

Robust estimation for functional quadratic regression models

Graciela Boente¹ and Daniela Parada²

¹ Universidad de Buenos Aires and CONICET

² Universidad de Buenos Aires

October 4, 2022

Abstract

Functional quadratic regression models postulate a polynomial relationship rather than a linear one between a scalar response and a functional covariate. As in functional linear regression, vertical and specially high-leverage outliers may affect the classical estimators. For that reason, providing reliable estimators in such situations is an important issue. Taking into account that the functional polynomial model is equivalent to a regression model that is a polynomial of the same order in the functional principal component scores of the predictor processes, our proposal combines robust estimators of the principal directions with robust regression estimators based on a bounded loss function and a preliminary residual scale estimator. Fisher-consistency of the proposed method is derived under mild assumptions. The results of a numerical study show the benefits of the robust proposal over the one based on sample principal directions and least squares for the considered contaminating scenarios. The usefulness of the proposed approach is also illustrated through the analysis of a real data set which also reveals that when the potential outliers are removed the classical method behave very similarly to the robust one computed with all the data.

AMS Subject Classification: 62G35

Key words and phrases: Functional Principal Components; Functional Data Analysis; Functional Quadratic Models; Robust estimation

1 Introduction

In the last decades, functional explanatory variables have been included in regression models either nonparametrically or through parametric models. Within the field of functional data analysis, some excellent overviews are provided in Ferraty and Vieu (2006) who presents a careful treatment of nonparametric models and also in the books by Ramsay and Silverman (2002, 2005), Horváth and Kokoszka (2012) and Hsing and Eubank (2015) who make emphasis on the functional linear model. Various aspects of this last model including implementations and asymptotic theory, have been studied among others in Cardot et al. (2003), Shen and Faraway (2004), Cardot and Sarda (2005), Cai and Hall (2006), Hall and Horowitz (2007), Frerero-Bande et al. (2017) and Reiss et al. (2017). The functional linear model imposes a structural linear constraint on the regression relationship which may or may not be satisfied. Some procedures to test the goodness of fit in such models have been discussed among others in García-Portugués et al. (2014), Cuesta-Albertos et al. (2019) and Patilea and Sánchez-Sellero (2020).

The linear constraint circumvents the *curse of dimensionality* present when considering fully nonparametric models since in the infinite-dimensional function space, the elements of a finite sample of random functions are very far away from each other. However, as pointed out in Yao and Müller (2010) and Horváth and Reeder (2013), this linear model imposes a constraint on the regression relationship that may be too restrictive for some applications. To preserve a reasonable structural constraint, but at the same time improving the model flexibility within the class of parametric models, Yao and Müller (2010) defined a functional polynomial model analogous to the extension from simple linear regression to polynomial regression. As in functional linear regression, regularization is key step to define the estimators. For that reason, Yao and Müller (2010) and Horváth and Reeder (2013) project the predictor on the eigenfunctions basis of the process, which is then truncated at a reasonable number of included components, leading to a parsimonious representation. With this representation, Yao and Müller (2010) have shown that the functional polynomial regression model can be represented as a polynomial regression model in the functional principal component scores of the predictor process.

In this paper, we consider independent and identically distributed observations with the same distribution as (y, X) , where the response $y \in \mathbb{R}$ is related to the functional explanatory variable $X \in L^2(\mathcal{I})$ according to the quadratic model $y = \alpha_0 + \langle \beta_0, X \rangle + \langle X, \Upsilon_0 X \rangle + \sigma_0 \epsilon$, where $\langle \cdot, \cdot \rangle$ denotes the usual $L^2(\mathcal{I})$ inner product, $\sigma_0 > 0$ is a residual scale parameter, and ϵ is the error term, independent of X . In this model, the regression parameter β_0 is assumed to be in $L^2(\mathcal{I})$ and $\Upsilon_0 : L^2(\mathcal{I}) \rightarrow L^2(\mathcal{I})$ is a linear operator, that without loss of generality may be assumed to be self-adjoint, that is, if $\Upsilon_0 u(t) = \int_{\mathcal{I}} v_0(s, t) u(s) ds$ then $v_0(s, t) = v_0(t, s)$. Furthermore, we will also assume that Υ_0 is Hilbert–Schmidt, that is, $\int_{\mathcal{I}} \int_{\mathcal{I}} v_0^2(s, t) ds dt < \infty$. The quadratic term $\langle X, \Upsilon_0 X \rangle$ appearing in the model reflects that beyond the effect that the values $X(t)$, $t \in \mathcal{I}$, have on the response, the products $\{X(s)X(t)\}$, for $s, t \in \mathcal{I}$, are also included as additional predictors.

As it has been extensively described, small proportions of outliers and other atypical observations can affect seriously the estimators for regression models and the situation in functional linear or quadratic models is not an exception. Robust proposals for functional linear regression models using P –splines or B –splines were considered in Maronna and Yohai (2013), Boente et al. (2020) and Kalogridis and Van Aelst (2021), while an approach combining robust functional principal components and robust linear regression was studied in Kalogridis and Van Aelst (2019).

As mentioned in Hubert et al. (2015), different types of outliers may arise when considering functional data. These author pointed out that, in the functional setting, atypical data might

consist of curves that behave differently from the others displaying a persistent behaviour either in shift, amplitude and/or shape making more difficult their detection. Several detection criteria have been given in the literature based on different notions of depths, dimension reduction and/or visualization tools. Among others, we can mention the procedures described in Febrero-Bande et al. (2007, 2008), Hyndman and Shang (2010), Sun and Genton (2011), Arribas-Gil and Romo (2014), Rousseeuw et al. (2018), Dai and Genton (2019).

However, it should be noticed that when providing robust procedures for linear regression models with covariates in \mathbb{R}^p , outliers in the covariates are not automatically eliminated in a first step using some diagnostic method. The main reason is that the atypical data in the explanatory variables may not always be bad high-leverage observations, since some of them may help in the fitting process. MM –estimators with bounded loss functions provide an alternative choice for robust regression, in which good leverage points are not discarded. The same approach should be followed when dealing with functional covariates and quadratic models, so even when different outlier detection rules exist, it is better to adapt the best practices of robust estimation to this setting.

In this paper, we adapt the robust procedures for multiple linear regression estimators to the functional quadratic regression model. More precisely, we first compute robust estimators of the principal directions with the aim of providing finite-dimensional candidates for the estimators of both the functional regression parameter and the quadratic operator. We then apply MM –regression estimators (Yohai, 1987) that are based on a bounded loss function and a preliminary residual scale estimator to the residuals obtained from these finite-dimensional spaces. The initial scale estimator ensures that the estimators of β_0 and Υ_0 are scale equivariant, while the bounded loss function and the robust principal directions guarantee that the resulting procedure will be robust against high-leverage outliers. It is worth mentioning that the presence of outliers in the functional covariates may affect the estimation procedure when the sample principal components are used to estimate the regression function and quadratic operator, even when MM –estimators are used. The main reason is that a distorted estimator of the principal direction will affect the scores of all the observations in that direction, that is why robust estimators of the principal direction are needed. Among others, one may consider the spherical principal components introduced in Locantore et al. (1999) and studied in Gervini (2008), Boente et al. (2014) and Boente et al. (2019) or the projection–pursuit approach considered in Hyndman and Ullah (2007) and Bali et al. (2011).

We illustrate our approach with the Tecator data set (see Ferraty and Vieu, 2006). This food quality–control data contains 215 samples of finely chopped meat with different percentages of fat, protein and moisture content. For each sample, a spectrometric curve of absorbances was measured using a Tecator Infratec Food and Feed Analyzer. To predict the fat content of a meat sample from its absorbance spectrum, Yao and Müller (2010) fitted a functional quadratic model, while Horváth and Reeder (2013) tested the significance of the quadratic term. However, Boente and Vahnovan (2017) and Febrero-Bande and de la Fuente (2012), among others, showed the presence of atypical data in the spectrometric curves. Thus, a reliable analysis of the Tecator data set requires procedures protecting from outliers in the absorbance spectrum.

The rest of the paper is organized as follows. The model and our proposed estimators are described in Section 2. Fisher–consistency of the procedure is studied in Section 3 both for finite–dimensional and infinite–dimensional processes. In Section 4, the performance and advantages of the proposed methods are illustrated for finite–samples. Section 5 contains the Tecator data set analysis, while final comments are given in Section 6.

2 Model and estimators

As mentioned in the Introduction, the functional quadratic regression model assumes that the observations (y_i, X_i) , $1 \leq i \leq n$, are independent and identically distributed realizations of the random element (y, X) , where $y \in \mathbb{R}$ is the response variable, X is a stochastic process on $L^2(\mathcal{I})$, the space of square integrable functions on the interval \mathcal{I} . The relationship between the response and the explanatory variable is given by:

$$y = \alpha_0 + \langle \beta_0, X \rangle + \langle X, \Upsilon_0 X \rangle + \sigma_0 \epsilon, \quad (1)$$

where $\langle \cdot, \cdot \rangle$ denotes the usual $L^2(\mathcal{I})$ inner product, ϵ is independent of X , $\sigma_0 > 0$ is the unknown error scale parameter, $\beta_0 \in L^2(\mathcal{I})$ is the regression coefficient and $\Upsilon_0 : L^2(\mathcal{I}) \rightarrow L^2(\mathcal{I})$ is the linear self-adjoint and Hilbert–Schmidt operator corresponding to the quadratic term, where \mathcal{I} is a compact interval. For simplicity, we will assume that $\mathcal{I} = [0, 1]$. At this instance, to avoid requiring moments to the errors, but at the same time to identify the regression function, we require that ϵ has a symmetric distribution $G(\cdot)$ with scale parameter 1.

Just as in Kalogridis and Van Aelst (2019) who considered the functional linear regression model, to obtain a proper finite-dimensional approximation of X , we assume that $\mathbb{E}\|X\|^2 < \infty$, where $\|X\|^2 = \langle X, X \rangle$. From now on, we denote as ϕ_j , $j \geq 1$, the eigenfunctions of the covariance operator Γ of X and as λ_j , $j \geq 1$, the related eigenvalues ordered such that $\lambda_j \geq \lambda_{j+1}$, for all j . In such a case, the Karhunen–Loëve representation of X is $X = \mu + \sum_{j \geq 1} \xi_j \phi_j$, where $\mu = \mathbb{E}(X)$ and the scores $\xi_j = \langle X - \mu, \phi_j \rangle$ are uncorrelated random variables with mean zero and variance λ_j .

Note that in Yao and Müller (2010) and Horváth and Reeder (2013) model (1) is written in terms of the centered process $X^{(c)} = X - \mu$ as

$$y = \alpha_0^* + \langle \beta_0^*, X^{(c)} \rangle + \langle X^{(c)}, \Upsilon_0 X^{(c)} \rangle + \sigma_0 \epsilon. \quad (2)$$

Clearly, the parameters in both models (1) and (2) are related as follows $\alpha_0^* = \alpha_0 + \langle \mu, \beta_0 \rangle + \langle \mu, \Upsilon_0 \mu \rangle$ and $\beta_0^* = \beta_0 + 2 \Upsilon_0 \mu$. Taking into account the Karhunen–Loéve of the process X , Yao and Müller (2010) suggest to estimate α_0^* , β_0^* and Υ_0 using the scores on the linear space spanned by the first eigenfunctions of the covariance operator. Moreover, Yao and Müller (2010) derived explicit expressions for the coefficients $b_{0,j}^*$, $j \geq 1$ and $v_{0,j\ell}$, $j, \ell \geq 1$ of β_0^* and Υ_0 , respectively in (2) and suggested to estimate them by plugging-in the unknown scores by their predicted values and replacing the expectations by their sample counterparts. To define the final estimators of β_0^* and Υ_0 , they approximated their infinite expansions by a small one that uses only p estimated eigenfunctions. Horváth and Reeder (2013) used a finite approximation and a least squares approach to estimate the parameters and to construct a test for significance of the quadratic operator.

Let us consider model (1), similar expansions than those given below can be obtained when using the centered model (2), replacing α_0 and β_0 by α_0^* , β_0^* , respectively and X by $X^{(c)}$, so that $x_j = \langle X, \phi_j \rangle$ needs to be replaced by $\langle X^{(c)}, \phi_j \rangle = \xi_j$ and \widehat{x}_{ij} by $\langle \widehat{X}_i - \widehat{\mu}, \widehat{\phi}_j \rangle = \widehat{\xi}_{ij}$, for proper estimators $\widehat{\mu}$ of μ and $\widehat{\phi}_j$ of ϕ_j . Section 2.1 revisits some well known robust estimators for these quantities.

To motivate the estimators to be used, we begin by expanding β_0 and Υ_0 over the basis of eigenfunctions. Note that $\{\phi_j \otimes \phi_\ell\}_{j \geq 1, \ell \geq 1}$ is a proper basis on the space of self-adjoint Hilbert–Schmidt operator. Hence, we have the following expansions for β_0 and Υ_0

$$\beta_0 = \sum_{j=1}^{\infty} b_{0,j} \phi_j \quad \Upsilon_0 = \sum_{j=1}^{\infty} v_{0,jj} \phi_j \otimes \phi_j + \sum_{j=1}^{\infty} \sum_{\ell=j+1}^{\infty} v_{0,j\ell} (\phi_j \otimes \phi_\ell + \phi_\ell \otimes \phi_j),$$

where $b_{0,j} = \langle \beta, \phi_j \rangle$ and $v_{0,j\ell} = \langle \phi_j, \Upsilon_0 \phi_\ell \rangle = v_{0,\ell j}$ with $\sum_{j \geq 1} b_{0,j}^2 < \infty$ and $\sum_{j \geq 1} \sum_{\ell \geq 1} v_{0,j\ell}^2 < \infty$. Thus, replacing in (1), we get that

$$\begin{aligned}
y &= \alpha_0 + \langle \beta_0, X \rangle + \langle X, \Upsilon_0 X \rangle + \sigma_0 \epsilon \\
&= \alpha_0 + \sum_{j=1}^{\infty} b_{0,j} x_j + \sum_{j=1}^{\infty} v_{0,jj} x_j^2 + \sum_{j=1}^{\infty} \sum_{\ell=j+1}^{\infty} v_{0,j\ell} \langle X, (\phi_j \otimes \phi_\ell + \phi_\ell \otimes \phi_j) X \rangle + \sigma_0 \epsilon \\
&= \alpha_0 + \sum_{j=1}^{\infty} b_{0,j} x_j + \sum_{j=1}^{\infty} v_{0,jj} x_j^2 + 2 \sum_{j=1}^{\infty} \sum_{\ell=j+1}^{\infty} v_{0,j\ell} x_j x_\ell + \sigma_0 \epsilon \\
&= \alpha_0 + \sum_{j=1}^{\infty} b_{0,j} x_j + \sum_{j=1}^{\infty} \sum_{\ell=j}^{\infty} (2 - \mathbf{1}_{j=\ell}) v_{0,j\ell} x_j x_\ell + \sigma_0 \epsilon,
\end{aligned}$$

where $x_j = \langle X, \phi_j \rangle = \xi_j + \langle \mu, \phi_j \rangle$.

It is worth mentioning that even when robust estimators of the principal directions are obtained, for atypical trajectories X_i their predicted scores $\hat{\xi}_{ij} = \langle X_i - \hat{\mu}, \hat{\phi}_j \rangle$ may be distorted. Hence, the least squares procedure used in Horváth and Reeder (2013) will not lead to resistant estimators. Moreover, vertical outliers which correspond to atypical values only in the responses may also be present in the sample, affecting also these estimators. For that reason, we will follow a different approach combining robust estimators of the principal directions and robust regression estimators.

More precisely, assume that robust estimators of the location μ and the eigenfunctions ϕ_j are available and denote them $\hat{\mu}$ and $\hat{\phi}_j$, respectively. In such a case, one may predict X_i using a small number p of principal directions as $\hat{X}_i = \hat{\mu} + \sum_{j=1}^p \hat{\xi}_{ij} \hat{\phi}_j$, which allows to approximate the regression function $g(X) = \alpha_0 + \langle \beta_0, X \rangle + \langle X, \Upsilon_0 X \rangle$ at X_i as

$$g(X_i) \approx g(\hat{X}_i) = \alpha_0 + \langle \beta_0, \hat{X}_i \rangle + \langle \hat{X}_i, \Upsilon_0 \hat{X}_i \rangle = \alpha_0 + \sum_{j=1}^p \langle \hat{\phi}_j, \beta_0 \rangle \hat{x}_{ij} + \sum_{j=1}^p \sum_{\ell=1}^p \langle \hat{\phi}_j, \Upsilon_0 \hat{\phi}_\ell \rangle \hat{x}_{ij} \hat{x}_{i\ell},$$

where $\hat{x}_{ij} = \langle \hat{X}_i, \hat{\phi}_j \rangle = \langle \hat{\mu}, \hat{\phi}_j \rangle + \hat{\xi}_{ij}$. Noticing that $\langle \hat{\phi}_j, \Upsilon_0 \hat{\phi}_\ell \rangle = \langle \hat{\phi}_\ell, \Upsilon_0 \hat{\phi}_j \rangle$, since Υ_0 is self adjoint, we can write

$$\begin{aligned}
g(\hat{X}_i) &= \alpha_0 + \sum_{j=1}^p \langle \hat{\phi}_j, \beta_0 \rangle \hat{x}_{ij} + \sum_{j=1}^p \sum_{\ell=j+1}^p 2 \langle \hat{\phi}_j, \Upsilon_0 \hat{\phi}_\ell \rangle \hat{x}_{ij} \hat{x}_{i\ell} + \sum_{j=1}^p \langle \hat{\phi}_j, \Upsilon_0 \hat{\phi}_j \rangle \hat{x}_{ij}^2 \\
&= \alpha_0 + \sum_{j=1}^p b_j \hat{x}_{ij} + \sum_{j=1}^p \sum_{\ell=j}^p u_{j\ell} \hat{x}_{ij} \hat{x}_{i\ell}.
\end{aligned}$$

As mentioned above, the unknown coefficients $b_j = \langle \hat{\phi}_j, \beta_0 \rangle$ and $u_{j\ell} = (2 - \mathbf{1}_{j=\ell}) \langle \hat{\phi}_j, \Upsilon_0 \hat{\phi}_\ell \rangle$ are estimated in Horváth and Reeder (2013) using a least squares approach.

The above expansions suggest that one possible way to estimate β_0 and Υ_0 is to restrict the set of possible candidates to those belonging to the linear spaces spanned by $\hat{\phi}_1, \dots, \hat{\phi}_p$ and $\{\hat{\phi}_j \otimes \hat{\phi}_\ell\}_{1 \leq j, \ell \leq p}$, respectively. To ensure resistance to atypical data, including vertical outliers and atypical observations in the covariates, we will use *MM*–estimators combined with robust estimators of the principal directions, as described below in Section 2.2.

2.1 Some robust principal direction estimators

As mentioned in the Introduction, several robust estimators for the principal directions have been considered in the literature since the spherical principal components introduced in Locantore et al. (1999). As it is well known, the spherical principal directions are the eigenfunctions of the sample sign covariance function, which is just the sample covariance function of the centered curves projected on the unit sphere. More precisely, let $\hat{\mu}$ stand for an estimator of the location of X such as the sample spatial median $\hat{\mu}_{\text{SM}} = \text{argmin}_{\theta \in L^2(\mathcal{I})} \sum_{i=1}^n (\|X_i - \theta\| - \|X_i\|)$ and define the operator $\hat{\Gamma}^{\text{S}}$ as

$$\hat{\Gamma}^{\text{S}} = \frac{1}{n} \sum_{i=1}^n \mathbb{E} \left\{ \frac{(X_i - \hat{\mu}) \otimes (X_i - \hat{\mu})}{\|X_i - \hat{\mu}\|^2} \right\}.$$

Gervini (2008) and Cardot et al. (2013) have shown that $\hat{\mu}_{\text{SM}}$ is a consistent estimator of the spatial median $\mu_{\text{SM}} = \text{argmin}_{\theta \in L^2(\mathcal{I})} \mathbb{E} (\|X - \theta\| - \|X\|)$. Consistency of $\hat{\Gamma}^{\text{S}}$ to the sign operator defined as

$$\Gamma^{\text{S}} = \mathbb{E} \left\{ \frac{(X - \mu) \otimes (X - \mu)}{\|X - \mu\|^2} \right\},$$

was derived in Theorem 1 in Boente et al. (2019), whenever $\hat{\mu}$ is consistent to μ . These authors also obtained the asymptotic distribution of $\hat{\Gamma}^{\text{S}}$ and that of its eigenfunctions, that is, the asymptotic distribution of the spherical principal directions, see Proposition 1 in Boente et al. (2019).

It is worth mentioning that when considering the spherical principal directions, one need to choose a robust estimator for the location μ of the process X to center the data. As discussed in Boente et al. (2019), several robust location functionals and their related estimators may be considered. Among others, the geometric median or spatial median defined above is the usual choice when using the spatial operator. However, other choices are possible including the α –trimmed mean defined in Fraiman and Muñiz (2001) or the M –estimators defined in Sinova et al. (2018) which are consistent under some model assumptions. Also, estimators defined through a suitable depth notion may be used defining the related median as the deepest point. Note that all these procedures provide Fisher–consistent estimators when considering a symmetric process around $\mu \in \mathcal{H}$, meaning that $X - \mu$ and $\mu - X$ have the same distribution.

As when estimating μ , one important issue to be considered when defining robust estimators of the directions ϕ_j is that they are indeed estimating the target directions, a property which is usually known as Fisher–consistency. Theorem 3 in Gervini (2008) shows that if the process is finite–dimensional, i.e., $X = \mu + \sum_{k=1}^q \xi_k \phi_k$ and the standardized scores $(\xi_1/\sqrt{\lambda_1}, \dots, \xi_q/\sqrt{\lambda_q})$, $\lambda_1 \geq \dots \geq \lambda_q > 0$, have a symmetric distribution with exchangeable marginals, then the eigenfunctions of Γ^{S} are ϕ_j , $1 \leq j \leq q$. Furthermore, as mentioned in Boente et al. (2014), for infinite–dimensional processes, if X is an elliptical process $\mathcal{E}(\mu, \Gamma)$, then Γ^{S} has the same eigenfunctions as Γ and in the same order. These two properties do not require the existence of second moments, making the procedure adequate when we suspect that atypical curves may arise among the functional covariates.

Other procedures to robustly estimate the principal directions include the projection–pursuit approach considered in Hyndman and Ullah (2007) and generalized in Bali et al. (2011) to include a penalization, so as to ensure that the principal direction estimators are smooth. The projection–pursuit estimators provide a Fisher–consistent method at elliptical processes and consistent estimators, under mild conditions. A procedure based on projecting the observations over a known basis and performing robust principal components analysis on the coefficients has been

proposed in Sawant et al. (2012). Robust alternatives based on estimating the eigenspace have been also considered. In this direction, we can mention the M –type smoothing spline estimators proposed in Lee et al. (2013) who proposed a sequential algorithm that robustly fits one–dimensional linear spaces. Other alternatives are the S –estimators defined in Boente and Salibián-Barrera (2015) or those defined in Cevallos-Valdiviezo (2016) who, as in Sawant et al. (2012), consider the coefficients of the data over a finite–dimensional basis and then apply a robust multivariate method to estimate principal subspaces. It is worth mentioning that, even when, for elliptically distributed random processes, these last two procedures are Fisher–consistent methods to estimate the linear space spanned by the first eigenfunctions, they do not give estimators of the principal directions themselves but to the linear space spanned by them, so a proper basis in that space should then be selected.

From now on, $\hat{\phi}_j$, $1 \leq j \leq p$, will stand for the principal direction estimators obtained by one of these methods.

2.2 The estimators of β_0 and Υ_0

As mentioned above, one way to regularize the problem and avoid the curse of dimensionality imposed by dealing with functional covariates is to restrict the set of possible candidates for the estimators of β_0 and Υ_0 to those belonging to the linear spaces spanned by $\hat{\phi}_1, \dots, \hat{\phi}_p$ and $\{\hat{\phi}_j \otimes \hat{\phi}_\ell\}_{1 \leq j, \ell \leq p}$. For that purpose, from now on, we denote as $\text{vech}(\cdot)$ the half–vectorization that stacks the columns of the lower triangular portion of the matrix under each other.

To define our estimators, for any symmetric matrix \mathbf{V} , we define $u_{j\ell} = (2 - \mathbf{1}_{j=\ell})v_{j\ell}$ and $\mathbf{u} = \text{vech}(\{u_{j\ell}\})_{1 \leq j \leq \ell \leq p} = \text{vech}(\{(2 - \mathbf{1}_{j=\ell})v_{j\ell}\})_{1 \leq j \leq \ell \leq p} \in \mathbb{R}^{p \times (p+1)/2}$. Furthermore, given $\mathbf{b} \in \mathbb{R}^p$ and symmetric matrix $\mathbf{V} \in \mathbb{R}^{p \times p}$, let $\beta_{\mathbf{b}}$ and $\Upsilon_{\mathbf{u}}$ stand for

$$\begin{aligned} \beta_{\mathbf{b}} &= \sum_{j=1}^p b_j \hat{\phi}_j, \\ \Upsilon_{\mathbf{u}} &= \sum_{j=1}^{\infty} \sum_{\ell=1}^{\infty} v_{j\ell} \hat{\phi}_j \otimes \hat{\phi}_\ell = \sum_{j=1}^p \sum_{\ell=j}^p (2 - \mathbf{1}_{j=\ell}) v_{j\ell} \hat{\phi}_j \otimes \hat{\phi}_\ell = \sum_{j=1}^p \sum_{\ell=j}^p u_{j\ell} \hat{\phi}_j \otimes \hat{\phi}_\ell. \end{aligned} \quad (3)$$

To define the robust estimators, we use robust regression MM –estimators (Yohai, 1987), that is, we compute a residual scale estimator using an initial robust regression estimator and then we calculate a regression M –estimator using a bounded loss function and standardized residuals.

In what follows the loss functions $\rho_j : \mathbb{R} \rightarrow \mathbb{R}_+$, $j = 0, 1$ to be used below correspond to bounded ρ –functions as defined in Maronna et al. (2019). The Tukey’s bisquare function $\rho_{T,c}(t) = \min(1 - (1 - (t/c)^2)^3, 1)$ provides an example of bounded ρ –function. The tuning parameter $c > 0$ is chosen to balance the robustness and efficiency properties of the associated estimators.

We define the residuals $r_i(a, \beta_{\mathbf{b}}, \Upsilon_{\mathbf{u}})$, $1 \leq i \leq n$, with respect to the corresponding approximations $\beta_{\mathbf{b}}$ and $\Upsilon_{\mathbf{u}}$ as

$$r_i(a, \beta_{\mathbf{b}}, \Upsilon_{\mathbf{u}}) = y_i - a - \sum_{j=1}^p b_j \hat{x}_{ij} - \sum_{j=1}^p \sum_{\ell=1}^p v_{j\ell} \hat{x}_{ij} \hat{x}_{i\ell} = y_i - a - \mathbf{b}^T \hat{\mathbf{x}}_i - \mathbf{u}^T \hat{\mathbf{z}}_i,$$

where $\hat{\mathbf{x}}_i = (\hat{x}_{i1}, \dots, \hat{x}_{ip})^T$, $\hat{\mathbf{z}}_i = (\hat{z}_{i,1}, \dots, \hat{z}_{i,q})^T$ with $\hat{\mathbf{z}}_i = \text{vech}(\{(\hat{x}_{ij} \hat{x}_{i\ell})\})_{1 \leq j \leq \ell \leq p} \in \mathbb{R}^q$, $q = p \times (p+1)/2$, and $\hat{x}_{ij} = \langle X_i, \hat{\phi}_j \rangle$.

First, we compute an S –estimator of regression and its associated residual scale. Let ρ_0 be a bounded ρ –function and $s_n(a, \beta_{\mathbf{b}}, \eta_{\mathbf{a}})$ be the M –scale estimator of the residuals given as the solution to the following equation:

$$\frac{1}{n - (p + q)} \sum_{i=1}^n \rho_0 \left(\frac{r_i(a, \beta_{\mathbf{b}}, \Upsilon_{\mathbf{u}})}{s_n(a, \beta_{\mathbf{b}}, \Upsilon_{\mathbf{u}})} \right) = b, \quad (4)$$

where $b = E(\rho_0(\epsilon))$. This choice of b ensures that the scale estimators are indeed Fisher–consistent. Note that as in Boente et al. (2020), we use $1/(n - (p + q))$ instead of $1/n$ in (4) above to control the effect of a possibly large number of parameters $(p + q)$ relative to the sample size (see Maronna et al., 2019). Recall that if $\rho_0 = \rho_{T, c_0}$, the choices $c_0 = 1.54764$ and $b = 1/2$ above yield a scale estimator that is Fisher–consistent when the errors have a normal distribution, and with a 50% breakdown point in finite–dimensional regression models. S –regression estimators are defined as the minimizers of the M –scale above:

$$(\hat{a}_{\text{INI}}, \hat{\mathbf{b}}_{\text{INI}}, \hat{\mathbf{u}}_{\text{INI}}) = \underset{a, \mathbf{b}, \mathbf{u}}{\text{argmin}} s_n(a, \beta_{\mathbf{b}}, \Upsilon_{\mathbf{u}}). \quad (5)$$

The associated residual scale estimator is

$$\hat{\sigma} = s_n(\hat{a}_{\text{INI}}, \beta_{\hat{\mathbf{b}}_{\text{INI}}}, \Upsilon_{\hat{\mathbf{u}}_{\text{INI}}}) = \min_{a, \mathbf{b}, \mathbf{u}} s_n(a, \beta_{\mathbf{b}}, \Upsilon_{\mathbf{u}}).$$

Let ρ_1 be a ρ –function such that $\rho_1 \leq \rho_0$ and $\sup_t \rho_1(t) = \sup_t \rho_0(t)$. As it is well known, if $\rho_0 = \rho_{T, c_0}$ and $\rho_1 = \rho_{T, c_1}$, then $\rho_0 \leq \rho_1$ when $c_1 > c_0$. We now compute an M –estimator using the residual scale estimator $\hat{\sigma}$ and the loss function ρ_1 as

$$(\hat{a}, \hat{\mathbf{b}}, \hat{\mathbf{u}}) = \underset{a, \mathbf{b}, \mathbf{u}}{\text{argmin}} L_n(a, \mathbf{b}, \mathbf{u}) = \underset{a, \mathbf{b}, \mathbf{u}}{\text{argmin}} \sum_{i=1}^n \rho_1 \left(\frac{r_i(a, \beta_{\mathbf{b}}, \Upsilon_{\mathbf{u}})}{\hat{\sigma}} \right), \quad (6)$$

where $L_n(a, \mathbf{b}, \mathbf{u}) = \sum_{i=1}^n \rho_1(r_i(a, \beta_{\mathbf{b}}, \Upsilon_{\mathbf{u}})/\hat{\sigma})$. Note that \hat{a} provides an estimator of α_0 , that will be denoted $\hat{\alpha}$. If we denote as $\hat{u}_{j\ell}$, the elements of a symmetric matrix such that $\hat{\mathbf{u}} = \text{vech}(\{\hat{u}_{j\ell}\}_{1 \leq j \leq \ell \leq p})$, the resulting estimators of the regression function β_0 and the quadratic operator Υ_0 are given by

$$\hat{\beta} = \sum_{j=1}^p \hat{b}_j \hat{\phi}_j, \quad \text{and} \quad \hat{\Upsilon} = \sum_{j=1}^p \hat{u}_{jj} \hat{\phi}_j \otimes \hat{\phi}_j + \sum_{1 \leq j < \ell \leq p} \frac{1}{2} \hat{u}_{j\ell} \left(\hat{\phi}_j \otimes \hat{\phi}_\ell + \hat{\phi}_\ell \otimes \hat{\phi}_j \right). \quad (7)$$

It is worth mentioning that if model (2) is considered, given a robust consistent estimator $\hat{\mu}$ of μ , estimators of α_0^* and β_0^* may be constructed from those obtained in (7) as

$$\hat{\alpha}^* = \hat{\alpha} + \langle \hat{\mu}, \hat{\beta} \rangle + \langle \hat{\mu}, \hat{\Upsilon} \hat{\mu} \rangle \quad \text{and} \quad \hat{\beta}^* = \hat{\beta} + 2 \hat{\Upsilon} \hat{\mu}. \quad (8)$$

Note that when defining both $\hat{\alpha}^*$ and $\hat{\beta}^*$ in the above expressions, only the coordinates of $\hat{\mu}$ on the finite–dimensional basis $\hat{\phi}_1, \dots, \hat{\phi}_p$ are used.

It is worth mentioning that the transformation made in (8) to construct the estimators $\hat{\alpha}^*$ and $\hat{\beta}^*$ is equivalent to directly obtaining estimators of α_0^* , β_0^* and Υ_0 using MM –estimators with the predicted scores. More precisely, let us denote $\hat{\xi}_i = (\hat{\xi}_{i1}, \dots, \hat{\xi}_{ip})^T$, $\hat{\mathbf{z}}_i^* = (\hat{z}_{i,1}^*, \dots, \hat{z}_{i,q}^*)^T$ with

$\widehat{\mathbf{z}}_i^* = \text{vech}(\{\widehat{\xi}_{ij} \widehat{\xi}_{i\ell}\})_{1 \leq j \leq \ell \leq p} \in \mathbb{R}^q$, $q = p \times (p+1)/2$, and $\widehat{\xi}_{ij} = \langle X_i - \widehat{\mu}, \widehat{\phi}_j \rangle = x_{ij} - \langle \widehat{\mu}, \widehat{\phi}_j \rangle$ and the possible candidates for estimating β_0^* as

$$\beta_{\mathbf{b}^*}^* = \sum_{j=1}^p b_j^* \widehat{\phi}_j,$$

where $\mathbf{b}^* \in \mathbb{R}^p$. The possible candidates for estimating the quadratic operator are given by (3). The residuals are now defined as

$$r_i^*(a^*, \beta_{\mathbf{b}^*}^*, \Upsilon_{\mathbf{u}}) = y_i - a^* - \sum_{j=1}^p b_j^* \widehat{\xi}_{ij} - \sum_{j=1}^p \sum_{\ell=1}^p v_{j\ell} \widehat{\xi}_{ij} \widehat{\xi}_{i\ell} = y_i - a^* - \mathbf{b}^{*\top} \widehat{\boldsymbol{\xi}}_i - \mathbf{u}^{\top} \widehat{\mathbf{z}}_i^*,$$

where we use the upper-script * to make clear that we are dealing with the centered model. Then, one may consider S -regression estimators to obtain estimators of σ_0 , that is,

$$\widehat{\sigma}^* = s_n^*(\widehat{a}_{\text{INI}}^*, \beta_{\widehat{\mathbf{b}}_{\text{INI}}}^*, \Upsilon_{\widehat{\mathbf{u}}_{\text{INI}}}) = \min_{a^*, \mathbf{b}^*, \mathbf{u}} s_n^*(a^*, \beta_{\mathbf{b}^*}^*, \Upsilon_{\mathbf{u}}),$$

where $s_n^*(a^*, \beta_{\mathbf{b}^*}^*, \Upsilon_{\mathbf{u}})$ is defined as in (4), that is,

$$\frac{1}{n - (p + q)} \sum_{i=1}^n \rho_0 \left(\frac{r_i^*(a^*, \beta_{\mathbf{b}^*}^*, \Upsilon_{\mathbf{u}})}{s_n^*(a^*, \beta_{\mathbf{b}^*}^*, \Upsilon_{\mathbf{u}})} \right) = b.$$

The M -estimator of the coefficient is obtained using the residual scale estimator $\widehat{\sigma}^*$ and the loss function ρ_1 as

$$(\widehat{\alpha}^*, \widehat{\mathbf{b}}^*, \widehat{\mathbf{u}}^*) = \underset{a^*, \mathbf{b}^*, \mathbf{u}}{\text{argmin}} L_n^*(a^*, \mathbf{b}^*, \mathbf{u}) = \underset{a^*, \mathbf{b}^*, \mathbf{u}}{\text{argmin}} \sum_{i=1}^n \rho_1 \left(\frac{r_i^*(a^*, \beta_{\mathbf{b}^*}^*, \Upsilon_{\mathbf{u}})}{\widehat{\sigma}^*} \right). \quad (9)$$

The resulting estimators of β_0^* and Υ_0 are then equal to

$$\widehat{\beta}^* = \sum_{j=1}^p \widehat{b}_j^* \widehat{\phi}_j, \quad \text{and} \quad \widehat{\Upsilon} = \sum_{j=1}^p \widehat{u}_{jj}^* \widehat{\phi}_j \otimes \widehat{\phi}_j + \sum_{1 \leq j < \ell \leq p} \frac{1}{2} \widehat{u}_{j\ell}^* \left(\widehat{\phi}_j \otimes \widehat{\phi}_\ell + \widehat{\phi}_\ell \otimes \widehat{\phi}_j \right), \quad (10)$$

where we used the notation $\widehat{\mathbf{u}}^* = \text{vech}(\{\widehat{u}_{j\ell}^*\}_{1 \leq j \leq \ell \leq p})$. Taking into account the relations between $\widehat{\mathbf{x}}_i$ and $\widehat{\mathbf{z}}_i$ with $\widehat{\boldsymbol{\xi}}_i$ and $\widehat{\mathbf{z}}_i^*$, respectively, straightforward calculations allow to see that, for any $a \in \mathbb{R}$, $\mathbf{b} \in \mathbb{R}^p$ and symmetric matrix $\mathbf{V} \in \mathbb{R}^{p \times p}$, we have $r_i(a, \beta_{\mathbf{b}}, \Upsilon_{\mathbf{u}}) = r_i^*(a^*, \beta_{\mathbf{b}^*}^*, \Upsilon_{\mathbf{u}})$, where

$$\begin{aligned} a^* &= a + \sum_{j=1}^p b_j \widehat{\mu}_j + \sum_{j=1}^p \sum_{\ell=1}^p v_{j\ell} \widehat{\mu}_j \widehat{\mu}_\ell = a + \mathbf{b}^{\top} \widehat{\boldsymbol{\mu}} + \sum_{j=1}^p \sum_{\ell=j}^p (2 - \mathbf{1}_{j=\ell}) v_{j\ell} \widehat{\mu}_j \widehat{\mu}_\ell = a + \mathbf{b}^{\top} \widehat{\boldsymbol{\mu}} + \mathbf{u}^{\top} \widehat{\boldsymbol{\nu}}, \\ b_j^* &= b_j + \sum_{\ell=1}^p (v_{j\ell} + v_{\ell j}) \widehat{\mu}_\ell = b_j + 2 \sum_{\ell=1}^p v_{j\ell} \widehat{\mu}_\ell = b_j + 2 \langle \Upsilon_{\mathbf{u}} \widehat{\boldsymbol{\mu}}, \widehat{\phi}_j \rangle = b_j + 2 \sum_{\ell=j}^p u_{j\ell} \widehat{\mu}_\ell = b_j + 2 \mathbf{u}^{(j)\top} \widehat{\boldsymbol{\mu}}, \end{aligned}$$

with $\widehat{\mu}_j = \langle \widehat{\boldsymbol{\mu}}, \widehat{\phi}_j \rangle$, $\widehat{\boldsymbol{\mu}} = (\widehat{\mu}_1, \dots, \widehat{\mu}_p)^{\top}$, $\widehat{\boldsymbol{\nu}} = \text{vech}(\{\langle \widehat{\mu}_j \widehat{\mu}_\ell \rangle\}_{1 \leq j \leq \ell \leq p}) \in \mathbb{R}^q$ and $\mathbf{u} = (\mathbf{u}^{(1)\top}, \dots, \mathbf{u}^{(p)\top})^{\top}$ where $\mathbf{u}^{(j)\top} \in \mathbb{R}^{p-j+1}$. Hence, due to the equivariance of M -estimators, we have that $\widehat{\sigma}^* = \widehat{\sigma}$, $\widehat{\mathbf{u}}^* = \widehat{\mathbf{u}}$, $\widehat{\alpha}^* = \widehat{\alpha} + \langle \widehat{\boldsymbol{\mu}}, \widehat{\boldsymbol{\beta}} \rangle + \langle \widehat{\boldsymbol{\mu}}, \widehat{\Upsilon} \widehat{\boldsymbol{\mu}} \rangle$ and $\widehat{b}_j^* = \widehat{b}_j + 2 \widehat{u}_{jj} \langle \widehat{\phi}_j, \widehat{\boldsymbol{\mu}} \rangle + \sum_{\ell=j+1}^p \widehat{u}_{j\ell} \langle \widehat{\phi}_\ell, \widehat{\boldsymbol{\mu}} \rangle$ which leads to the estimators defined in (8). Even though either considering model (1) or (2) there is one-to-one transformation that relate the MM -estimators in one model to those in the other one, when considering Fisher-consistency it will be better to use the proposed procedure under model (2). The main reason is that, unless the kernel of the covariance operator of X reduces to $\{0\}$, the parameters are not uniquely identified. Under model (1), this lack of uniqueness also affects the intercept parameter, while under model (2) it only involves β_0^* and Υ_0 .

2.3 Additional remarks

Smooth estimators The above considered estimators of the regression parameter β_0 and the quadratic kernel v_0 will be Fisher-consistent under mild regularity conditions (see Section 3) and our simulation study will show that they also are resistant to high-leverage trajectories. However, if smoothness of the estimated function and kernel is a requirement, two possibilities arise. On the one hand, as done in the functional linear model by Kalogridis and Van Aelst (2019), the practitioner may add a penalty term in the loss functions $L_n(a, \mathbf{b}, \mathbf{u})$ or $L_n^*(a^*, \mathbf{b}^*, \mathbf{u})$ defined in (6) or (9), respectively. However, unlike the method proposed by these authors, even when working with the centered trajectories and model (2), the quadratic model does not allow to obtain easily the penalized coefficients transforming those obtained from (6) as in ridge regression, since the predicted squared scores $\hat{\xi}_{ij}^2$ are not centered. Instead of adding computational burden to the procedure, we suggest to use the smoothed robust principal components defined in Bali et al. (2011) obtained penalizing the scale. The choice of this basis, which is an orthonormal basis, guarantees the smoothness of the regression and the quadratic kernel estimators.

Sparse trajectories The estimators defined in Section 2.2 only depend on proper predictors of the scores and estimators of the location μ and the eigenfunctions ϕ_j , since $\hat{x}_{ij} = \langle X_i, \hat{\phi}_j \rangle = \langle \hat{\mu}, \hat{\phi}_j \rangle + \hat{\xi}_{ij}$. Hence, as mentioned in the classical case by Yao and Müller (2010), they can be implemented when the functional predictors are derived from sparse and irregular measurements. The non-robust procedure proposed in Yao et al. (2005) predicts the scores and estimates the principal directions via the so-called Principal Analysis by Conditional Estimation (PACE) algorithm, implemented in R through the package `fdaPACE` developed by Chen et al. (2020).

When the practitioner suspects that outliers may be present among the functional covariates, the center function μ may be estimated by aggregating the available information, for instance, using a robust local M -estimator as in Boente and Salibián-Barrera (2021) or the M -type smoothing spline one defined in Kalogridis and Van Aelst (2021). The stepwise procedure proposed in Boente and Salibián-Barrera (2021) may be used to estimate the scatter operator Γ and its eigenfunctions. Besides, the scores may be predicted using the conditional distribution of the scores given the observed trajectories. The robust MM -estimators defined in (10) can be obtained using the predicted scores $\hat{\xi}_{ij}$ and the estimator $\hat{\mu}$ of μ .

Semi-functional models The estimators defined above can be extended to other functional models, such as those involving a nonparametric component using B -splines to approximate the unknown function. More specifically, consider the model

$$y_i = \langle X_i, \beta_0 \rangle + \langle X_i, \Upsilon_0 X_i \rangle + \eta_0(z_i) + \sigma_0 \epsilon_i,$$

where $z_i \in \mathcal{J}$, $1 \leq i \leq n$, is another explanatory variable and $\eta_0 : \mathcal{J} \rightarrow \mathbb{R}$ is an unknown smooth function with \mathcal{J} a compact interval which, without loss of generality, we will assume equal to $\mathcal{J} = [0, 1]$. Note that in order to identify η_0 the intercept coefficient is avoided in the above model. To define MM -estimators in this setting, we consider B -splines estimators of η_0 . More precisely, we fix a desired spline order ℓ and consider m_n knots to approximate η_0 . The corresponding B -spline basis has dimension $k = k_n = m_n + \ell$, see Corollary 4.10 in Schumaker (1981) and will be denoted $\{B_j : 1 \leq j \leq k_n\}$. In the sequel, $\eta_{\mathbf{a}}$ stands for the spline $\eta_{\mathbf{a}}(z) = \sum_{j=1}^k a_j B_j(z)$.

The residuals are now defined as

$$r_i(\eta_{\mathbf{a}}, \beta_{\mathbf{b}}, \Upsilon_{\mathbf{u}}) = y_i - \sum_{j=1}^p b_j \hat{x}_{ij} - \sum_{j=1}^p \sum_{\ell=j}^p u_{j\ell} \hat{z}_{ij\ell} - \sum_{j=1}^k a_j B_j(z_i) = y_i - \mathbf{b}^T \hat{\mathbf{x}}_i - \mathbf{u}^T \hat{\mathbf{z}}_i - \mathbf{a}^T \mathbf{B}_i,$$

with $\mathbf{B}_i = (B_1(z_i), \dots, B_k(z_i))^T$ and the estimators may be defined as before, but minimizing over $(\mathbf{a}, \mathbf{b}, \mathbf{u}) \in \mathbb{R}^{k+p+q}$ in (5) and (6).

3 Fisher-consistency

From now on, denote as P the probability measure related to (y, X) where the response y and the functional covariates satisfy the quadratic model (1) and as P_X the probability measure of X . Let Γ be the covariance operator of X and denote as ϕ_j , $j \geq 1$, its eigenfunctions with related eigenvalues $\lambda_1 \geq \lambda_2 \geq \dots$. In this section, we will study the functionals associated to the estimators of the centered model (2). For notation simplicity, we omit the upper-script $*$. Two situations will be considered. In the first one, as in Kalogridis and Van Aelst (2019) we will assume that the process is a finite-dimensional one, that is, $\lambda_j = 0$, for $j > q$ and some $q \geq 1$. Therefore, only the components of β_0 and Υ_0 over the linear space induced by the corresponding eigenfunctions will be identifiable. This motivates the definition of the projections given in (11), below. In the second case, we will consider an infinite-dimensional process where the kernel of Γ , denoted $\ker(\Gamma)$, reduces to $\{0\}$, in which case smoothness assumptions will be required to the eigenfunctions of Γ .

3.1 Fisher-consistency for finite-dimensional processes

Given p , define the projections of μ , β_0 and Υ_0 over the finite-dimensional spaces spanned by ϕ_1, \dots, ϕ_p and $\{\phi_j \otimes \phi_\ell\}_{1 \leq j, \ell \leq p}$ as

$$\mu_p = \sum_{j=1}^p \langle \mu, \phi_j \rangle \phi_j, \quad \beta_{0,p} = \sum_{j=1}^p \langle \beta_0, \phi_j \rangle \phi_j \quad \text{and} \quad \Upsilon_{0,p} = \sum_{j=1}^p \sum_{\ell=1}^p \langle \phi_j, \Upsilon_0 \phi_\ell \rangle \phi_j \otimes \phi_\ell. \quad (11)$$

The functional related to the estimation procedure described in Section 2.2 can be defined as follows. Let $\mu_R(P_X)$ be a location functional for the process X . For $1 \leq j \leq p$ denote as $\phi_{R,j}(P_X)$ any robust principal component direction functional from which the estimators are constructed and as $\lambda_{R,j}(P_X)$ the related eigenvalues ordered such that $\lambda_{R,j}(P_X) \geq \lambda_{R,j+1}(P_X)$. For each fixed p , define $\mathbf{x}_p(P_X) = (\langle X - \mu_R(P_X), \phi_{R,1}(P_X) \rangle, \dots, \langle X - \mu_R(P_X), \phi_{R,p}(P_X) \rangle)^T$ and $\mathbf{z}_p(P_X) = \text{vech}(\{(x_j(P_X) x_\ell(P_X))\}_{1 \leq j \leq \ell \leq p}) \in \mathbb{R}^q$, $q = p \times (p+1)/2$, with $x_j(P_X) = \langle X - \mu_R(P_X), \phi_{R,j}(P_X) \rangle$.

Given a ρ -function ρ_1 denote as $\beta(P)$ and $\Upsilon(P)$ the functionals,

$$\begin{aligned} \beta(P) &= \sum_{j=1}^p b_j(P) \phi_{R,j}(P_X), \\ \Upsilon(P) &= \sum_{j=1}^p u_{jj}(P) \phi_{R,j}(P_X) \otimes \phi_{R,j}(P_X) + \frac{1}{2} \sum_{1 \leq j < \ell \leq p} u_{j\ell}(P) (\phi_{R,j}(P_X) \otimes \phi_{R,\ell}(P_X) + \phi_{R,\ell}(P_X) \otimes \phi_{R,j}(P_X)) \\ &= \sum_{1 \leq j, \ell \leq p} v_{j\ell}(P) \phi_{R,j}(P_X) \otimes \phi_{R,\ell}(P_X), \end{aligned} \quad (12)$$

where $v_{jj}(P) = u_{jj}(P)$, $v_{j\ell}(P) = v_{\ell j}(P) = u_{j\ell}(P)/2$ and $(\alpha(P), \mathbf{b}(P), \mathbf{u}(P))$ are such that

$$(\alpha(P), \mathbf{b}(P), \mathbf{u}(P)) = \underset{a, \mathbf{b}, \mathbf{u}}{\operatorname{argmin}} \mathbb{E} \rho_1 \left(\frac{y - a - \mathbf{b}^T \mathbf{x}_p(P_X) - \mathbf{u}^T \mathbf{z}_p(P_X)}{\sigma_0} \right). \quad (13)$$

For simplicity, we denote as \mathcal{F} the space of linear, self-adjoint and Hilbert-Schmidt operators $\Upsilon : L^2(0, 1) \rightarrow L^2(0, 1)$ and as \mathcal{F}_p the finite-dimensional linear space of \mathcal{F} defined as

$$\mathcal{F}_p = \left\{ \Upsilon \in \mathcal{F} : \Upsilon = \sum_{1 \leq j, \ell \leq p} v_{j\ell} \phi_j \otimes \phi_\ell \text{ with } v_{j\ell} = v_{\ell j} \right\}.$$

Moreover, \mathcal{H}_p will stand for the linear space spanned by the first p eigenfunctions of Γ , that is, $\mathcal{H}_p = \{\beta \in L^2(0, 1) : \beta = \sum_{j=1}^p b_j \phi_j \text{ for some } b_j \in \mathbb{R}\}$. Then, the set of the possible candidates allowing to define $(\alpha(P), \beta(P), \Upsilon(P))$ equals $\mathcal{C}_p = \mathbb{R} \times \mathcal{H}_p \times \mathcal{F}_p$.

Throughout this section, we will consider the following assumptions

C1 : The function $\rho : \mathbb{R} \rightarrow [0, \infty)$ is bounded, continuous, even, non-decreasing on $[0, +\infty)$, and such that $\rho(0) = 0$. Moreover, $\lim_{u \rightarrow \infty} \rho(u) \neq 0$ and if $0 \leq u < v$ with $\rho(v) < \sup_u \rho(u)$ then $\rho(u) < \rho(v)$. Furthermore, assume that $\sup_u \rho(u) = 1$.

C2 : The random variable ϵ has a density function $f_0(t)$ that is even, non-increasing in $|t|$, and strictly decreasing for $|t|$ in a neighbourhood of 0.

C3 : $\mu_R(\cdot)$ and $\phi_{R,j}(\cdot), 1 \leq j \leq p$, are Fisher-consistent at P_X .

C4 : X has a finite-dimensional Karhunen-Loëve decomposition given by $X = \mu + \sum_{j=1}^q \xi_j \phi_j$.

C5 : $\mathbb{P}(\langle X - \mu, \beta \rangle + \langle X - \mu, \Upsilon(X - \mu) \rangle = a) < 1$, for any $(a, \beta, \Upsilon) \in \mathcal{C}_q$ such that $(a, \beta, \Upsilon) \neq 0$, where q is given in **C4**.

Remark 3.1. Condition **C1** corresponds to the requirements in Maronna et al. (2019) for a bounded ρ -function. Condition **C2** is a usual assumption when considering robust estimators in linear regression models. Conditions ensuring Fisher-consistency of the principal direction functional and of the location functional required in **C3** were discussed in Section 2.1. It is worth mentioning that, when assumption **C3** holds, (12) and (13) can be written as

$$(\alpha(P), \beta(P), \Upsilon(P)) = \underset{a \in \mathbb{R}, \beta \in \mathcal{H}_p, \Upsilon \in \mathcal{F}_p}{\operatorname{argmin}} L(a, \beta, \Upsilon, \mu, \sigma_0),$$

where

$$L(a, \beta, \Upsilon, \nu, \sigma) = \mathbb{E} \rho_1 \left(\frac{y - a - \langle X - \nu, \beta \rangle - \langle X - \nu, \Upsilon(X - \nu) \rangle}{\sigma} \right).$$

Moreover, under **C4**, we have that

$$L(\alpha_0, \beta_0, \Upsilon_0, \mu, \sigma) = L(\alpha_0, \beta_{0,q}, \Upsilon_{0,q}, \mu, \sigma) = L(\alpha_0, \beta_{0,q}, \Upsilon_{0,q}, \mu_q, \sigma) = \mathbb{E} \rho_1 \left(\frac{y - \mathbf{b}^T \mathbf{x}_q - \mathbf{u}^T \mathbf{z}_q}{\sigma} \right),$$

where μ_q is defined in (11), $\mathbf{x}_q = (x_1, \dots, x_q)^T = (\langle X - \mu, \phi_1 \rangle, \dots, \langle X - \mu, \phi_q \rangle)^T = (\langle X - \mu_q, \phi_1 \rangle, \dots, \langle X - \mu_q, \phi_q \rangle)^T$ and $\mathbf{z}_q = \operatorname{vech}(\{x_j x_\ell\})_{1 \leq j \leq \ell \leq q}$.

Note that, for any $\beta = \sum_{j=1}^q b_j \phi_j \in \mathcal{H}_q$ and $\Upsilon = \sum_{1 \leq j, \ell \leq q} v_{j\ell} \phi_j \otimes \phi_\ell \in \mathcal{F}_q$, we have that $\langle X - \mu, \beta \rangle + \langle X - \mu, \Upsilon(X - \mu) \rangle = \boldsymbol{\xi}^T \mathbf{b} + \boldsymbol{\xi}^T \mathbf{V} \boldsymbol{\xi}$, where $\boldsymbol{\xi} = (\xi_1, \dots, \xi_q)^T$, $\mathbf{V} \in \mathbb{R}^{q \times q}$ is the symmetric

matrix with (j, ℓ) -element $v_{j\ell}$ and $\mathbf{b} = (b_1, \dots, b_q)^\top$. Hence, assumption **C5** holds if $\Lambda_q^{-1/2} \boldsymbol{\xi}$ is absolutely continuous. If in addition $\Lambda_q^{-1/2} \boldsymbol{\xi}$ is an spherically distributed random vector, we obtain assumption (C2) in Kalogridis and Van Aelst (2019). Furthermore, **C5** is valid not only under **C4**, but also when X is elliptically distributed, i.e., $X \sim \mathcal{E}(\mu, \Gamma, \phi)$, as defined in Bali and Boente (2009) and Γ does not have finite rank.

Remark 3.2. A more restrictive assumption than **C5**, is to require that $\mathbb{P}(\langle X - \mu, \beta \rangle + \langle X - \mu, \Upsilon(X - \mu) \rangle = a) < 1$, for any $(a, \beta, \Upsilon) \in \mathbb{R} \times L^2(0, 1) \times \mathcal{F}$. In such case, the kernel of the covariance operator Γ , denoted $\ker(\Gamma)$, reduces to $\{0\}$. However, our set of possible candidates is a finite-dimensional space and for that reason, **C4** and **C5** are required. In particular, note that when **C4** holds, $\ker(\Gamma)$ is the infinite-dimensional linear space orthogonal to the linear space spanned by ϕ_1, \dots, ϕ_q . In this case, as mentioned in Cardot et al. (2003) for the functional linear regression model, the parameters α_0 , β_0 and Υ_0 are not uniquely defined. Effectively, for any $\gamma \in \ker(\Gamma)$, $\mathbb{P}(\langle X - \mu, \gamma \rangle = 0) = 1$, so that $\mathbb{P}(\langle X - \mu, \beta_0 \rangle = \langle X - \mu, \beta_0 + \gamma \rangle) = 1$ and the model may be reparametrized using $\beta_0 + \gamma$. Similarly, the linear operator $\Upsilon_0 + \gamma \otimes \gamma$ also provides a valid parametrization for the quadratic parameter in model (2), meaning that the parameters in (2) (or (1)) are not identifiable. Hence, under assumption **C4**, the linear and quadratic parameters should be defined via equivalence class identifying all the parameters (β_0, Υ_0) whose projection over $\mathcal{H}_q \times \mathcal{F}_q$ is the same. Taking into account that model (2) remains unchanged if we replace β_0 and Υ_0 by $\beta_{0,q}$ and $\Upsilon_{0,q}$, respectively, it is sensible to define $\beta_{0,q}$ and $\Upsilon_{0,q}$ as in (11), that is, as the projection of β_0 and Υ_0 over \mathcal{H}_q and \mathcal{F}_q , respectively. Recall that \mathcal{H}_q is the range of the covariance operator of X . Thus, our target will be to estimate $\beta_{0,q}$ and $\Upsilon_{0,q}$ and Fisher-consistency in this case means that the projections of $\beta(P)$ and $\Upsilon(P)$ over \mathcal{H}_q and \mathcal{F}_q , are indeed $\beta_{0,q}$ and $\Upsilon_{0,q}$.

It is worth mentioning that similar arguments to those considered in Lemma S.1.1 in Boente et al. (2020) allow to show that, if **C2** holds and ρ_1 satisfies **C1**, then for any $a \in \mathbb{R}$, $\beta \in L^2(0, 1)$ and any operator $\Upsilon \in \mathcal{F}$, we have that $L(\alpha, \beta, \Upsilon, \mu, \sigma) \geq L(\alpha_0, \beta_0, \Upsilon_0, \mu, \sigma)$, for any $\sigma > 0$. Furthermore, if $\mathbb{P}(\langle X - \mu, \beta \rangle + \langle X - \mu, \Upsilon(X - \mu) \rangle = a) < 1$, for any $(a, \beta, \Upsilon) \in \mathbb{R} \times L^2(0, 1) \times \mathcal{F}$, $(\alpha_0, \beta_0, \Upsilon_0)$ is the unique minimizer of $L(\alpha, \beta, \Upsilon, \mu, \sigma)$. However, the set of possible candidates for our functionals is not the space $\mathbb{R} \times L^2(0, 1) \times \mathcal{F}$ but the reduced space $\mathcal{C}_p = \mathbb{R} \times \mathcal{H}_p \times \mathcal{F}_p$, for that reason **C4** and **C5** are required and the following Lemma whose proof is relegated to the Appendix shows that the functionals $\alpha(P)$, $\beta(P)$ and $\Upsilon(P)$ are indeed Fisher-consistent.

Proposition 3.1. Assume that **C2**, **C3**, **C4** and **C5** hold. Let ρ_1 be a function satisfying **C1**. Given $p \geq q$ and any $\sigma > 0$, let $(\alpha(P), \beta(P), \Upsilon(P))$ be defined through (13) and (12). Then, we have that, $\alpha(P) = \alpha_0$, $\pi(\beta(P), \mathcal{H}_q) = \beta_{0,q}$ and $\pi(\Upsilon(P), \mathcal{F}_q) = \Upsilon_{0,q}$, where we have denoted as $\pi(u, \mathcal{L})$ the orthogonal projection of u over the finite-dimensional space \mathcal{L} . In particular, when $p = q$, $L(\alpha, \beta, \Upsilon, \sigma)$ is uniquely minimized over the set \mathcal{C}_q .

3.2 Fisher-consistency for infinite-dimensional processes

In order to consider the situation of purely infinite-dimensional processes, that is, when Γ does not have finite rank, we will strengthen the dependence of the functionals $(\alpha(P), \beta(P), \Upsilon(P))$ defined through (12) and (13) on the dimension p by denoting them as $(\alpha_p(P), \beta_p(P), \Upsilon_p(P))$. The following result shows that the lowest value of $L(\alpha, \beta, \Upsilon, \mu, \sigma_0)$ over \mathcal{C}_p converges to $L(\alpha_0, \beta_0, \Upsilon_0, \mu, \sigma_0)$ which is the smallest possible value. This is the infinite-dimensional counterpart of the classical result for robust linear regression.

Proposition 3.2. Let ρ_1 be a function satisfying **C1** and let $(\alpha_p(P), \beta_p(P), \Upsilon_p(P))$ be defined through (12) and (13). Assume that **C2** and **C3** hold. Then, we have that,

$$\lim_{p \rightarrow \infty} L(\alpha_p(P), \beta_p(P), \Upsilon_p(P), \mu, \sigma_0) = \lim_{p \rightarrow \infty} \underset{a \in \mathbb{R}, \beta \in \mathcal{H}_p, \Upsilon \in \mathcal{F}_p}{\operatorname{argmin}} L(\alpha, \beta, \Upsilon, \mu, \sigma_0) = L(\alpha_0, \beta_0, \Upsilon_0, \mu, \sigma_0).$$

In order to show that, when X does not have a finite-dimensional expansion as in **C4**, the functional $(\alpha_p(P), \beta_p(P), \Upsilon_p(P))$ is still Fisher-consistent in the sense that it converges to the true parameters, we will need some additional assumptions.

C6 : The eigenfunctions of the covariance operator Γ are differentiable and such that $\phi'_j \in L^2(0, 1)$, for all $j \geq 1$.

C7 : $\mathbb{P}(\langle X - \mu, \beta \rangle + \langle X - \mu, \Upsilon(X - \mu) \rangle = a) < c < 1$, for any $a \in \mathbb{R}$, $\beta \in L^2(0, 1)$ and any operator $\Upsilon \in \mathcal{F}$ such that $(a, \beta, \Upsilon) \neq 0$.

From now on, $\mathcal{W}^{1,2} = \mathcal{W}^{1,2}(0, 1)$ stands for the Sobolev space

$$\mathcal{W}^{1,2}(0, 1) = \{f \in L^2(0, 1) : \text{the weak derivative of } f \text{ exists and } \int_0^1 \{f'(t)\}^2 dt < \infty\},$$

with norm given by $\|f\|_{\mathcal{W}^{1,2}}^2 = \|f\|_{L^2(0,1)}^2 + \|f'\|_{L^2(0,1)}^2$. Besides, we will also denote as $\mathcal{W}_2^{1,2}$ the Sobolev space of two-dimensional functions in $\mathcal{T} = (0, 1) \times (0, 1)$, that is,

$$\mathcal{W}_2^{1,2} = \{f \in L^2(\mathcal{T}) : \text{the weak derivatives of } f \text{ exist for any } \nu = (\nu_1, \nu_2) \text{ such that } |\nu| \leq 1, \text{ and } D^{(\nu)} f \in L^2(\mathcal{T})\},$$

where $D^{(\nu)} f$ stands for the partial derivative $D^{(\nu)} f = \partial^{|\nu|} f / \partial t^{\nu_1} \partial s^{\nu_2}$. We consider the norm in $\mathcal{W}_2^{1,2}$ given by $\|f\|_{\mathcal{W}_2^{1,2}}^2 = \sum_{|\nu| \leq 1} \|D^{(\nu)} f\|_{L^2(\mathcal{T})}^2$.

Assumption **C6** means that $\phi_j \in \mathcal{W}^{1,2}$, while Assumption **C7** is the functional version of assumption (A.3) in Yohai (1987) adapted to functional quadratic models. We have the following result that states Fisher-consistency in the sense that the considered functional provides a finite-dimensional approximation to the true parameters when the process is infinite-dimensional.

Proposition 3.3. Assume that $\mathbb{E}\|X\|^2 < \infty$ and that **C2**, **C3** and **C6** hold. Let ρ_1 be a function satisfying **C1** and assume that **C7** holds with $c < 1 - b_{\rho_1}$, where $b_{\rho_1} = L(\alpha_0, \beta_0, \Upsilon_0, \mu, \sigma_0)$. Then, if $(\alpha_p(P), \beta_p(P), \Upsilon_p(P))$ are defined through (12) and (13), we have that,

$$\lim_{p \rightarrow \infty} |\alpha_p(P) - \alpha_0| + \|\beta_p(P) - \beta_0\|_{L^2(0,1)} + \|\Upsilon_p(P) - \Upsilon_0\|_{\mathcal{F}} = 0.$$

It is worth mentioning that if we denote as $v_p(P)$ and v_0 the kernels related to the operators $\Upsilon_p(P)$ and Υ_0 , that is,

$$(v_p(P))(t, s) = \sum_{1 \leq j, \ell \leq p} v_{j\ell}(P) \phi_{R,j}(P_X)(t) \phi_{R,\ell}(P_X)(s) \quad v_0(t, s) = \sum_{j=1}^{\infty} \sum_{\ell=1}^{\infty} v_{0,j\ell} \phi_j(t) \phi_{\ell}(s),$$

where $v_{0,j\ell} = \langle \phi_j, \Upsilon_0 \phi_{\ell} \rangle$ and $v_{j\ell}(P)$ are given in (12), then using the Fisher-consistency of the principal direction functionals we get that $\|\Upsilon_p(P) - \Upsilon_0\|_{\mathcal{F}} = \|v_p(P) - v_0\|_{L^2((0,1) \times (0,1))}$. Moreover, under **C3** and **C6**, $\beta_p(P) \in \mathcal{W}^{1,2}$, while $v_p(P) \in \mathcal{W}_2^{1,2}$.

4 Simulation study

In this section, we report the results of a Monte Carlo study designed to investigate the finite-sample properties of the robust estimators proposed for the functional quadratic regression model:

$$y_i = \alpha_0 + \langle \beta_0, X_i \rangle + \langle X_i, \Upsilon_0 X_i \rangle + \sigma_0 \epsilon_i, \quad i = 1, \dots, n. \quad (14)$$

We considered several choices for the parameters, including the case where $\Upsilon_0 = 0$, that is, where the true model is a linear one. The first setting mimics the one considered in Boente et al. (2020) for the covariate distribution and some of the contamination schemes. The second one corresponds to the functional quadratic model studied in Yao and Müller (2010). In both cases, we selected $\alpha_0 = 0$ and $\mathcal{I} = [0, 1]$ and for each setting we generated $n_R = 1000$ samples of size $n = 300$.

We compared two estimators: the classical procedure based on least squares (LS), and the MM -estimators (MM) from Section 2. The MM -estimators were computed using a bounded ρ -function ρ_0 to obtain the residual scale estimator in (4) and also a bounded ρ_1 for the M -step (6). For $j = 0, 1$, we choose $\rho_j = \rho_{T, c_j}$, the bisquare function, with tuning constants $c_0 = 1.54764$ ($b = 1/2$) and $c_1 = 3.444$. All calculations were performed in R.

To compute the estimators of the principal directions we use the eigenfunctions of the sample covariance when considering the classical procedure and the spherical principal directions for the robust one, since the former are very sensitive to atypical curves. Denote λ_k^S the eigenvalues of Γ^S . When second moment exists, the values λ_k^S are shrunk with respect to those of the scatter operator as follows $\lambda_k^S = \lambda_k \mathbb{E} \left(\xi_k^2 / \sum_{j \geq 1} \lambda_j \xi_j^2 \right)$. To avoid situations in which the eigenvalues related to the sign operator are too close and will not allow to identify easily the order of the estimated eigenfunctions, it is better to order the eigenfunctions $\hat{\phi}_j$ according to the values of a robust scale of the projected data, $\langle X_i - \hat{\mu}, \hat{\phi}_j \rangle$, $1 \leq i \leq n$, which are resistant estimators $\hat{\lambda}_j$ of the j -th eigenvalue of Γ .

Both for the classical and robust method, we select the dimension p used in the regularization as the smallest number explaining at least 90% of total variation obtained. In the classical case, the total variation is obtained using the eigenvalues of the sample covariance, while when considering the robust procedure, the eigenvalue estimators $\{\hat{\lambda}_j\}$ defined above as a robust scale of the projected data, are taken. We use as robust scale the M -scale computed with the bisquare function.

To evaluate the performance of each estimator, we looked at their integrated squared bias and mean integrated squared error. These were computed on a grid of $M = 100$ equally spaced points on $[0, 1]$ and $[0, 1] \times [0, 1]$, for $\hat{\beta}$ and \hat{v} , respectively. More specifically, if $\hat{\beta}_j$ is the estimate of the function β obtained with the j -th sample ($1 \leq j \leq n_R$) and \hat{v}_j is the estimate of v , we compute approximations for the integrated square bias as

$$\begin{aligned} \text{Bias}^2(\hat{\beta}) &= \frac{1}{M} \sum_{s=1}^M \left(\frac{1}{n_R} \sum_{j=1}^{n_R} \hat{\beta}_j(t_s) - \beta_0(t_s) \right)^2, \\ \text{Bias}^2(\hat{v}) &= \frac{1}{M^2} \sum_{s=1}^M \sum_{\ell=1}^M \left(\frac{1}{n_R} \sum_{j=1}^{n_R} \hat{v}_j(t_s, t_\ell) - v_0(t_s, t_\ell) \right)^2, \end{aligned}$$

and of the integrated squared errors as

$$\begin{aligned} \text{MISE}(\hat{\beta}) &= \frac{1}{M} \sum_{s=1}^M \frac{1}{n_R} \sum_{j=1}^{n_R} \left(\hat{\beta}_j(t_s) - \beta_0(t_s) \right)^2, \\ \text{MISE}(\hat{v}) &= \frac{1}{M^2} \sum_{s=1}^M \sum_{\ell=1}^M \frac{1}{n_R} \sum_{j=1}^{n_R} (\hat{v}_j(t_s, t_\ell) - v_0(t_s, t_\ell))^2, \end{aligned}$$

where $t_1 \leq \dots \leq t_M$ are equispaced points on $\mathcal{I} = [0, 1]$. Note that when $v_0 = 0$, $\text{Bias}^2(\hat{v})$ measures the squared bias of the estimated coefficients, while for the other quadratic kernels it also gives a measure of how biased are the principal direction estimators. This difference is also inherited by the mean integrated squared error. As mentioned in He and Shi (1998) who studied estimators under a nonparametric regression model and in Boente et al. (2020) who considered estimators of the slope and of the nonparametric component under a functional partial linear model, the squared Bias and the MISE may be heavily influenced by numerical errors at or near the boundaries of the grid. For that reason, we also consider trimmed versions of the above computed without the q first and last points on the grid, that is,

$$\begin{aligned} \text{Bias}_{\text{TR}}^2(\hat{\beta}) &= \frac{1}{M-2q} \sum_{s=q+1}^{M-q} \left(\frac{1}{n_R} \sum_{j=1}^{n_R} \hat{\beta}_j(t_s) - \beta_0(t_s) \right)^2, \\ \text{Bias}_{\text{TR}}^2(\hat{v}) &= \frac{1}{(M-2q)^2} \sum_{s=q+1}^{M-q} \sum_{\ell=q+1}^{M-q} \left(\frac{1}{n_R} \sum_{j=1}^{n_R} \hat{v}_j(t_s, t_\ell) - v_0(t_s, t_\ell) \right)^2, \\ \text{MISE}_{\text{TR}}(\hat{\beta}) &= \frac{1}{M-2q} \sum_{s=q+1}^{M-q} \frac{1}{n_R} \sum_{j=1}^{n_R} \left(\hat{\beta}_j(t_s) - \beta_0(t_s) \right)^2, \\ \text{MISE}_{\text{TR}}^2(\hat{v}) &= \frac{1}{(M-2q)^2} \sum_{s=q+1}^{M-q} \sum_{\ell=q+1}^{M-q} \frac{1}{n_R} \sum_{j=1}^{n_R} (\hat{v}_j(t_s, t_\ell) - v_0(t_s, t_\ell))^2. \end{aligned}$$

We chose $q = [M \times 0.05]$ which uses the central 90% interior points in the grid, which for both models was an equally spaced grid of points in $[0, 1]$ with size $M = 100$.

4.1 Model 1

In this section, we considered the functional quadratic regression model (14), where $\sigma_0 = 1$ and the regression parameter equals the one used in Boente et al. (2020), that is, $\beta_0(t) = \sum_{j=1}^{50} b_{j,0} \phi_j(t)$ with the basis $\phi_1(t) \equiv 1$, $\phi_j(t) = \sqrt{2} \cos((j-1)\pi t)$, $j \geq 2$, and $\mathbf{b}_0 = (b_{1,0}, \dots, b_{50,0})^T$ where $b_{1,0} = 0.3$ and $b_{j,0} = 4(-1)^{j+1} j^{-2}$, $j \geq 2$. We label this model as **Model 1**. Besides, we considered three possible choices for the quadratic operator, that will be labelled **Model**_{1,0} to **Model**_{1,2} and correspond to:

- **Model**_{1,0}: $\Upsilon_{0,0} = 0$ which means that the true model is a linear one.
- **Model**_{1,1}: $\Upsilon_{0,1} = \sum_{j=1}^{50} \sum_{\ell=1}^{50} c_{j\ell,1} \phi_j \otimes \phi_\ell$ with $\mathbf{C}_1 = (c_{j\ell,1})_{1 \leq j, \ell \leq 50} = 5\mathbf{b}_1 \mathbf{b}_1^T$ and $\mathbf{b}_1 = \mathbf{b}_0$ with \mathbf{b}_0 defined above.

- **Model_{1,2}:** $\Upsilon_{0,2} = \sum_{j=1}^5 \sum_{\ell=1}^5 c_{j\ell,2} \phi_{2(j-1)+1} \otimes \phi_{2(\ell-1)+1}$ with $\mathbf{C}_2 = (c_{j\ell,2})_{1 \leq j, \ell \leq 5} = 5\mathbf{b}_2 \mathbf{b}_2^T$, where $\mathbf{b}_2 = (b_{1,2}, \dots, b_{5,2})^T$, $b_{1,2} = b_{2,2} = 0.3$, $b_{j,2} = 3(-1)^{j+1}j^{-2}$, for $j = 3, 4, 5$.

Figure 1 shows the function β_0 and the surface $v_{0,j}(s, t)$, $j = 1, 2$, associated to each choice of a non-null operator Υ_0 .

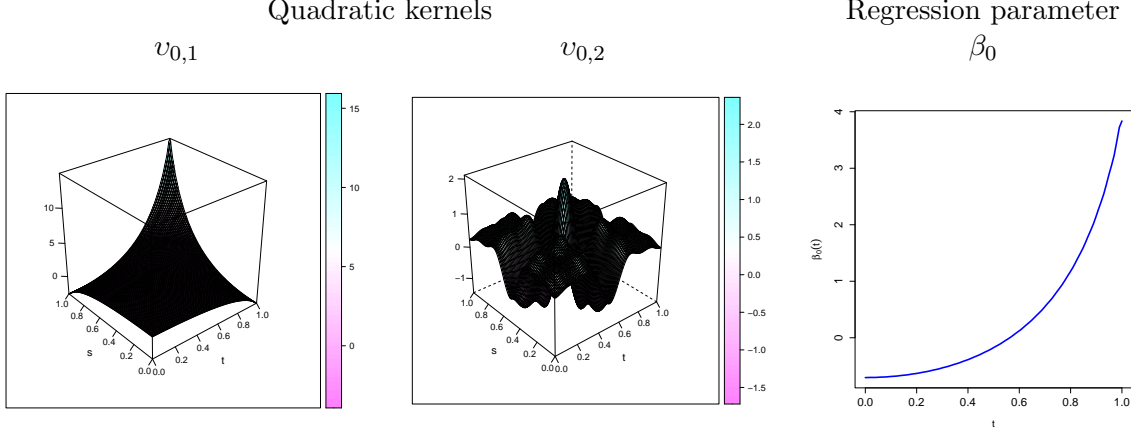


Figure 1: True parameters.

The process that generates the functional covariates $X_i(t)$ was Gaussian with mean 0 and covariance operator with eigenfunctions $\phi_j(t)$. For uncontaminated samples that will be denoted C_0 , the scores ξ_{ij} were independent Gaussian random variables $\xi_{ij} \sim N(0, j^{-2})$, and the errors $\epsilon_i \sim N(0, 1)$, independent of X_i . Taking into account that $\text{VAR}(\xi_{ij}) \leq 1/2500$ when $j > 50$, the process was approximated numerically using the first 50 terms of its Karhunen–Loève representation.

Table 1 reports the squared bias and MISE and their trimmed counterparts for samples without outliers.

$\Upsilon_{0,0}$				$\Upsilon_{0,1}$				$\Upsilon_{0,2}$				
$\hat{\beta}$	\hat{v}											
Bias ²	MISE											
LS	0.2958	2.7659	0.0270	58.0046	0.2966	2.7919	23.5860	86.4361	0.2958	2.7636	1.2817	59.5208
MM	0.2983	3.4331	0.0488	80.3626	0.3006	3.4731	22.7776	109.9980	0.2973	3.4421	1.2584	82.2667
Bias _{TR} ²	MISE _{TR}											
LS	0.0656	2.3135	0.0214	48.8398	0.0665	2.3384	3.4632	55.7912	0.0654	2.3099	1.4807	50.5278
MM	0.0624	2.9323	0.0370	68.3566	0.0622	2.9664	3.1481	76.5740	0.0625	2.9411	1.4579	70.3716

Table 1: Integrated squared bias and mean integrated squared errors and their trimmed versions (multiplied by 10) over $n_R = 1000$ clean samples under **Model 1**.

We note that the boundary effect is more pronounced for the estimators of Υ_0 , but it is present for $\hat{\beta}$ as well. In particular, due to the shape near $(1,1)$ of $v_{0,1}$ the squared bias is seven times larger than the trimmed one.

Based on this observation, in what follows, we report the trimmed measures in all Tables and Figures.

We considered three contamination scenarios. The first one contains outliers in the response variables and is expected to affect mainly the estimation of β_0 and α_0 . The other ones include high-leverage outliers in the functional explanatory variables, which typically affect the estimation of the linear regression parameter or the quadratic operator. Specifically, we constructed our samples as follows:

- Scenario $C_{1,\mu}$: here only the regression errors are contaminated in order to produce “vertical outliers”. Their distribution G is given by $G(u) = 0.9 \Phi(u) + 0.1 \Phi((u - \mu)/0.5)$, with Φ the standard normal distribution function.
- Scenario $C_{2,\mu}$: in these settings, we introduce high-leverage outliers by contaminating the functional covariates X_i and the errors simultaneously. Outliers in the X_i ’s are generated by perturbing the distribution of the second score in the Karhunen–Loève representation of the process. We denote with the superscript (co) the contaminated observations. Specifically, we sample $v_i \sim Bi(1, 0.10)$ and then:

- if $v_i = 0$, let $\epsilon_i^{(co)} = \epsilon_i$ and $X_i^{(co)} = X_i$;
- if $v_i = 1$, let $\epsilon_i^{(co)} \sim N(\mu, 0.25)$ and $X_i^{(co)} = \sum_{j=1}^{50} \xi_{ij}^{(co)} \phi_j$, with $\xi_{ij}^{(co)} \sim N(0, j^{-2})$ for $j \neq 2$ and $\xi_{i2}^{(co)} \sim N(\mu/2, 0.25)$.

The responses are generated as $y_i^{(co)} = \langle \beta_0, X_i^{(co)} \rangle + \langle X_i^{(co)}, \Upsilon_0 X_i^{(co)} \rangle + \epsilon_i^{(co)}$.

- Scenario $C_{3,\mu,\delta}$: high-leverage outliers are introduced contaminating the functional covariates X_i and modifying the responses as in Maronna and Yohai (2013). More precisely, outliers in the covariates are generated by adding a constant to the coefficient process, that is, we sample $v_i \sim Bi(1, 0.10)$ and then:

- if $v_i = 0$, let $y_i^{(co)} = y_i$ and $X_i^{(co)} = X_i$;
- if $v_i = 1$, let $X_i^{(co)} = \sum_{j=1}^{50} \xi_{ij}^{(co)} \phi_j$ where $\xi_{ij}^{(co)} \sim N(\mu, j^{-2})$, while $y_i^{(co)} = \delta y_i$.

Both $C_{1,\mu}$ and $C_{2,\mu}$ depend on the parameter $\mu \in \mathbb{R}$. In this experiment, we looked at values of μ varying between 8 and 20 with a step of 2. They produce a range of contamination scenarios ranging from mild to severe. Besides, in contamination $C_{3,\mu,\delta}$, we combine values of $\mu = 2, 4, 6, 8$ with $\delta = 0.2, 0.4, 0.6, 0.8$ to affect the quadratic component. When considering the contamination schemes, Table 2 reports the maximum value of the trimmed squared bias and MISE over the different values of μ and/or δ and we simply label the situation as C_j , for $j = 1, 2, 3$ to avoid burden notation.

As an illustration of the type of outliers generated, Figure 2 shows 25 randomly chosen functional covariates $X_i(t)$, for one sample generated under C_0 (with no outliers), one obtained under $C_{2,12}$ and the other one under $C_{3,4,0.4}$.

The plots in Figures 3 to Figures 5 summarize the effect of the contamination scenarios for the different choices of Υ_0 and different values of μ when considering $C_{1,\mu}$ and $C_{2,\mu}$. For $C_{3,\mu,\delta}$, we choose $\mu = 2$ and vary δ . Each plot corresponds to one contamination scenario and one parameter estimator. Within each panel, the solid and dashed lines correspond to the measures for the least squares and MM –estimators, respectively. There are two lines per estimation method: the one

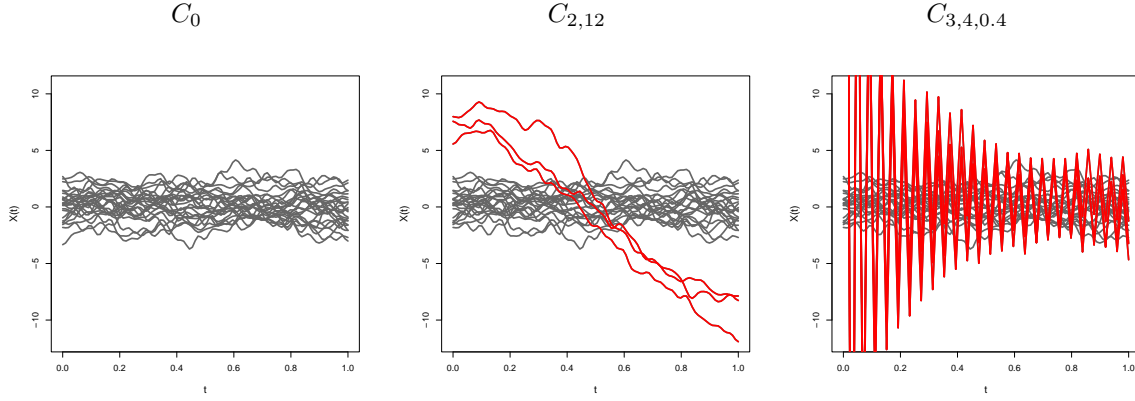


Figure 2: 25 trajectories $X_i(t)$ with and without contamination.

$\Upsilon_{0,0}$				$\Upsilon_{0,1}$				$\Upsilon_{0,2}$					
	$\hat{\beta}$	\mid	\hat{v}		$\hat{\beta}$	\mid	\hat{v}		$\hat{\beta}$	\mid	\hat{v}		
	Bias _{TR} ²	MISE _{TR}											
C_0	LS	0.0656	2.3135	0.0214	48.8398	0.0665	2.3384	3.4632	55.7912	0.0654	2.3099	1.4807	50.5278
	MM	0.0624	2.9323	0.0370	68.3566	0.0622	2.9664	3.1481	76.5740	0.0625	2.9411	1.4579	70.3716
C_1	LS	0.0788	82.5051	1.6237	1867.4839	0.0803	82.5097	5.7713	1874.4401	0.0788	82.5052	3.0274	1869.5741
	MM	0.0591	2.9711	0.0461	69.2086	0.0595	3.0037	3.1985	77.3132	0.0590	2.9749	1.4963	70.9218
C_2	LS	2.6091	2.8690	1.0453	3.0408	2.5548	6.2146	86.3542	87.2354	2.6110	2.8761	5.3909	6.8795
	MM	0.3125	3.0785	1.5264	54.2488	0.2624	3.0535	7.4495	64.6150	0.3111	3.0842	3.0050	56.5554
C_3	LS	9.3426	9.3797	0.0000	0.0000	9.3422	9.5766	218.1688	218.1692	9.3426	9.3879	5.2112	5.2112
	MM	0.0844	3.9225	0.0366	55.2039	0.0845	4.0217	5.5522	65.8103	0.0854	3.9209	1.5840	57.0941

Table 2: Trimmed versions of the integrated squared bias and mean integrated squared errors (multiplied by 10) for clean and contaminated samples, **Model 1**. The reported values under contamination correspond to the worst situation.

with triangles shows the trimmed MISE, and the one with solid circles indicates the corresponding trimmed bias squared. We also include the values under C_0 for comparison, it is indicated in the horizontal axis as C_0 .

As expected, when the data do not contain outliers, all estimators behave similarly to each other (see Table 1). When estimating the quadratic kernel v_0 , the less efficient robust MM -estimator naturally results in higher MISE's. However, this efficiency loss is smaller for the estimators of β_0 . Note that the size of the squared bias and trimmed one are larger when using the quadratic operator $\Upsilon_{0,1}$ due to its shape near $(1, 1)$.

The serious damage caused to the least squares estimators by outliers can be seen in Figures 3 to 5. The behaviour clearly depends on the quadratic operator selected. For instance, when considering the quadratic operator $\Upsilon_0 = \Upsilon_{0,1}$, the trimmed bias and MISE of the least squares estimators of β_0 and v_0 are consistently much higher than those of the robust MM -estimators. The only exception is $C_{2,\mu}$ with $\mu = 8$, which corresponds to a mild contamination and leads to larger values of the MISE for the robust proposal, even when these values are smaller than those obtained for clean samples. The same behaviour is observed when considering $\Upsilon_0 = 0$ or $\Upsilon_0 = \Upsilon_{0,2}$ for the estimators of β_0 , where smaller values of the MISE are obtained for the classical procedure

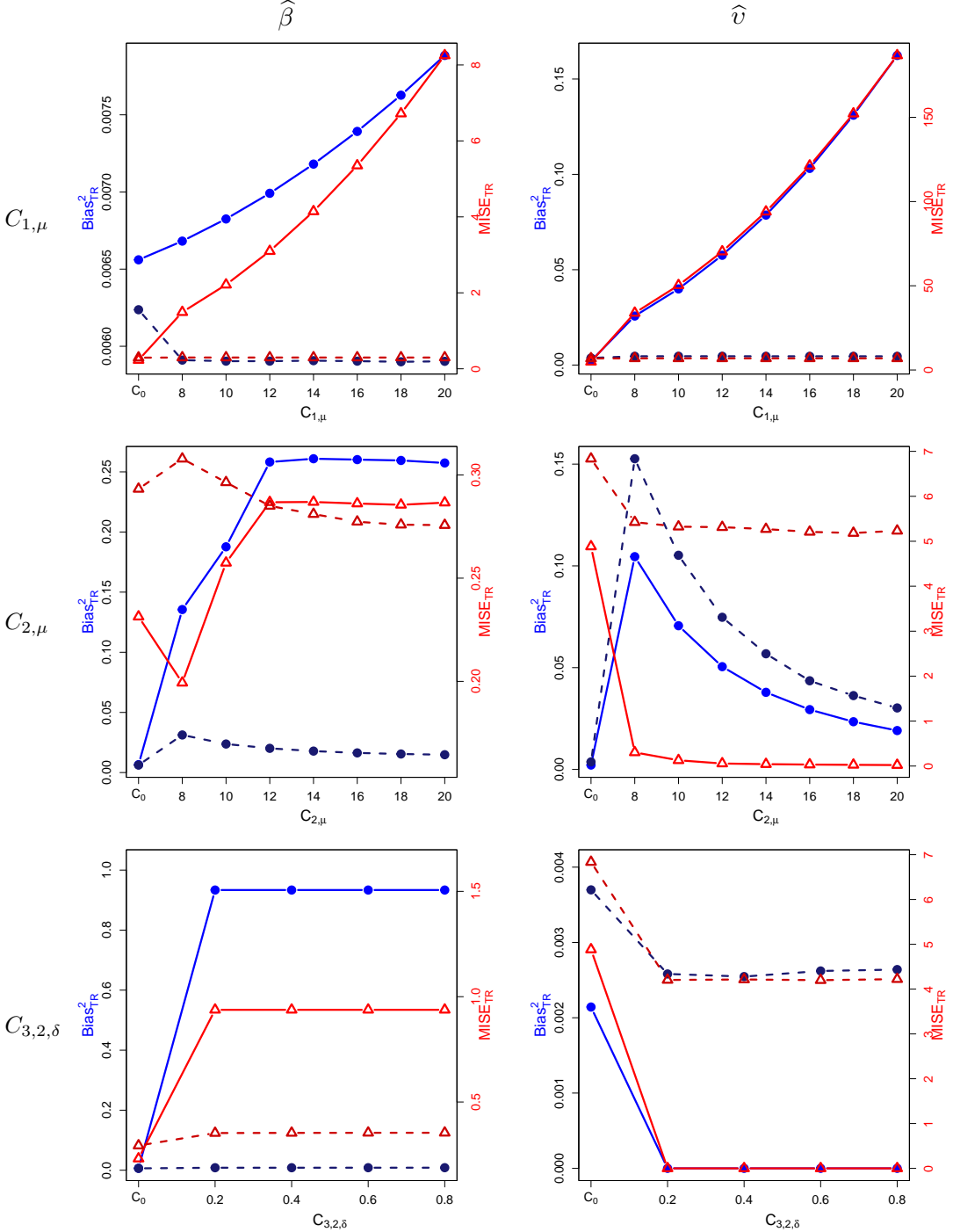


Figure 3: Plots of the trimmed squared bias and MISE of the estimators of β_0 and v_0 as a function of μ or δ for each contamination scenario, under **Model 1** with $\Upsilon_0 = 0$. The solid and dashed lines correspond to the least squares and MM -estimators, respectively. The squared bias is indicated with circles, and the MISE with triangles.

only under $C_{2,\mu}$ with $\mu = 8, 10$, even when its squared bias is consistently larger.

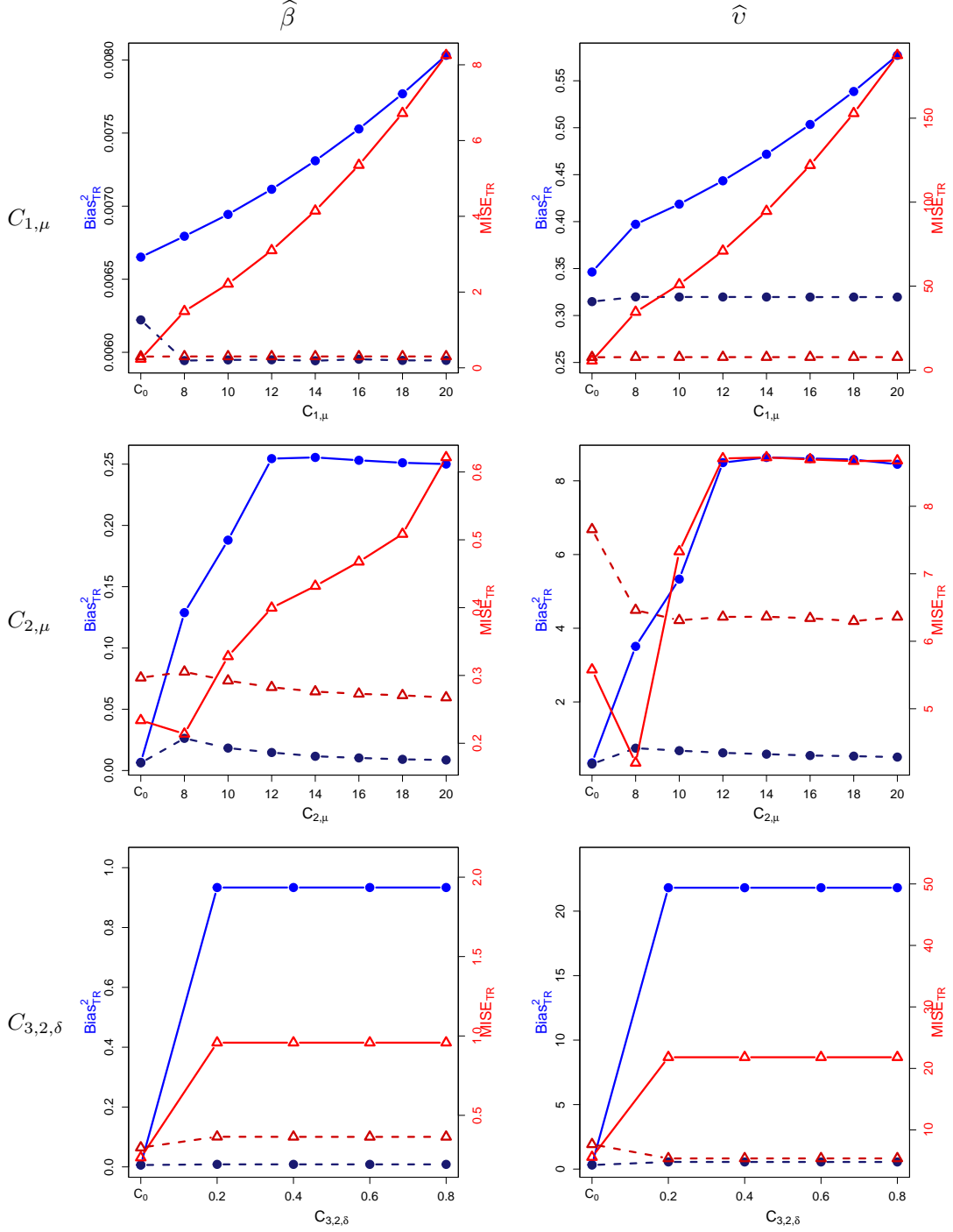


Figure 4: Plots of the trimmed squared bias and MISE of the estimators of β_0 and v_0 as a function of μ or δ for each contamination scenario, under **Model 1** with $\Upsilon_0 = \Upsilon_{0,1}$. The solid and dashed lines correspond to the least squares and MM -estimators, respectively. The squared bias is indicated with circles, and the MISE with triangles.

For the two quadratic kernels, different behaviours are obtained according to the contamination

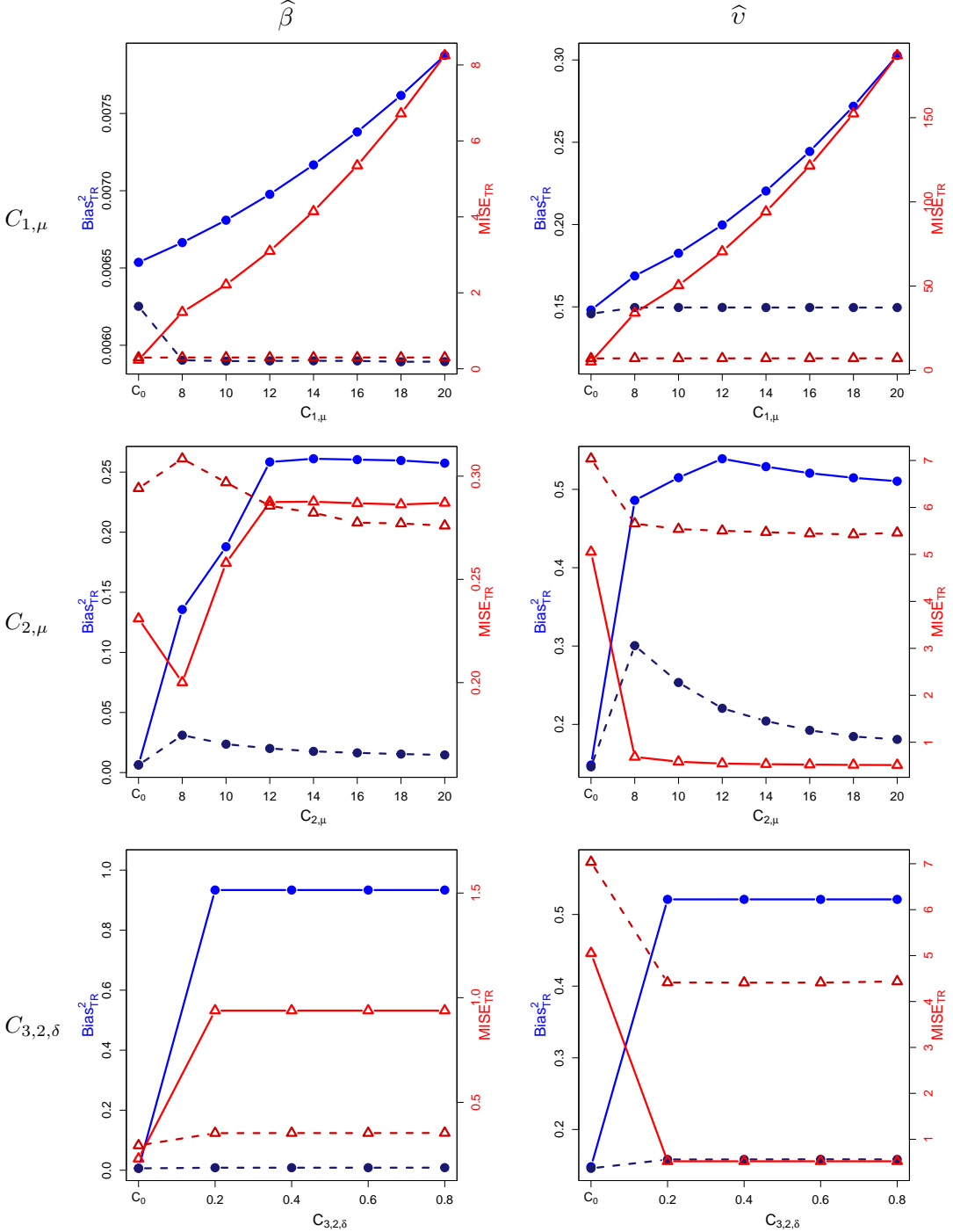


Figure 5: Plots of the trimmed squared bias and MISE of the estimators of β_0 and v_0 as a function of μ or δ for each contamination scenario, under **Model 1** with $\Upsilon_0 = \Upsilon_{0,2}$. The solid and dashed lines correspond to the least squares and MM -estimators, respectively. The squared bias is indicated with circles, and the MISE with triangles.

schemes. Contamination $C_{1,\mu}$ affects both the bias and MISE of the least squares procedure and

the MM –estimator outperforms the classical one. When using $\Upsilon_0 = \Upsilon_{0,2}$, both under $C_{2,\mu}$ and $C_{3,2,\delta}$ the bias of the classical procedure is enlarged, but it attains smaller values of the MISE than the robust method. Quite surprisingly, the obtained MISE are smaller than those obtained for clean samples. In contrast, when there is no quadratic term, i.e., $\Upsilon_0 = 0$ both the bias and the MISE of the robust procedure are larger than those obtained for the classical one, but under $C_{2,\mu}$ the contamination effect on the bias reduces as μ increases.

In order to also explore visually the performance of these estimators, Figures 6 to 8 contain functional boxplots, as defined in Sun and Genton (2011), for the $n_R = 1000$ realizations of the different estimators for β_0 under C_0 and some of the three contamination settings. As in standard boxplots, the magenta central box of these functional boxplots represents the 50% inner band of curves, the solid black line indicates the central (deepest) function and the dotted red lines indicate outlying curves (in this case: outlying estimates $\hat{\beta}_j$ for some $1 \leq j \leq n_R$). We also indicate the target (true) function β_0 with a dark green dashed line. To avoid boundary effects, we show here the different estimates $\hat{\beta}_j$ evaluated on the 90 interior points of the grid of equally spaced points. In addition, to facilitate comparisons between contamination cases and estimation methods, the scales of the vertical axes are the same for all panels within each Figure. The ways in which the different outliers affect the classical estimators for β_0 can be seen in these figures. Note that under $C_{1,12}$ the classical $\hat{\beta}$ becomes highly variable, but mostly retains the same shape of the true β_0 , which lies within the central box. However, with high-leverage outliers (as in $C_{2,12}$ and particularly under $C_{3,4,0.4}$) the estimator becomes completely uninformative and does not reflect the shape of the true regression coefficient β_0 , for all the quadratic models considered.

To have a deeper insight on the effect of contamination on the quadratic component estimators, Figures 9 to 11 contain surface boxplots as defined in Genton et al. (2014) for the $n_R = 1000$ realizations of the different estimators for v_0 under C_0 and some of the three contamination settings. For these plots the notion of volume depth is used to order the surfaces. The median surface is represented in dark violet, the central region containing the 50% deepest surfaces is represented in blue, while the surfaces in pink indicate the whiskers, beyond whose limits a surface is declared as outlier. The green surface represents the true function v_0 .

The effect on the quadratic operator least squares estimators is observed in Figures 9 to 11, where the enlargement of the central 50% region under $C_{1,12}$ and the damaging effect of contamination $C_{2,12}$ become evident. This effect is also observed under $C_{3,4,0.4}$ when considering quadratic terms in the model, that is, when choosing $\Upsilon_0 = \Upsilon_{0,1}$ or $\Upsilon_0 = \Upsilon_{0,2}$. In the first case, the true surface lies beneath the surface plot limits while in the former one it crosses the limiting surfaces.

In contrast, the MM –estimators display a remarkably stable behaviour across contamination settings. Their bias and MISE curves show that the MM –estimators for β_0 are highly robust against the considered contamination scenarios. If we look at the behaviour of these estimators in Figures 6 to 8 we note that the central box and the “whiskers” for the MM –estimators remain almost constant for all the contamination schemes in considered simulation scenarios ($\Upsilon_0 = 0$, $\Upsilon_0 = \Upsilon_{0,1}$ or $\Upsilon_0 = \Upsilon_{0,2}$), in sharp contrast to what happens to the classical method. Contamination $C_{3,4,0.4}$ affects the boxplot for values smaller than 2, where they mimic the distorting effect introduced in the model but even in this case, the band preserves the shape. The results in Figures 9 to 11 show that the MM –estimators for v_0 are almost unaffected by the different types of outliers, and the surface boxplots remain very similar to each other.

Regarding the estimation of α_0 , Table 3 reports as summary measures: the absolute value of the mean which is a measure of the bias since $\alpha_0 = 0$; and the standard deviation as variability

		$\Upsilon_{0,0}$		$\Upsilon_{0,1}$		$\Upsilon_{0,2}$	
		Mean	SD	Mean	SD	Mean	SD
C_0	LS	1.74	114.45	0.07	115.27	0.01	114.64
	MM	3.26	130.02	7.86	131.10	1.49	130.33
C_1	LS	2019.87	723.84	2021.67	723.88	2021.59	723.88
	MM	2.58	130.92	6.85	131.26	0.85	131.28
C_2	LS	45.15	98.32	129.87	233.93	33.42	98.47
	MM	90.01	128.36	95.61	129.93	87.82	129.45
C_3	LS	1.52	74.54	1825.23	172.97	208.23	78.36
	MM	2.68	132.44	9.82	132.77	0.68	132.51

Table 3: Summary measures (multiplied by 1000) for α_0 estimates over clean and contaminated samples, **Model 1**. The reported values under contamination correspond to the worst situation.

measure. For the contamination settings, the maximum over the different values of μ and/or δ are reported. In all cases, the reported values correspond to the summary measures multiplied by 1000. Figure 12 presents the boxplots of the estimators for α_0 for clean samples and for some contamination scenarios. The true value is plotted with a green dashed line, for reference. Each row corresponds to different Υ_0 scenarios, while each column to a contamination setting. The boxplots of the classical estimators are given in magenta, while those of the robust ones are presented in blue. The reported results show that scheme $C_{1,\mu}$ affects the classical estimator of the intercept for any choice of the quadratic operator with maximum biases increased more than 1000 times and standard deviations enlarged more than 7 times. In contrast, under $C_{3,4,0.4}$, the largest effect is observed when considering $\Upsilon_{0,1}$. For this choice of the quadratic kernel, the classical procedure is also affected under $C_{2,12}$. The robust procedure is stable over the contaminations considered, even though some effect in the bias is observed under C_2 (see Table 3) it is much smaller than that of its classical counterpart when the quadratic operator is $\Upsilon_{0,1}$.

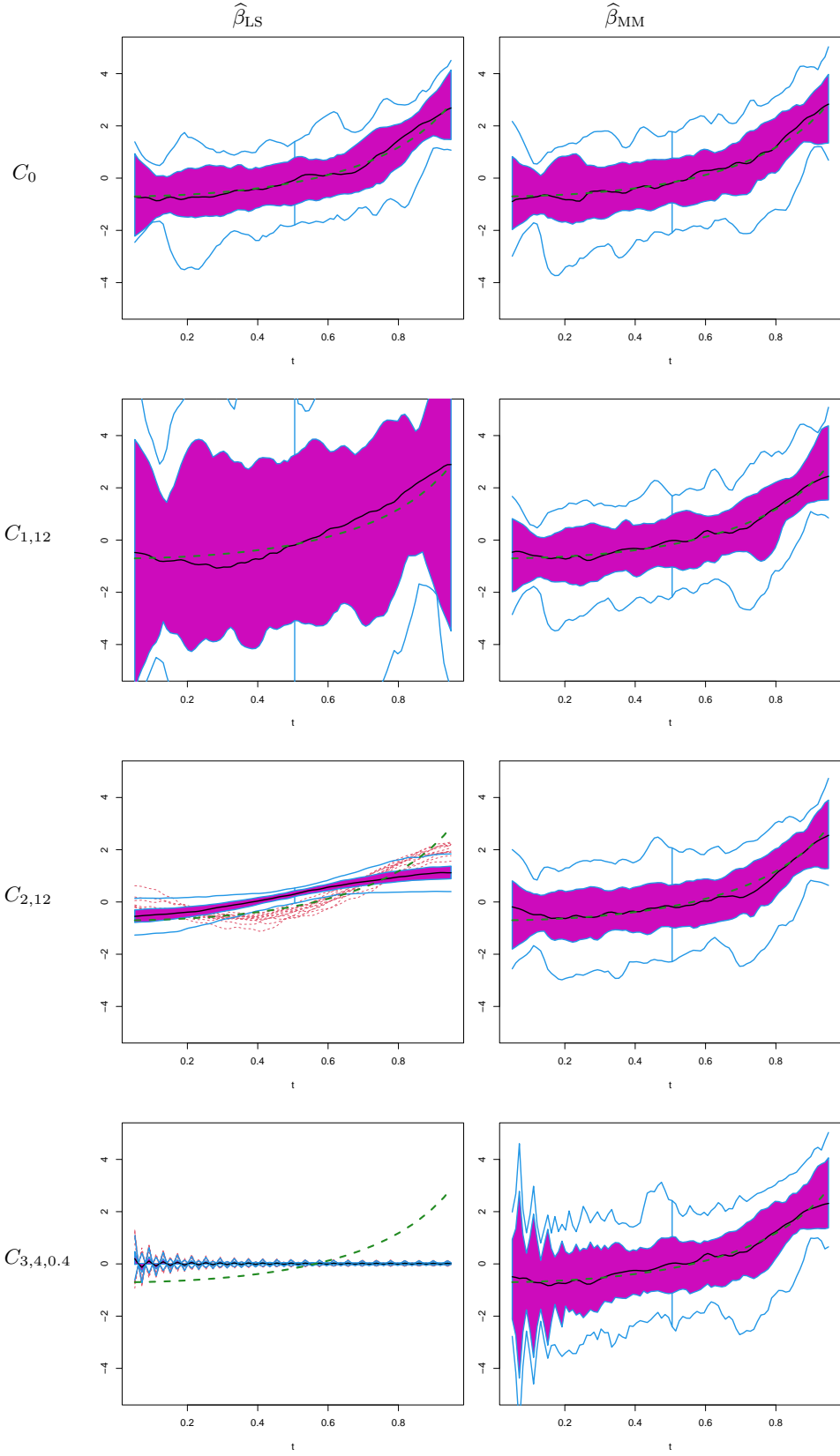


Figure 6: Functional boxplot of the estimators for β_0 under **Model 1** with $Y_0 = 0$. The true function is shown with a green dashed line, while the black solid one is the central curve of the $n_R = 1000$ estimates $\hat{\beta}$. Columns correspond to estimation methods, while rows to C_0 and to some of the three contamination settings.

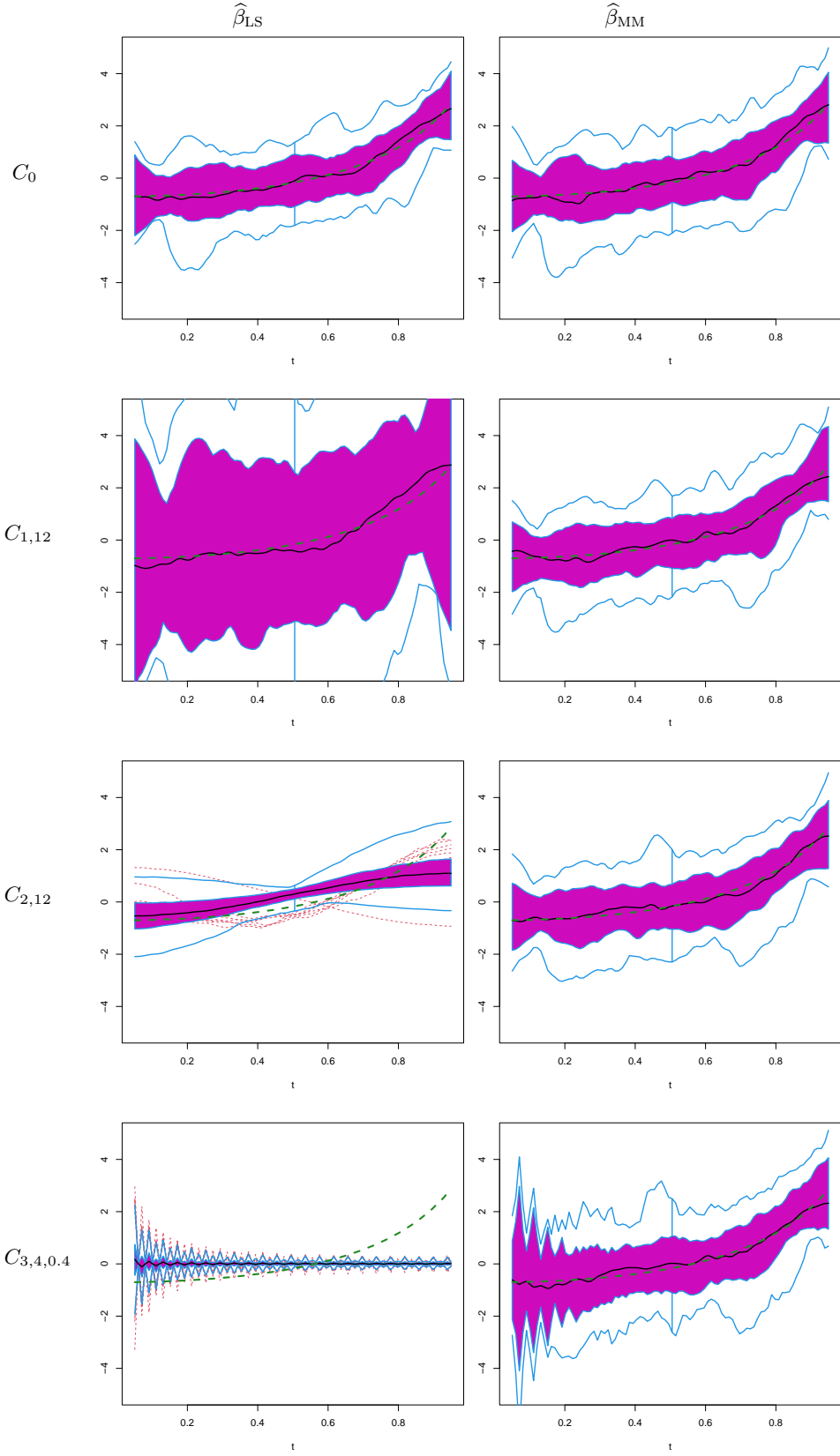


Figure 7: Functional boxplot of the estimators for β_0 under **Model 1** with $\Upsilon_0 = \Upsilon_{0,1}$. The true function is shown with a green dashed line, while the black solid one is the central curve of the $n_R = 1000$ estimates $\hat{\beta}$. Columns correspond to estimation methods, while rows to C_0 and to some of the three contamination settings.

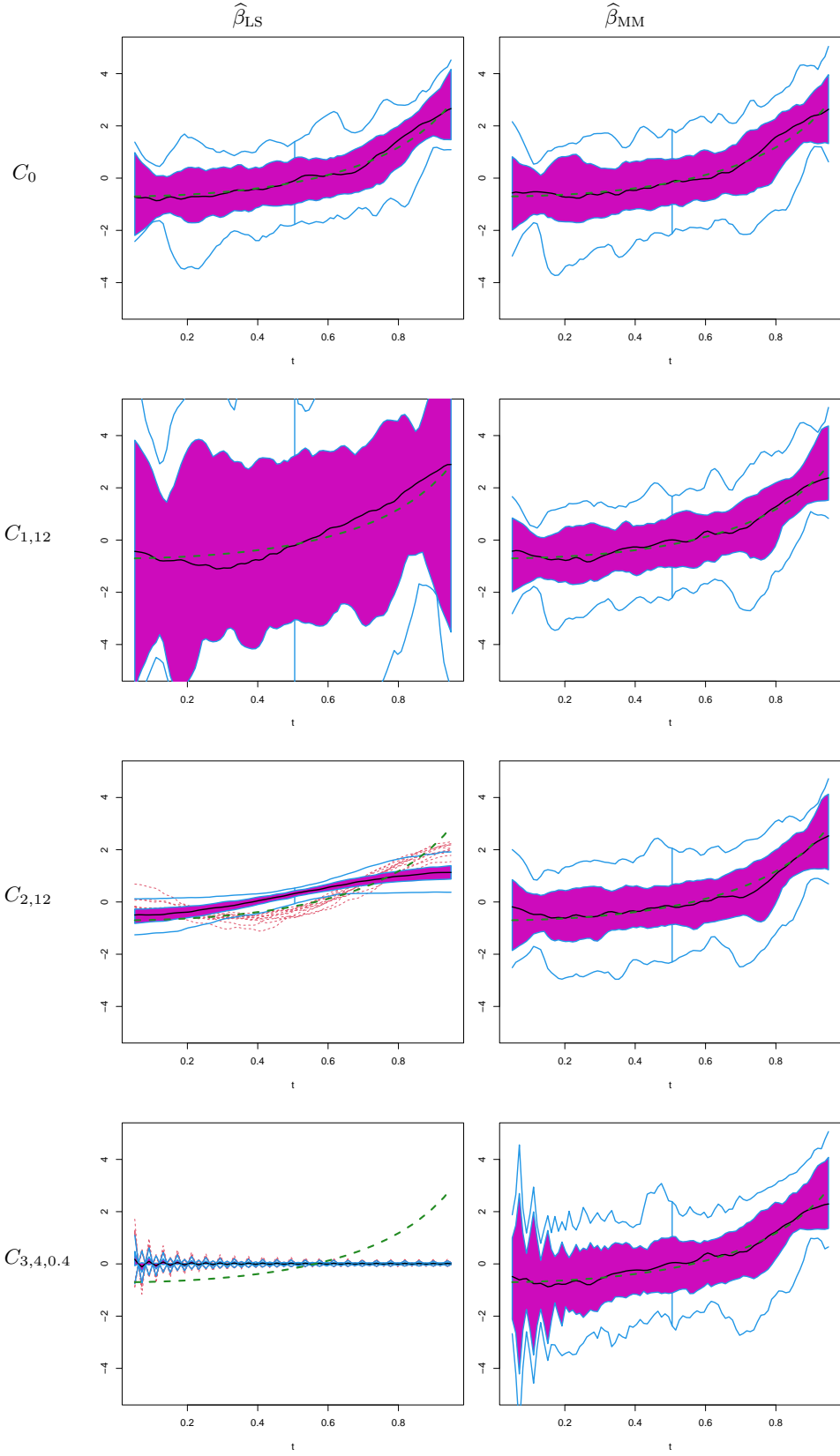


Figure 8: Functional boxplot of the estimators for β_0 under **Model 1** with $\Upsilon_0 = \Upsilon_{0,2}$. The true function is shown with a green dashed line, while the black solid one is the central curve of the $n_R = 1000$ estimates $\hat{\beta}$. Columns correspond to estimation methods, while rows to C_0 and to some of the three contamination settings.

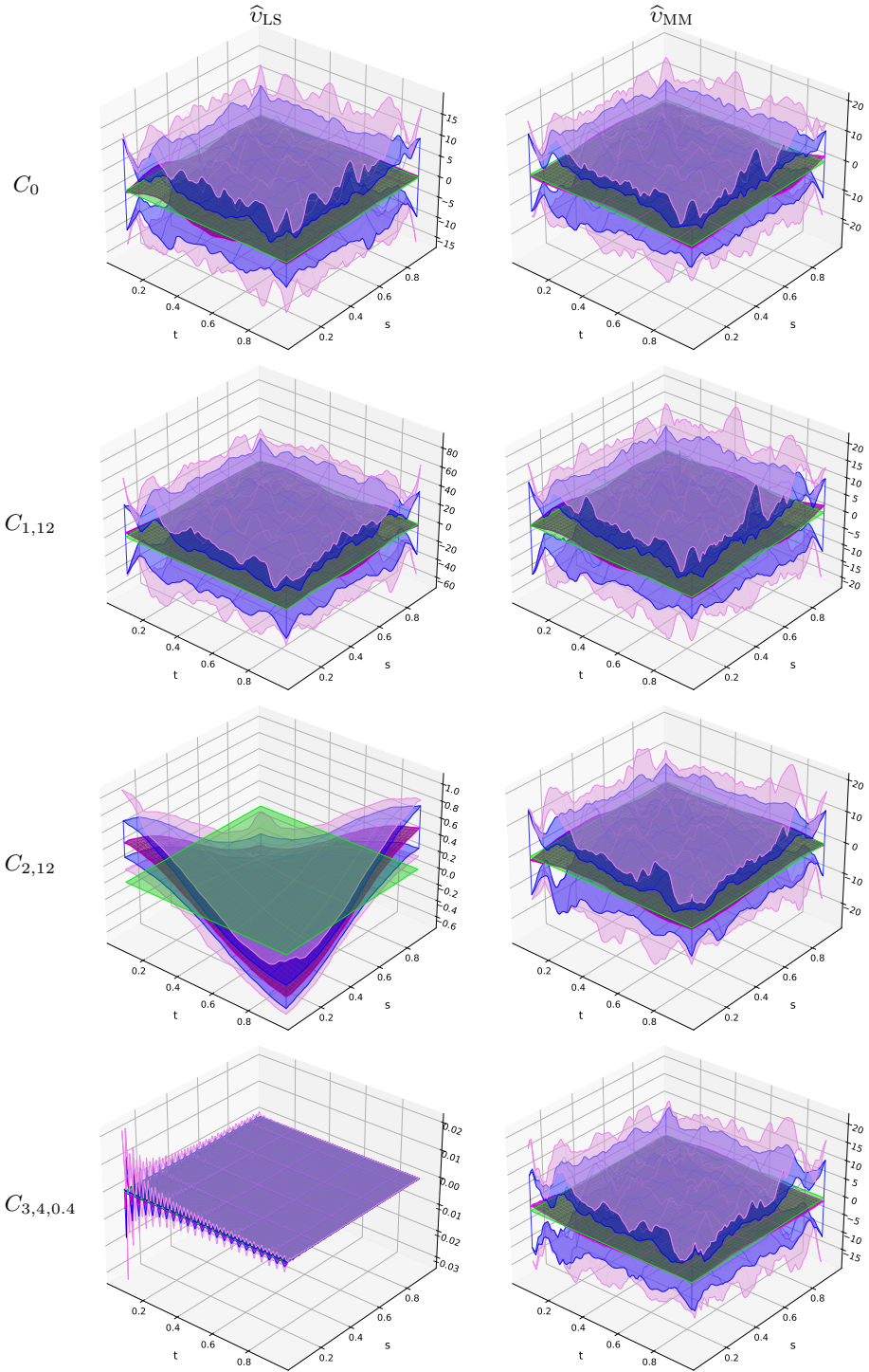


Figure 9: Surface boxplot of the estimators for v_0 under **Model 1** with $\Upsilon_0 = 0$. The true function is shown in green, while the purple surface is the central surface of the $n_R = 1000$ estimates \hat{v} . Columns correspond to estimation methods, while rows to C_0 and to some of the three contamination settings.

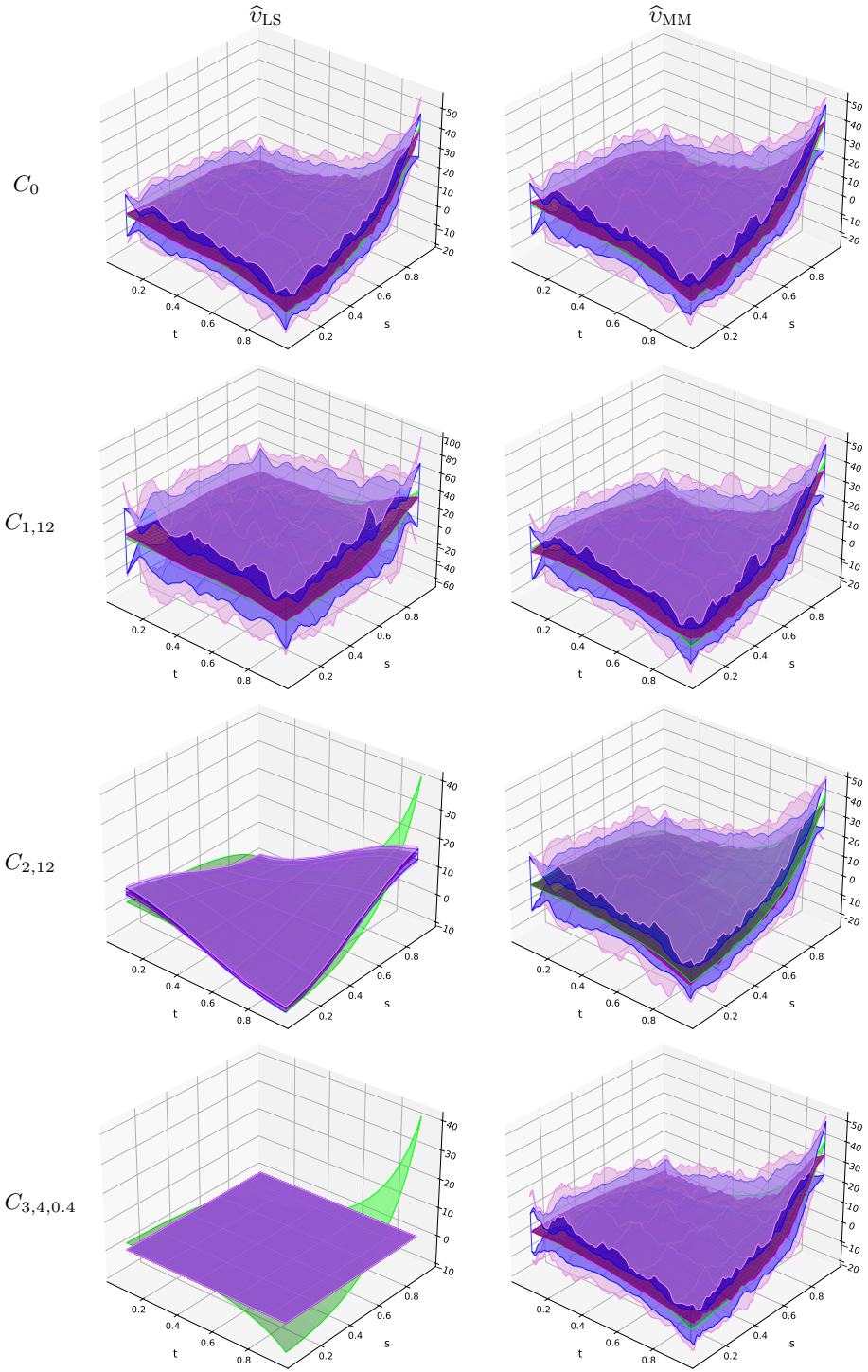


Figure 10: Surface boxplot of the estimators for v_0 under **Model 1** with $\Upsilon_0 = \Upsilon_{0,1}$. The true function is shown in green, while the purple surface is the central surface of the $n_R = 1000$ estimates \hat{v} . Columns correspond to estimation methods, while rows to C_0 and to some of the three contamination settings.

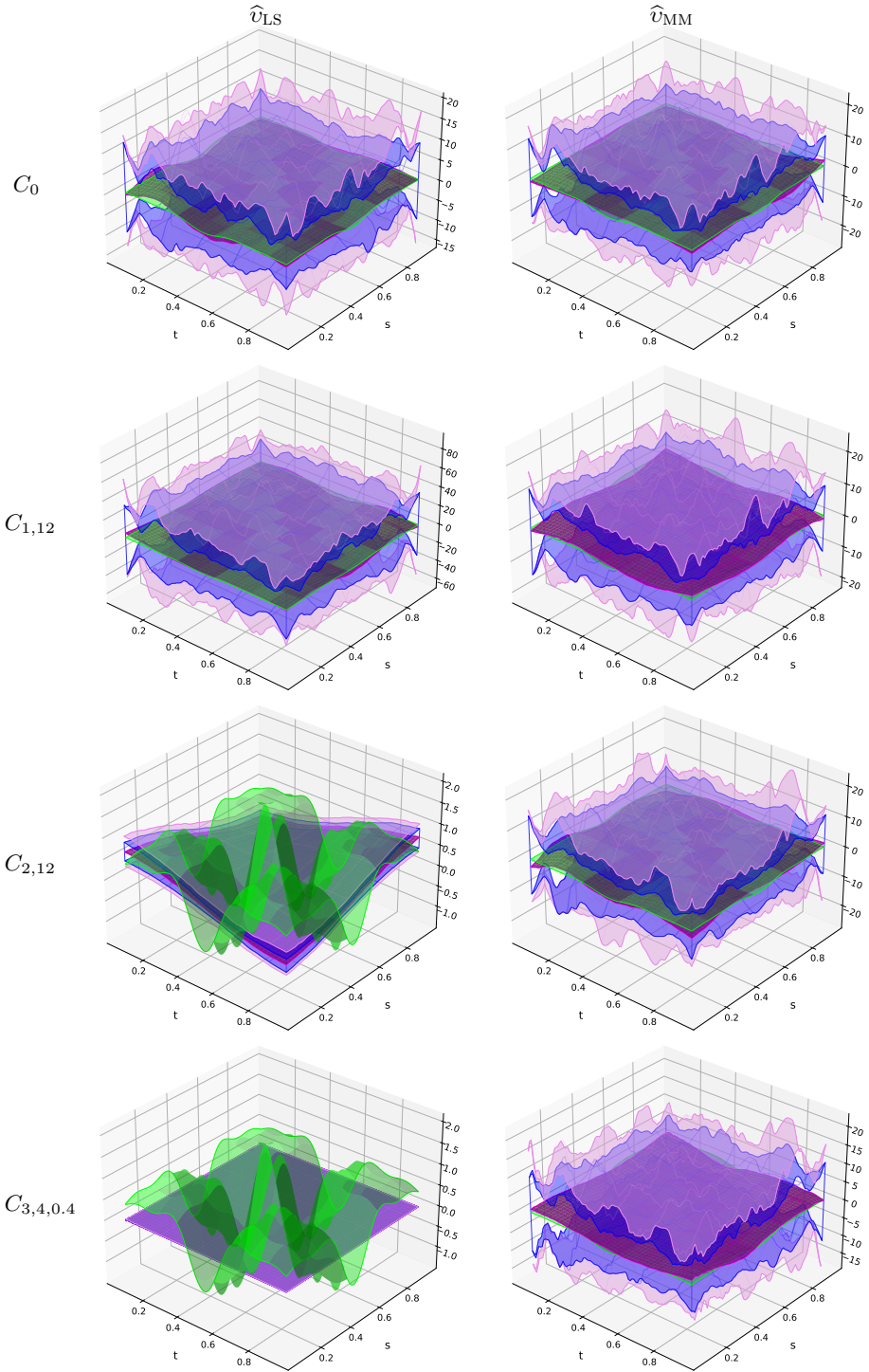


Figure 11: Surface boxplot of the estimators for v_0 under **Model 1** with $\Upsilon_0 = \Upsilon_{0,2}$. The true function is shown in green, while the purple surface is the central surface of the $n_R = 1000$ estimates \hat{v} . Columns correspond to estimation methods, while rows to C_0 and to some of the three contamination settings.

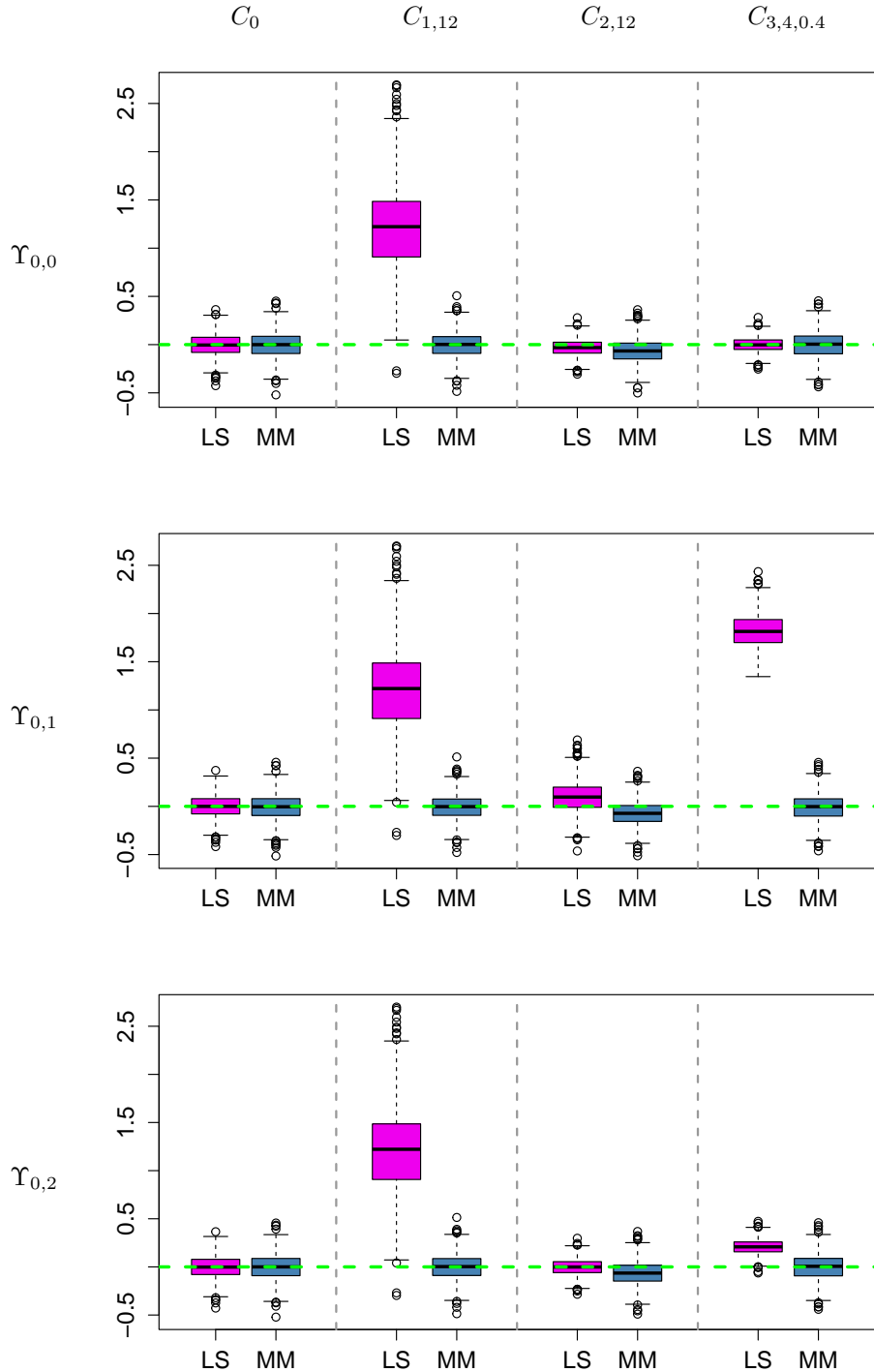


Figure 12: Boxplots of the estimators for α_0 for clean and contaminated samples, under **Model 1**. The true value is shown with a green dashed line. Rows correspond to different Υ_0 scenarios. Columns correspond to C_0 and to some of the three contamination settings. Magenta and blue boxplots correspond to classical and robust methods, respectively.

4.2 Model 2

In this section, we considered the functional quadratic regression model (14), where $\sigma_0 = 0.5$ and the regression parameter equals the one used in Yao and Müller (2010), that is, $\beta_0 = a_1\phi_1 + a_2\phi_2$ with $\phi_1(t) = -\sqrt{2}\cos(\pi t)$ and $\phi_2(t) = \sqrt{2}\sin(\pi t)$. We label this model as **Model 2**. The choice of the coefficients a_1 and a_2 depend on the quadratic operator selected. More precisely, when $\Upsilon_{0,0} = 0$, that is under a functional linear model, we chose $a_1 = 2$ and $a_2 = 0.5$. When considering a functional quadratic model with $\Upsilon_{0,1} = \phi_1 \otimes \phi_1 + \phi_2 \otimes \phi_2 + (1/2)(\phi_1 \otimes \phi_2 + \phi_2 \otimes \phi_1)$, the coefficients of β_0 equal $a_1 = a_2 = 1$. Figure 13 shows the functions β_0 related to the linear and quadratic model and the surface $v_{0,1}(s, t)$ associated to the non-null quadratic operator $\Upsilon_{0,1}$. For the quadratic kernel we present two viewpoints, since the surface plots are better appreciated with one of them due to the surface shape.

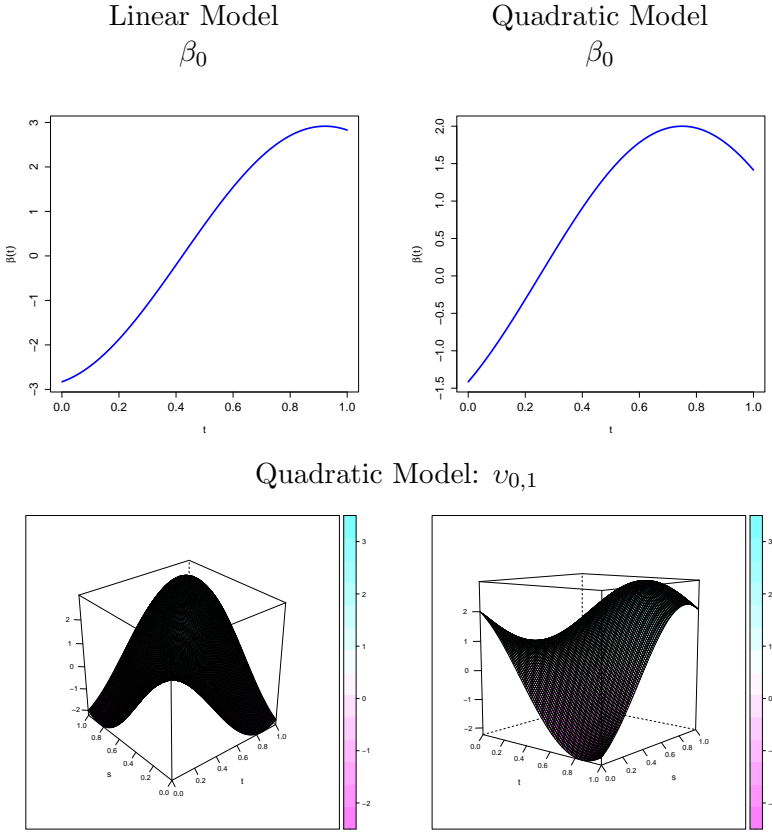


Figure 13: True parameters under Model 2. For the quadratic kernel we present two view points.

For clean samples, denoted C_0 , the errors are normally distributed $\epsilon_i \sim N(0, 1)$, independent from X_i . The functional covariates $X_i(t)$ were generated as Gaussian processes with mean 0 and covariance operator $\Gamma = 4\phi_1 \otimes \phi_1 + \phi_2 \otimes \phi_2$, that is, $X_{ij} = \xi_{i1}\phi_1 + \xi_{i2}\phi_2$ where ξ_{ij} are independent Gaussian random variables such that $\xi_{i1} \sim N(0, 4)$ and $\xi_{i2} \sim N(0, 1)$.

As in Model 1, we considered three contamination scenarios. Contaminations $C_{1,\mu}$ and $C_{2,\mu}$ are identical to the ones used in Model 1, and we include a third contamination, labelled $C_{3,\mu}$. The selected contamination schemes are then

- $C_{1,\mu}$: corresponds to “vertical outliers”. The distribution G of the errors ϵ is given by $G(u) = 0.9\Phi(u) + 0.1\Phi((u - \mu)/0.5)$, with Φ the standard normal distribution function. We chose μ varying between 8 and 20 with a step of 2.
- $C_{2,\mu}$: we sample $v_i \sim Bi(1, 0.10)$ and then:
 - if $v_i = 0$, let $\epsilon_i^{(co)} = \epsilon_i$ and $X_i^{(co)} = X_i$;
 - if $v_i = 1$, let $\sigma_0 \epsilon_i^{(co)} \sim N(\mu, \sigma_0^2/4)$ and $X_i^{(co)} = \xi_{i1}^{(co)} \phi_1 + \xi_{i2}^{(co)} \phi_2$, with $\xi_{i1}^{(co)} \sim N(0, 4)$ and $\xi_{i2}^{(co)} \sim N(\mu/2, 0.25)$.

The responses are generated as $y_i^{(co)} = \langle \beta_0, X_i^{(co)} \rangle + \langle X_i^{(co)} \Upsilon_0, X_i^{(co)} \rangle + \sigma_0 \epsilon_i^{(co)}$. The values of μ vary between 8 and 20 with a step of 2.

- $C_{3,\mu}$: we sample $v_i \sim Bi(1, 0.10)$ and then:
 - if $v_i = 0$, let $y_i^{(co)} = y_i$ and $X_i^{(co)} = X_i$;
 - if $v_i = 1$, let $X_i^{(co)} = \xi_{i1}^{(co)} \phi_1 + \xi_{i2}^{(co)} \phi_2$ where $\xi_{ij}^{(co)} = 2|\xi_{ij}|$, while $y_i^{(co)} = 2\mu|y_i|$.

The values of μ vary in $\{0.2, 0.4, 0.6, 0.8, 1.2, 1.4, 1.6, 1.8, 2.0, 2.2, 2.4\}$

As an illustration of the type of outliers generated with the second setting above, Figure 14 shows 25 randomly chosen functional covariates $X_i(t)$, for one sample generated under C_0 (with no outliers), one obtained under $C_{2,8}$ and the other one under $C_{3,1.2}$.

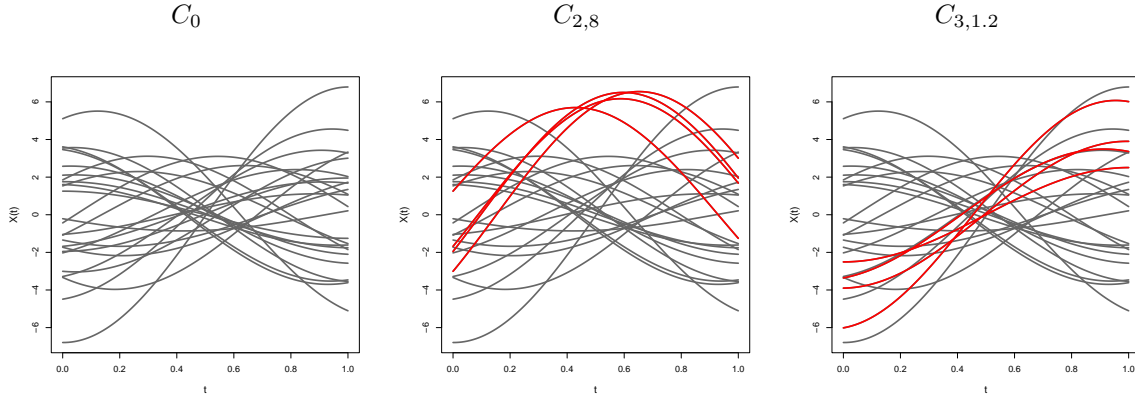


Figure 14: 25 trajectories $X_i(t)$ under **Model 2** with and without contamination.

The same summary measures as in Section 4.1 were computed. As in **Model 1**, Table 4 reports the maximum value of the squared bias and of the MISE over the different values of μ and/or δ and we simply label the situation as C_j , for $j = 1, 2, 3$ to avoid burden notation.

The plots in Figures 15 and Figures 16 summarize the effect of the contamination scenarios for the different choices of Υ_0 and different values of μ when considering $C_{1,\mu}$ and $C_{2,\mu}$. For $C_{3,\mu}$. Each plot corresponds to one contamination scenario and one parameter estimator. Within each panel, the solid and dashed lines correspond to the measures for the least squares and MM -estimators, respectively. As above, the line with triangles shows the trimmed MISE, and the one with solid circles indicates the corresponding trimmed bias squared. For this model, under all contamination schemes, the MISE of the classical procedure is much larger than those obtained for the robust

Linear Model				Quadratic Model					
	$\hat{\beta}$	\hat{v}			$\hat{\beta}$	\hat{v}			
	Bias _{TR} ²	MISE _{TR}							
C_0	LS	0.0145	0.0256	0.0000	0.0066	0.0037	0.0148	0.0142	0.0208
	MM	0.0148	0.0281	0.0000	0.0082	0.0038	0.0172	0.0142	0.0224
C_1	LS	0.0136	1.6399	0.0005	1.0112	0.0033	1.6302	0.0149	1.0257
	MM	0.0148	0.0285	0.0000	0.0083	0.0039	0.0176	0.0142	0.0224
C_2	LS	0.9683	1.0307	1.7754	1.7874	0.9578	1.0201	1.7892	1.8012
	MM	0.0161	0.0391	0.0139	0.0923	0.0052	0.0282	0.0281	0.1064
C_3	LS	1.7854	2.0006	0.5086	0.6485	13.8164	15.4307	15.5136	16.2597
	MM	0.0172	0.0329	0.0010	0.0134	0.0040	0.0178	0.0141	0.0223

Table 4: Trimmed versions of the integrated squared bias and mean integrated squared errors (multiplied by 10) for clean and contaminated samples, **Model 2**. The reported values under contamination correspond to the worst situation.

procedure, both when estimating the regression parameter or the quadratic operator. Regarding the Bias, except for $C_{1,\mu}$, the bias of the method based on least squares is highly affected by the contaminations considered. In particular, under $C_{3,\mu}$ the bias is increased more than 1000 times with respect to those obtained for clean samples. The robust proposal given in this paper is quite stable across all contaminations.

As when considering **Model 1**, to visualize the performance of the estimators of β_0 , Figures 18 and 19 contain functional boxplots of the estimators, under C_0 and some of the three contamination settings. To avoid boundary effects, we show here the different estimates $\hat{\beta}_j$ evaluated on central 90% interior points of the grid. In addition, to facilitate comparisons between contamination cases and estimation methods, the scales of the vertical axes are the same for all panels within each Figure.

The effect of contamination in this model is less striking than under **Model 1**. However, as in that model, under $C_{1,12}$ the classical estimator $\hat{\beta}$ becomes highly variable, but retains the shape of β_0 . In contrast, under $C_{3,1.2}$ when the data are generated according to a functional quadratic model the estimator becomes completely uninformative due to the distorted region containing the non-outlying curve estimators (see Figure 19). It is worth mentioning that when $\Upsilon_0 = 0$ and under the scheme $C_{3,1.2}$, the true curve is beyond the limits of the functional boxplot for values larger than 0.6, while under $C_{2,8}$ it lies near the boundary that limits the non-outlying curves but outside this region. It is worth mentioning that, for clean samples, the obtained estimators of β_0 have smaller variability than under **Model 1**, which is reflected on narrower bands. This fact may be explained by the ratio noise signal, which is much smaller under the model considered in Yao and Müller (2010) than under **Model 1**.

As under **Model 1**, the classical estimators of α_0 are sensitive to the contaminations considered. Table 5 reports, multiplied by 1000, the absolute bias, which in this case equals the absolute value of the mean, and the standard deviations over replications. For the contamination settings, the maximum over the different values of μ is reported. Figure 17 presents the boxplots of the estimators for α_0 for clean samples and for some contamination scenarios. The true value is plotted with a green dashed line, for reference. The first row corresponds to the case where the observations are

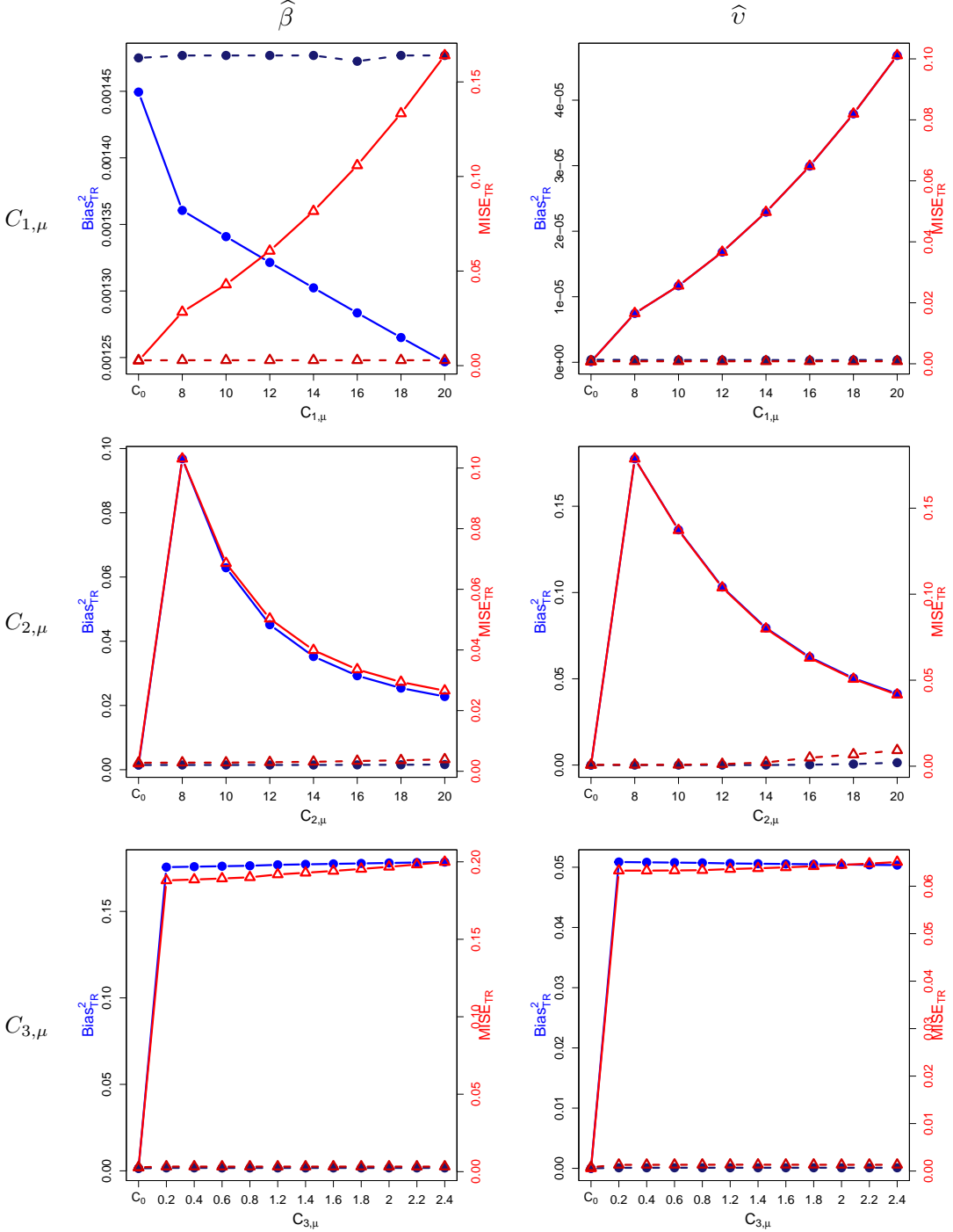


Figure 15: Plots of the trimmed squared bias and MISE of the estimators of β_0 and v_0 as a function of μ for each contamination scenario, under **Model 2** with $\Upsilon_0 = 0$. The solid and dashed lines correspond to the least squares and MM -estimators, respectively. The squared bias is indicated with circles, and the MISE with triangles.

generated according to a linear model ($\Upsilon_0 = 0$), while the second one to the quadratic model

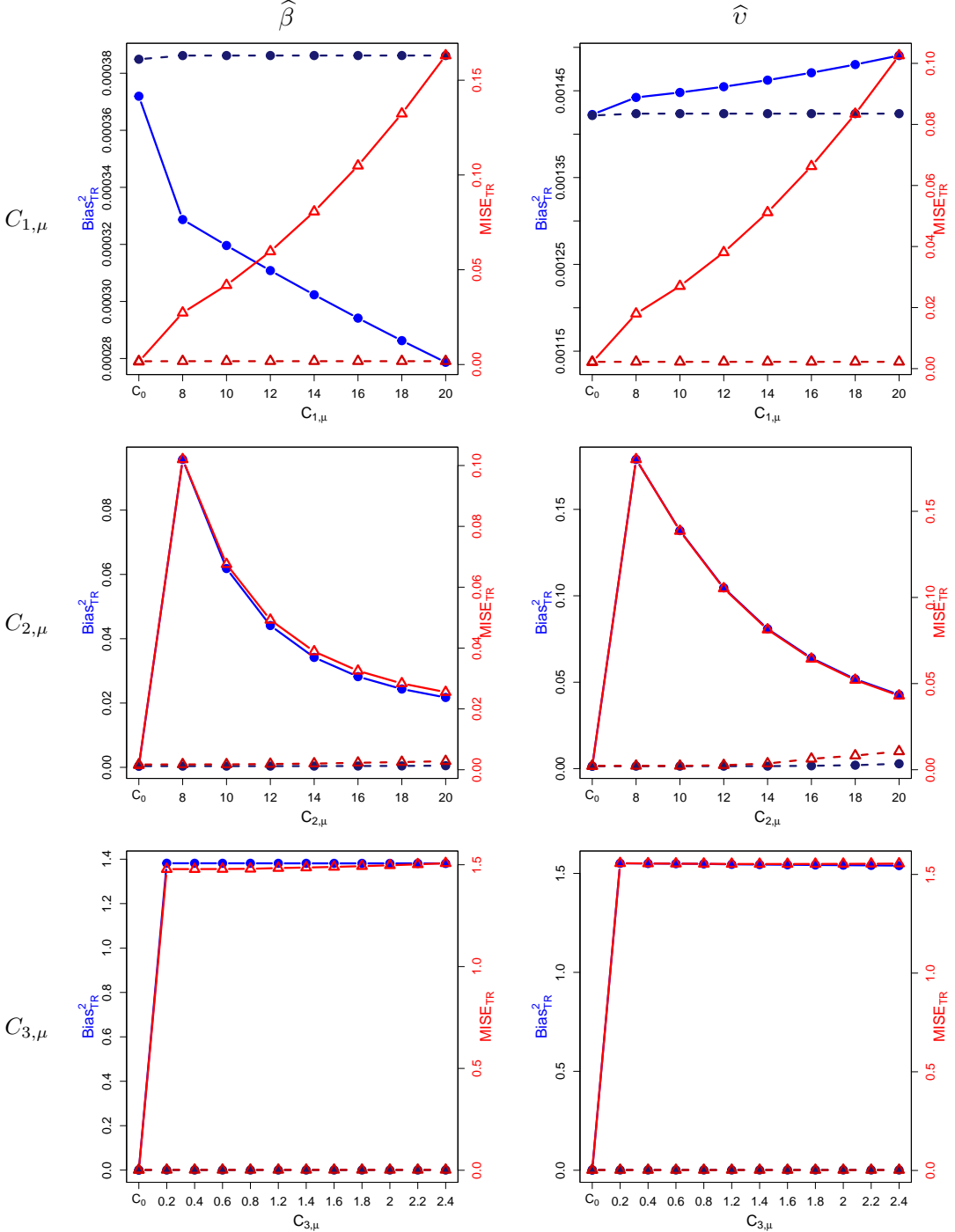


Figure 16: Plots of the trimmed squared bias and MISE of the estimators of β_0 and v_0 as a function of μ for each contamination scenario, under **Model 2** with $\Upsilon_0 = \Upsilon_{0,1}$. The solid and dashed lines correspond to the least squares and MM -estimators, respectively. The squared bias is indicated with circles, and the MISE with triangles.

considered ($\Upsilon_0 = \Upsilon_{0,1}$). Each column corresponds to a contamination setting. The boxplots of the

classical and robust estimators are given in magenta and blue, respectively. The reported results show that schemes $C_{1,\mu}$ and $C_{3,\mu}$ affect the classical estimator of the intercept for any choice of the quadratic operator with maximum biases increased more than ten thousand times and standard deviations enlarged more than one thousand times. In contrast, a smaller effect is observed under $C_{2,\mu}$ (see Figure 17). The robust procedure is stable over the contaminations considered, even though some effect in the bias is observed again under C_2 (see Table 5).

		$\Upsilon_{0,0}$		$\Upsilon_{0,1}$	
		Mean	SD	Mean	SD
C_0	LS	0.20	40.86	0.20	40.86
	MM	0.34	44.36	0.34	44.36
C_1	LS	1989.93	496.22	1989.93	496.22
	MM	0.65	44.85	0.13	44.81
C_2	LS	286.71	67.61	286.71	67.61
	MM	28.63	78.87	28.63	78.87
C_3	LS	340.05	200.35	2281.67	528.91
	MM	4.86	47.67	5.70	45.32

Table 5: Summary measures (multiplied by 1000) for α_0 estimates over clean and contaminated samples, **Model 1**. The reported values under contamination correspond to the worst situation.

The effect on the classical estimators of the quadratic operator is observed in Figures 20 and 21, where it is clear the enlargement of the central 50% region under $C_{1,12}$ and the damaging effect of contamination $C_{2,8}$ when $\Upsilon_0 = 0$, since the true surface is mostly beyond the area delimiting the non-atypical ones for values of t and s between 0.3 and 0.7. Under $C_{3,1,2}$, when the true model is a linear one, the whiskers are completely distorted even when the true surface lies within them. When considering quadratic terms in the model, this last contamination has an extreme effect, since the true surface crosses the limits of the surfaces plot. Note that an estimate of the trimmed total variance VAR_{TR} may be obtained as the difference between the MISE and the squared bias. Under C_0 , the BIAS_{TR} equals 0.037 for both estimators and the square root of VAR_{TR} equals 0.0257 for the classical procedure and 0.0286 for the robust one, so the bias is much larger than the variability. In contrast, under **Model 1** when considering $\Upsilon_0 = \Upsilon_{0,2}$ which varies within a similar range to that of the quadratic kernel under **Model 2**, the obtained estimate of the total variability ($\sqrt{\text{VAR}_{\text{TR}}}$) of $\hat{\Upsilon}$ equal 2.2147 and 2.6251 for the least squares and MM -procedure, respectively and the trimmed biases are more than five times smaller, since they equal 0.3848 and 0.3818, respectively. The difference arising produces a distorting effect on the surface plots obtained under **Model 2** and C_0 , which do not allow to see clearly the whiskers and central region. Furthermore, due to the stability of the robust procedure, the same behaviour arises for the MM -estimate under the considered contaminations.

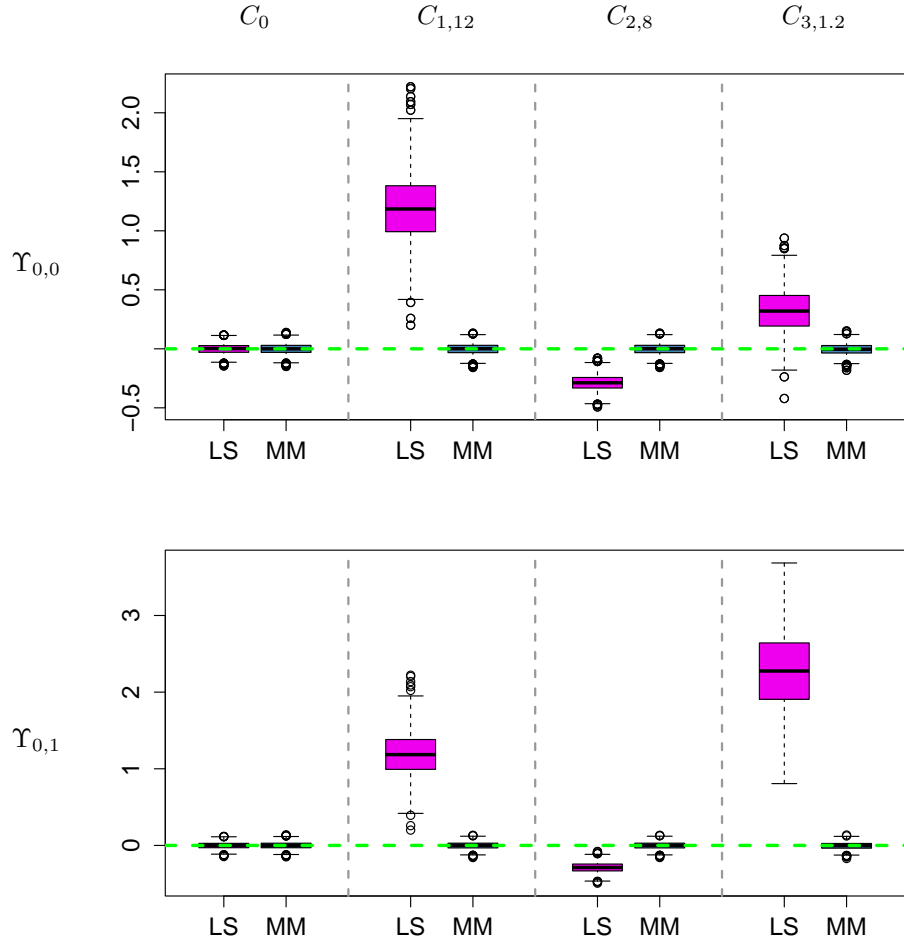


Figure 17: Boxplots of the estimators for α_0 for clean and contaminated samples, under **Model 2**. The true value is shown with a green dashed line. Rows correspond to different Υ scenarios. Columns correspond to C_0 and to some of the three contamination settings. Magenta and blue boxplots correspond to classical and robust methods, respectively.

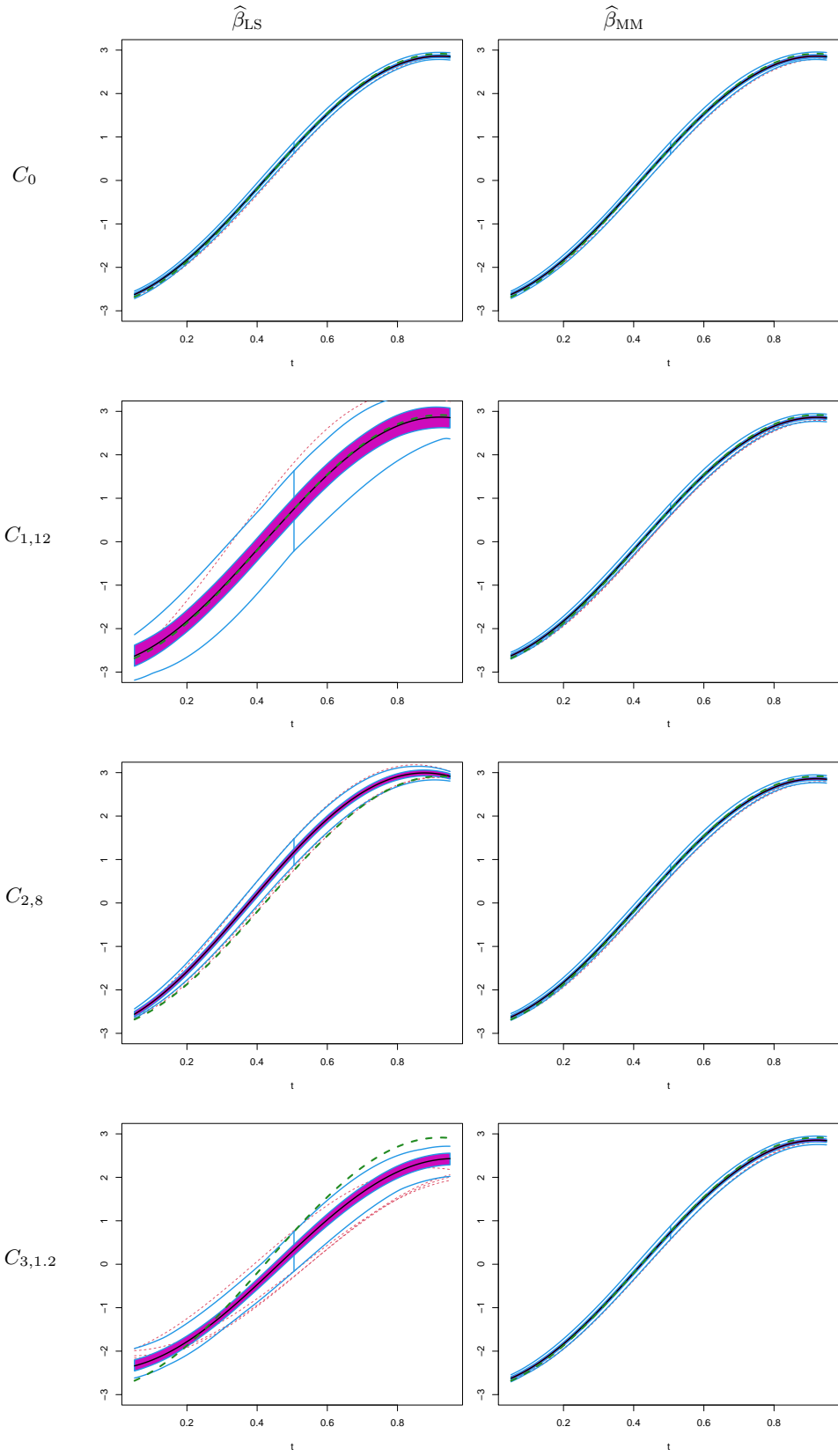


Figure 18: Functional boxplot of the estimators for β_0 under **Model 2** with $Y_0 = 0$. The true function is shown with a green dashed line, while the black solid one is the central curve of the $n_R = 1000$ estimates $\hat{\beta}$. Columns correspond to estimation methods, while rows to C_0 and to some of the three contamination settings.

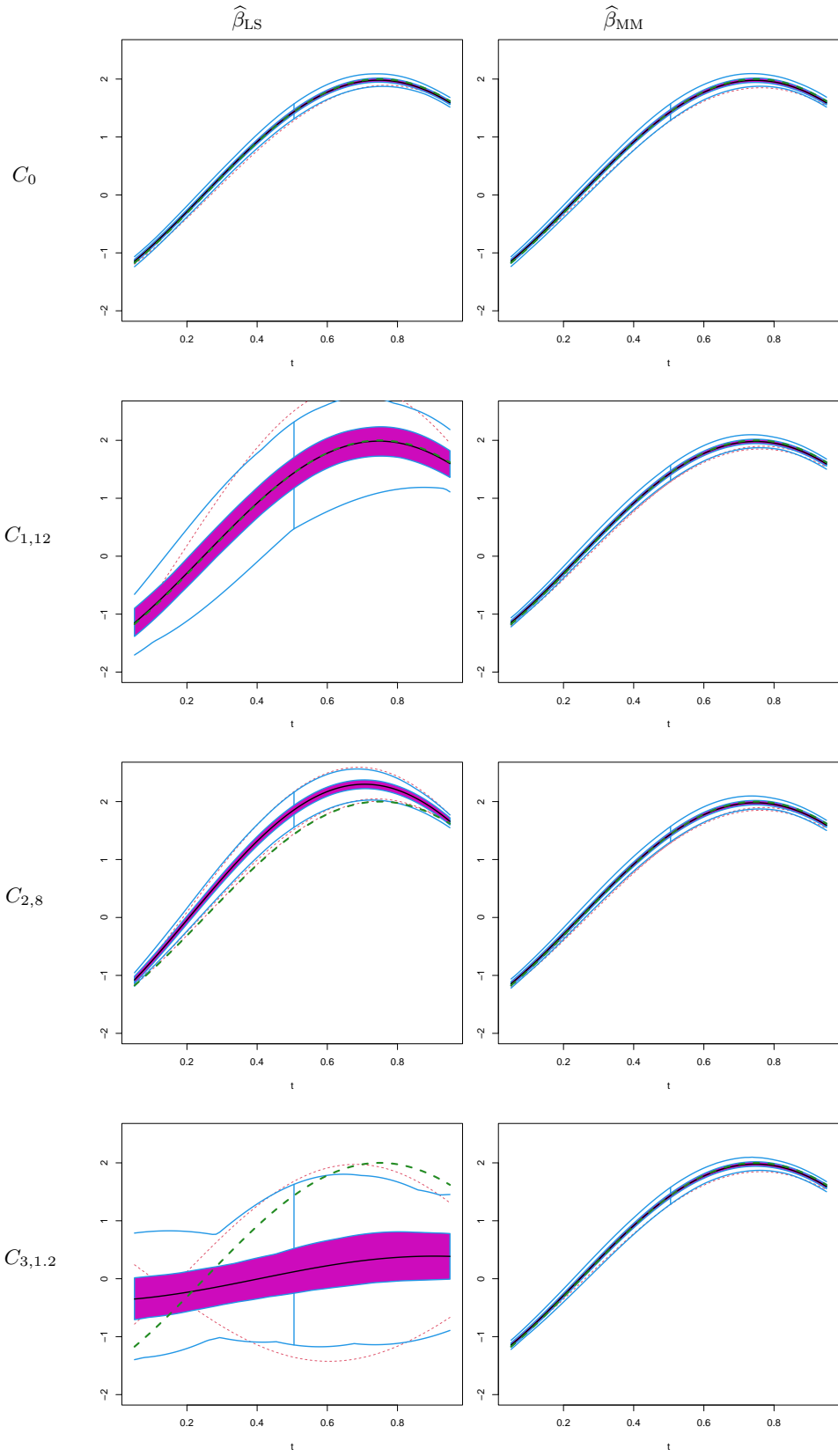


Figure 19: Functional boxplot of the estimators for β_0 under **Model 2** with $\Upsilon_0 = \Upsilon_{0,1}$. The true function is shown with a green dashed line, while the black solid one is the central curve of the $n_R = 1000$ estimates $\hat{\beta}$. Columns correspond to estimation methods, while rows to C_0 and to some of the three contamination settings.

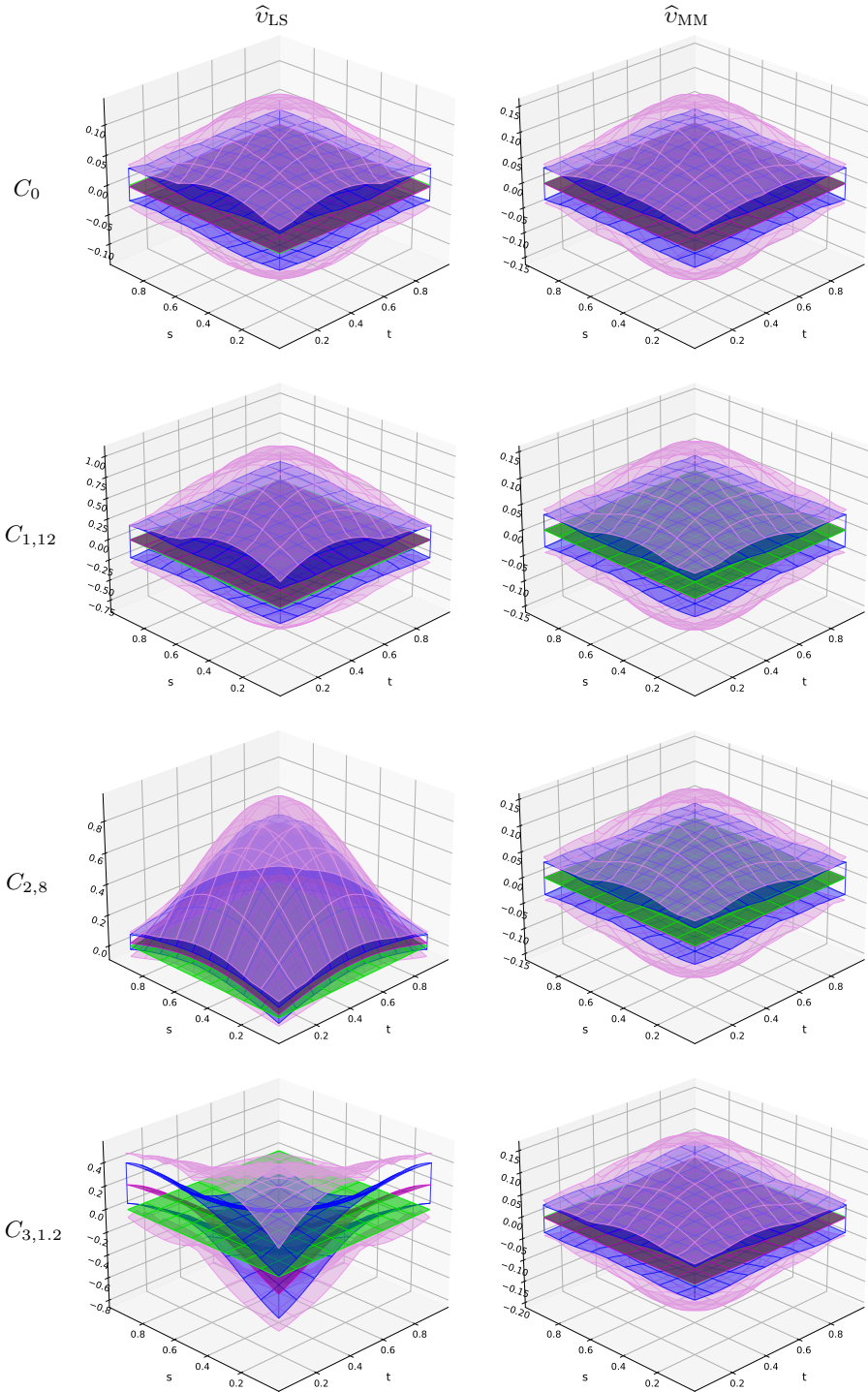


Figure 20: Surface boxplot of the estimators for v_0 under **Model 2** with $\Upsilon_0 = 0$. The true function is shown in green, while the purple surface is the central surface of the $n_R = 1000$ estimates \hat{v} . Columns correspond to estimation methods, while rows to some of the three contamination settings.

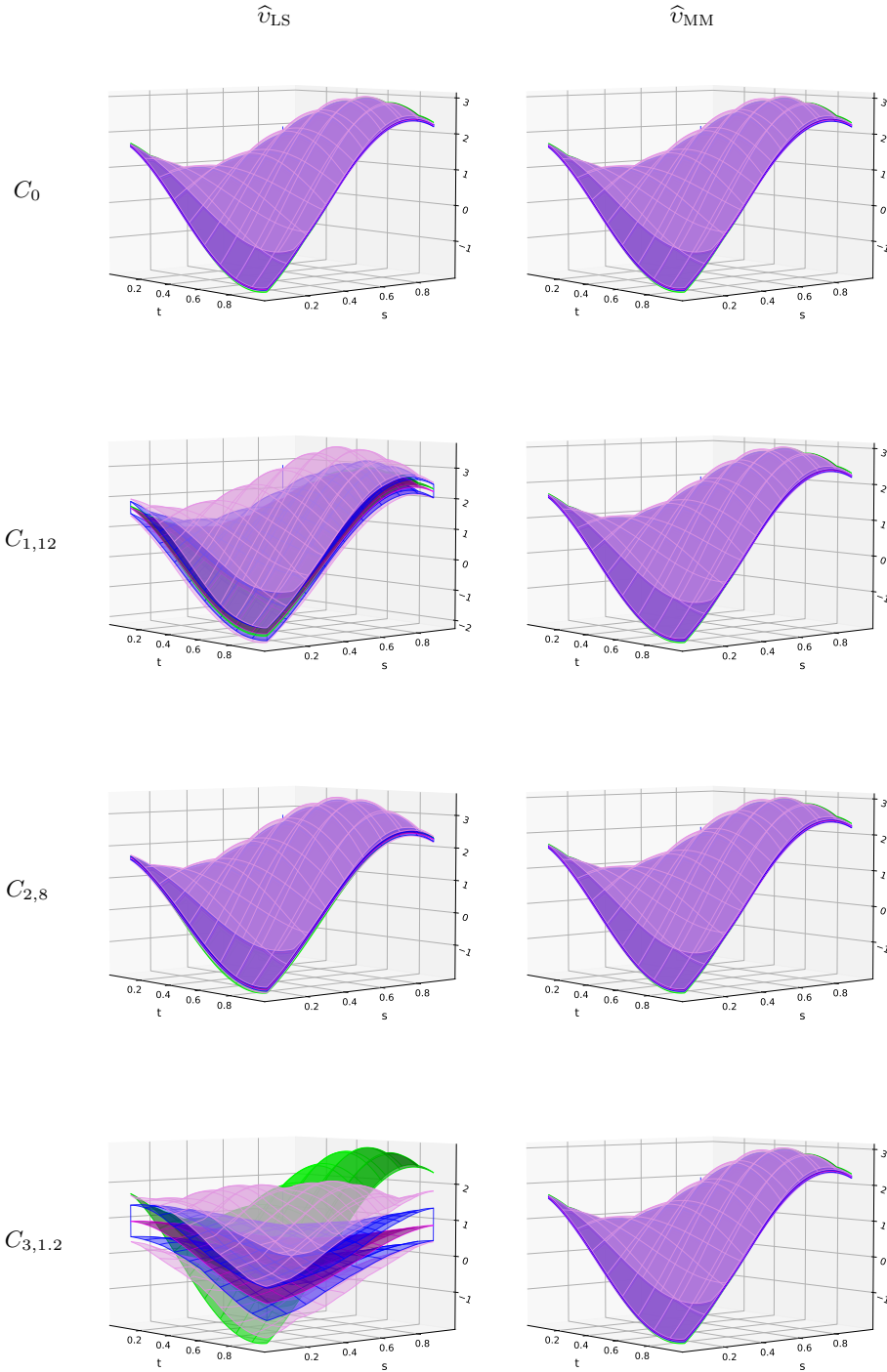


Figure 21: Surface boxplot of the estimators for v_0 under **Model 2** with $\Upsilon_0 = \Upsilon_{0,1}$. The true function is shown in green, while the purple surface is the central surface of the $n_R = 1000$ estimates \widehat{v} . Columns correspond to estimation methods, while rows to C_0 and to some of the three contamination settings.

5 Tecator Data

The Tecator data set was analysed, among others, in Ferraty and Vieu (2006), Aneiros-Pérez and Vieu (2006), Yao and Müller (2010), Shang (2014), Huang et al. (2015) and Boente et al. (2020) and it is available in the package `fda.usc` (Febrero-Bande and de la Fuente, 2012), see also <http://lib.stat.cmu.edu/datasets/tecator>. These data contain measurements taken on samples from finely chopped meat with different percentages of fat, protein and moisture content. Each observation consists of a spectrometric curve that corresponds to the absorbance measured on an equally spaced grid of 100 wavelengths between 850 and 1050 nm. The contents of fat protein and moisture were also recorded through analytic chemistry methods.

The goal of the analysis is to predict the fat content (y) using some characteristics of the spectrometric curve.

Huang et al. (2015) include also the variables water and protein contents to predict the fat content and compared several models in terms of their predictive properties. As a characteristic of the spectrometric curve, they used its second derivative which enters, as the functional covariate in the model linearly, while the other two variables appear either through an additive non-parametric component or a varying coefficient model.

In this section, as in Yao et al. (2005), we use a linear and a quadratic model to predict the fat content from the first derivative X of the spectrometric curve. The robust MM –estimators were calculated using the same ρ –functions as in our simulation study, and we choose $p = 4$ principal directions which explain more than 97% of the total variability.

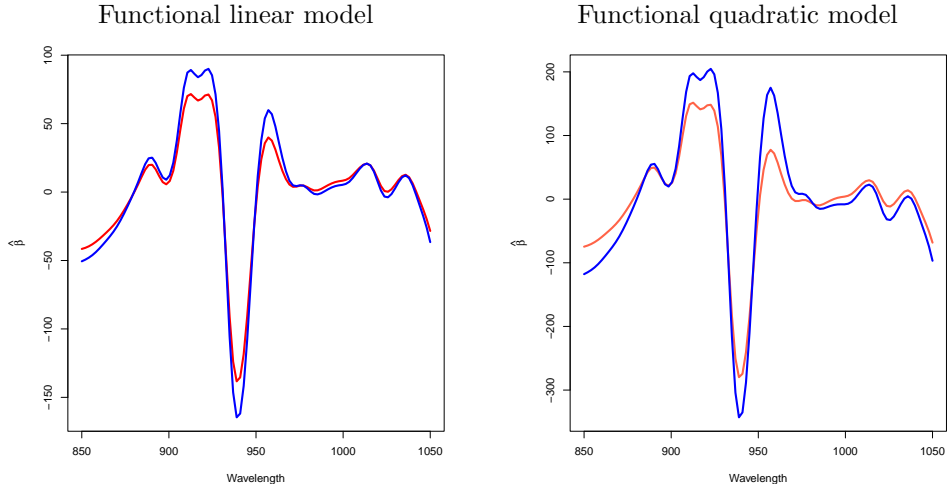


Figure 22: Estimators of β using a least squares (in solid red line) or an MM –estimator (in solid blue lines), when using a functional linear or quadratic model.

The red and blue lines in the left and right panels of Figure 22 show the estimators $\hat{\beta}$ obtained using the classical ($\hat{\beta}_{LS}$) and robust estimators ($\hat{\beta}_{MM}$) when fitting a linear or a quadratic model, respectively. Note that the robust estimators take larger absolute values for wavelengths varying between 900 and 980 nm. It is also worth mentioning that the shape of the estimators obtained when fitting a linear or a quadratic model is quite similar, even when they vary in their range which is enlarged when a quadratic model is assumed.

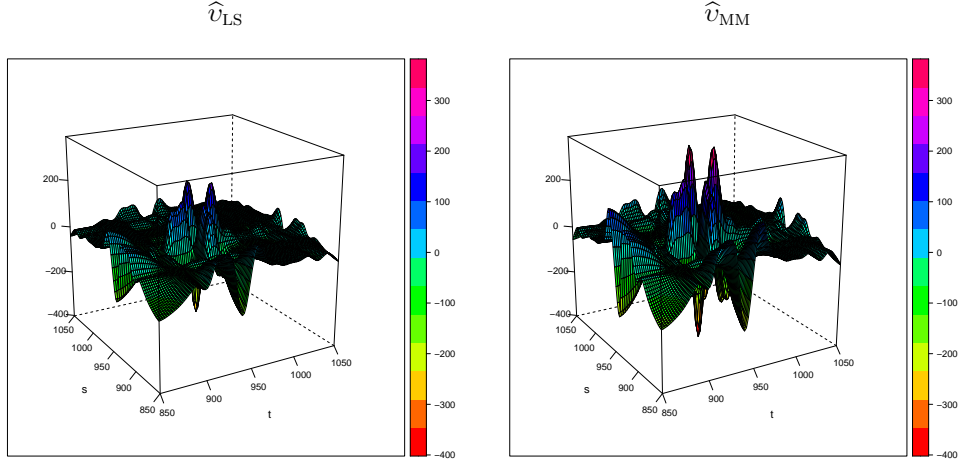


Figure 23: Estimators of v using a least squares, \hat{v}_{LS} , (left panel) or an MM –estimator, \hat{v}_{MM} , (right panel), when using a functional quadratic model.

Figure 23 presents the plot of the quadratic kernel estimates \hat{v}_{LS} and \hat{v}_{MM} obtained by each method when fitting a functional quadratic model. This Figure also reveals that the classical estimator presents a similar shape than the robust one but taking values in a smaller range, in particular, for the range of wavelengths close to 950 nm. The residual plots which are displayed in Figure 24 also show that the functional linear model does not seem to provide a reasonable fit neither for the classical nor for the robust method. Besides, when looking at the residuals from the robust quadratic fit, some atypical residuals are revealed. The boxplot of these residuals is given in the right panel of Figure 25 and identifies 32 observations as potential outliers, the corresponding covariates are displayed in red dashed lines in the left panel of Figure 25.

We fitted again a quadratic model using the classical procedure after eliminating the potential atypical observations. Figures 26 and 27 display the obtained estimators together with the classical and robust estimates computed with all the data. In Figure 26 the classical and robust estimators of β with all the data are displayed in red and blue solid lines, respectively, while the least squares estimate computed on the “cleaned” data set is presented in a dashed pink line. Note that for both the linear coefficient and the quadratic kernel, the shape of the classical estimators computed without the suspected atypical observations, resembles that of the robust ones. To visualize more clearly the similarity between the surfaces related to the quadratic kernel estimators, we present in Figure 28 the surfaces $\hat{D} = \hat{v}_{LS} - \hat{v}_{MM}$ and $\hat{D}^{(-\text{OUT})} = \hat{v}_{LS}^{(-\text{OUT})} - \hat{v}_{MM}$. This figure highlights the differences between the classical estimator computed with the whole data set and the robust one. Both when estimating the linear regression function or the quadratic operator, the classical estimators computed without the detected potential outliers are very close to the robust ones, that is, the robust estimator behaves similarly to the classical one if one were able to manually remove suspected outliers.

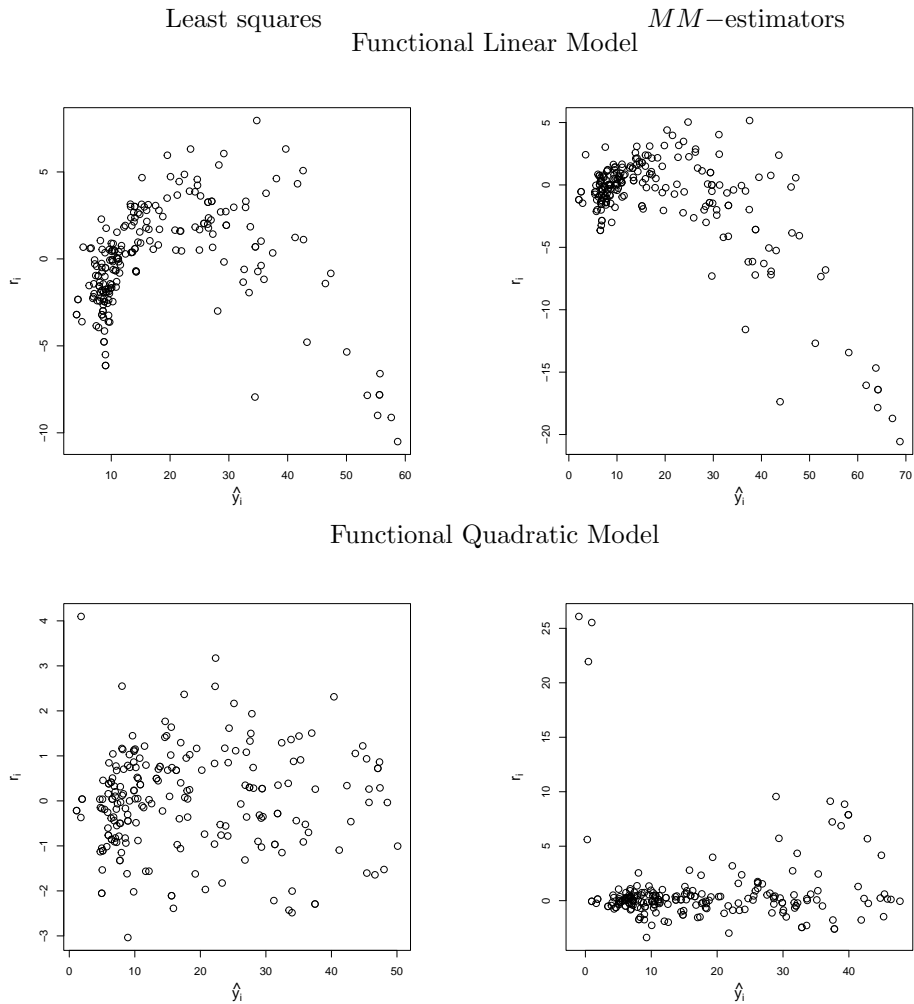


Figure 24: Residuals from a classical (left panels) or robust (right panels) fit, when using a functional linear (first line) or quadratic model (second line).

6 Final Comments

In this paper, we propose robust estimators based on robust principal component analysis for functional quadratic regression models. Our estimators are robust against outliers in the response variable and also in the functional explanatory variables. An extensive simulation study shows that our proposed estimators have good robustness and finite-sample statistical properties. For finite-dimensional processes, where only the coefficients of the regression and quadratic parameters over the linear spaces induced by the eigenfunctions of the covariance operator are identifiable, the proposed procedure is Fisher-consistent. In such a situation, our requirements are closely related to those considered in Kalogridis and Van Aelst (2019). However, we did not restrict our attention to this situation and we also derived Fisher-consistency when X is an infinite-dimensional process with $\ker(\Gamma) = \{0\}$, under smoothness conditions of the eigenfunctions of Γ .

We apply our method to a real data set and confirm that the robust MM -estimators remain reliable even when the data set contains atypical observations in the functional explanatory variables.

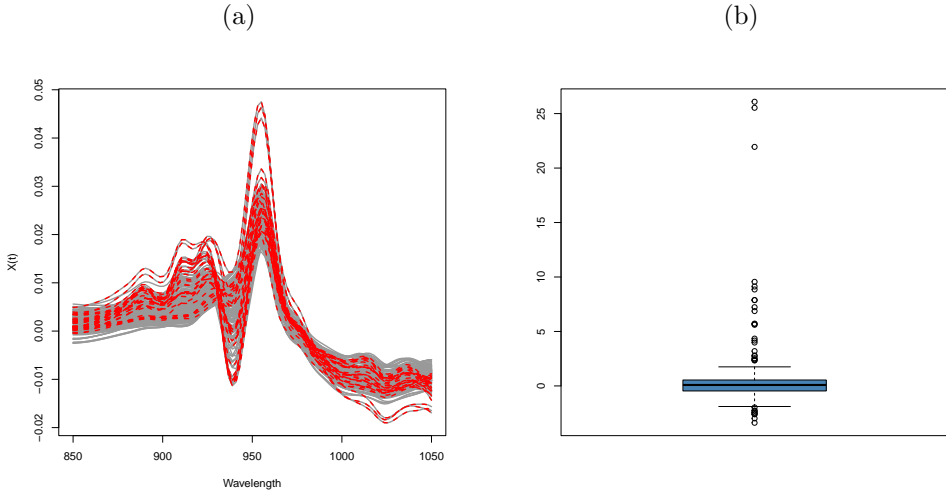


Figure 25: (a) Trajectories corresponding to the first derivative of the absorbance, in red we identify the covariates used in the the functional quadratic model for which the residuals are labelled as outliers by the boxplot. (b) Boxplot of the residuals from the robust quadratic fit.

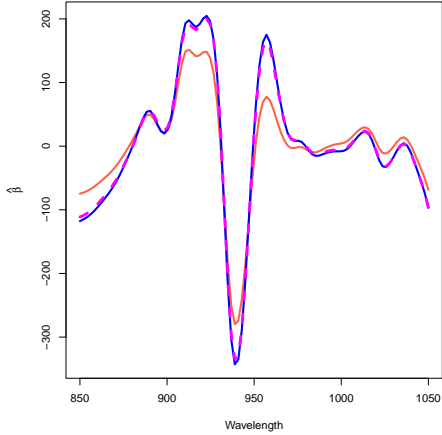


Figure 26: Estimators of β using a least squares (in solid red line) or an MM –estimator (in solid blue lines), when using a functional quadratic model. The dashed pink line corresponds to the classical estimators computed after eliminating the potential atypical observations.

Moreover, the residuals obtained from the robust fit provide a natural way to identify potential atypical observations.

Acknowledgements.

This research was partially supported by Universidad de Buenos Aires [Grant 20020170100022BA] and ANPCYT [Grant PICT 2018-00740] at Argentina (Graciela Boente), the Ministerio de Ciencia e Innovación, Spain (MCIN/AEI/10.13039/501100011033) [Grant PID2020-116587GB-I00] (Graciela Boente).

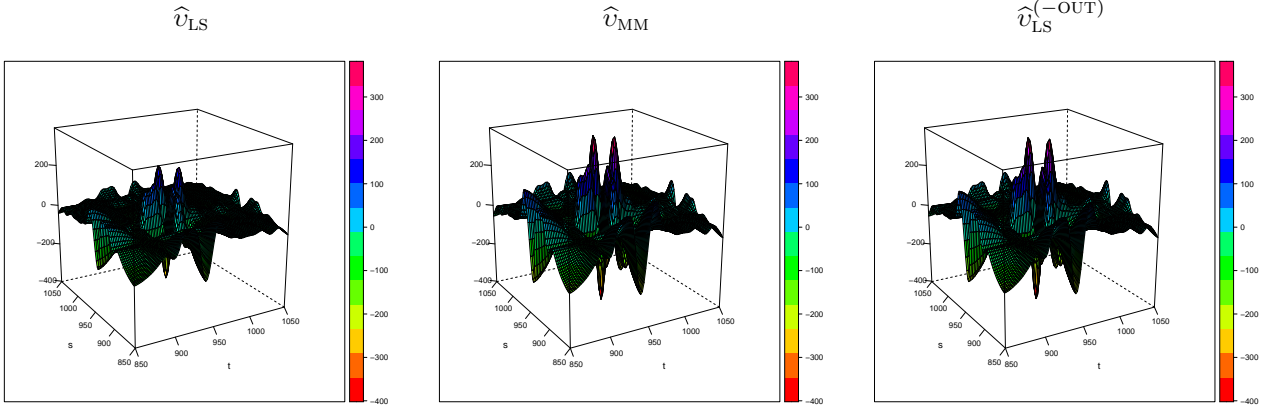


Figure 27: Estimates of v using a least squares approach (left panel), MM –method (middle panel) or the classical procedure after eliminating the potential atypical observations (right panel).

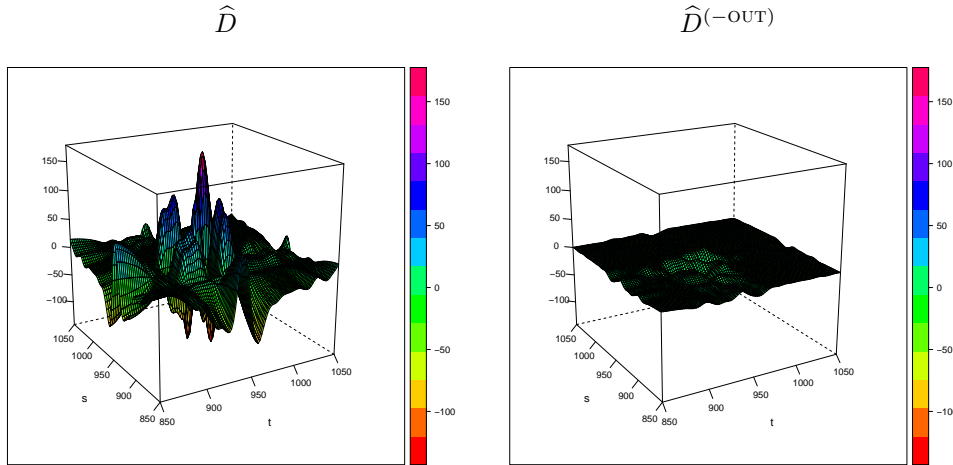


Figure 28: Plot of the surfaces $\hat{D}(s, t) = \hat{v}_{LS}(s, t) - \hat{v}_{MM}(s, t)$ and $\hat{D}^{(-OUT)}(s, t) = \hat{v}_{LS}^{(-OUT)}(s, t) - \hat{v}_{MM}(s, t)$.

7 Appendix

PROOF OF PROPOSITION 3.1. Note that the Fisher–consistency of μ_R and $\phi_{R,j}$ at P_X , i.e., $\mu_R(P_X) = \mu$ and $\phi_{R,j}(P_X) = \phi_j$, entail that $\mathbf{x}_p(P_X) = \mathbf{x}_p$ and $\mathbf{z}_p(P_X) = \mathbf{z}_p$ where $\mathbf{x}_p = (\langle X - \mu, \phi_1 \rangle, \dots, \langle X - \mu, \phi_p \rangle)^T$ and $\mathbf{z}_p = \text{vech}(\{(x_j x_\ell)\}_{1 \leq j \leq \ell \leq p})$. Moreover, if $p > q$ we have that $\langle X - \mu, \phi_j \rangle = 0$, for any $j > q$, so that $\mathbf{x}_p = (\mathbf{x}_q^T, 0, \dots, 0)^T$ and similarly for \mathbf{z}_p . Hence, for any $\mathbf{b}_p = (b_1, \dots, b_p) = (\mathbf{b}_q^T, \mathbf{b}_{p-q}^T)^T \in \mathbb{R}^p$ and any finite-dimensional candidate $\beta_{\mathbf{b}} = \sum_{j=1}^p b_j \phi_{R,j}(P_X)$ we have that $\langle X - \mu, \beta_{\mathbf{b}} \rangle = \mathbf{b}_q^T \mathbf{x}_q$. Similarly, for any self–adjoint Hilbert–Schmidt operator with finite range such that

$$\Upsilon = \sum_{1 \leq j, \ell \leq p} v_{j\ell} \phi_{R,j}(P_X) \otimes \phi_{R,\ell}(P_X),$$

we have that $\langle X - \mu, \Upsilon X \rangle = \mathbf{u}_q^T \mathbf{z}_q$, where $\mathbf{u}_p = \text{vech}(\{(2 - \mathbf{1}_{j=\ell})v_{j\ell}\})_{1 \leq j \leq \ell \leq p}$. Thus, for any $(a, \beta, \Upsilon) \in \mathcal{C}_p$, we have that

$$L(\alpha, \beta, \Upsilon, \mu_R(P_X), \sigma) = \mathbb{E} \rho_1 \left(\frac{y - \alpha - \mathbf{b}_q^T \mathbf{x}_q - \mathbf{u}_q^T \mathbf{z}_q}{\sigma} \right).$$

Define $\mathbf{b}_0 = (\langle \beta_0, \phi_1 \rangle, \dots, \langle \beta_0, \phi_q \rangle)^T$ and $v_{0,jj} = \langle \phi_j, \Upsilon_0 \phi_j \rangle$ and $v_{0,j\ell} = v_{0,\ell j} = \langle \phi_j, \Upsilon_0 \phi_\ell \rangle$, for $1 \leq j, \ell \leq q$ and $\mathbf{u}_0 = \text{vech}(\{(2 - \mathbf{1}_{j=\ell})v_{0,j\ell}\})_{1 \leq j \leq \ell \leq q}$. Then,

$$L(\alpha_0, \beta_{0,q}, \Upsilon_{0,q}, \mu, \sigma) = \mathbb{E} \rho_1 \left(\frac{y - \alpha_0 - \mathbf{b}_0^T \mathbf{x}_q - \mathbf{u}_0^T \mathbf{z}_q}{\sigma} \right) = \mathbb{E} \left(\rho_1 \left(\epsilon \frac{\sigma_0}{\sigma} \right) \right). \quad (15)$$

Lemma 3.1 of Yohai (1987) together with assumption **C1** and the fact that $\tilde{\epsilon} = \epsilon \sigma_0 / \sigma$ satisfy assumption **C2**, imply that for all $a \neq 0$,

$$\mathbb{E} \left[\rho_1 \left(\epsilon \frac{\sigma_0}{\sigma} - a \right) \right] > \mathbb{E} \left[\rho_1 \left(\epsilon \frac{\sigma_0}{\sigma} \right) \right]. \quad (16)$$

Thus, taking conditional expectation, we obtain that for any $(a, \beta, \Upsilon) \in \mathcal{C}_p$,

$$\begin{aligned} L(\alpha, \beta, \Upsilon, \mu_R(P_X), \sigma) &= \mathbb{E} \rho_1 \left(\frac{y - \alpha - \mathbf{b}_q^T \mathbf{x}_q - \mathbf{u}_q^T \mathbf{z}_q}{\sigma} \right) \\ &= \mathbb{E} \left\{ \mathbb{E} \left[\rho_1 \left(\epsilon \frac{\sigma_0}{\sigma} - \frac{(\alpha - \alpha_0) + (\mathbf{b}_q - \mathbf{b}_0)^T \mathbf{x}_q + (\mathbf{u}_q - \mathbf{u}_0)^T \mathbf{z}_q}{\sigma} \right) | X \right] \right\} \\ &\geq L(\alpha_0, \beta_{0,q}, \Upsilon_{0,q}, \sigma), \end{aligned}$$

where the last inequality is strict if **C5** holds and $(\alpha, \mathbf{b}_q, \mathbf{u}_q) \neq (\alpha_0, \mathbf{b}_0, \mathbf{u}_0)$. Therefore, if we denote as $\mathbf{b}_{0,p} = (\mathbf{b}_0^T, \mathbf{0}_{p-q}^T)$ and $\mathbf{u}_{0,p} = \text{vech}(\{(2 - \mathbf{1}_{j=\ell})v_{0,p,j\ell}\})_{1 \leq j \leq \ell \leq p}$, where $v_{0,p,j\ell} = v_{0,j\ell}$, for $1 \leq j, \ell \leq q$ and 0 otherwise, we have that the vector $(\alpha_0, \mathbf{b}_{0,p}, \mathbf{u}_{0,p})$ is a solution of (13), meaning that $\alpha(P) = \alpha_0$, $\pi(\beta(P), \mathcal{H}_q) = \beta_{0,q}$ and $\pi(\Upsilon(P), \mathcal{F}_q) = \Upsilon_{0,q}$.

If in addition **C5** holds and $p = q$, we have that $(\alpha_0, \mathbf{b}_0, \mathbf{u}_0)$ is the unique solution of (13). Effectively, given $(\alpha, \beta, \Upsilon) \in \mathcal{C}_q$, $(\alpha, \beta, \Upsilon) \neq 0$ let

$$\mathcal{A}_0 = \{X : \Phi(X) = \alpha - \alpha_0 + \langle X - \mu, \beta - \beta_{0,q} \rangle + \langle X - \mu, (\Upsilon - \Upsilon_{0,q})(X - \mu) \rangle = 0\},$$

and $a(X) = \Phi(X)/\sigma$. Then, we have that

$$L(\alpha, \beta, \Upsilon, \mu_R(P_X), \sigma) = \mathbb{E} \rho_1 \left(\epsilon \frac{\sigma_0}{\sigma} - \frac{\Phi(X)}{\sigma} \right) = \mathbb{E} \left\{ \rho_1 \left(\epsilon \frac{\sigma_0}{\sigma} \right) \mathbb{I}_{\mathcal{A}_0}(X) \right\} + \mathbb{E} \left\{ \mathbb{E} \left[\rho_1 \left(\epsilon \frac{\sigma_0}{\sigma} - a(X) \right) | X \right] \mathbb{I}_{\mathcal{A}_0^c}(X) \right\}.$$

Using (16) we get that, for any $X \notin \mathcal{A}_0$,

$$\begin{aligned} \mathbb{E} \left[\rho_1 \left(\epsilon \frac{\sigma_0}{\sigma} - a(X) \right) | X = X_0 \right] &= \mathbb{E} \left[\rho_1 \left(\epsilon \frac{\sigma_0}{\sigma} - a(X_0) \right) | X = X_0 \right] \\ &= \mathbb{E} \left[\rho_1 \left(\epsilon \frac{\sigma_0}{\sigma} - a(X_0) \right) \right] > \mathbb{E} \left[\rho_1 \left(\epsilon \frac{\sigma_0}{\sigma} \right) \right], \end{aligned}$$

where the last equality follows from the fact that the errors are independent of the covariates. Thus, taking into account that **C5** implies that $\mathbb{P}(\mathcal{A}_0^c) > 0$, we obtain

$$\begin{aligned} L(\alpha, \beta, \Upsilon, \mu_R(P_X), \sigma) &= \mathbb{E} \left\{ \rho_1 \left(\epsilon \frac{\sigma_0}{\sigma} \right) \mathbb{I}_{\mathcal{A}_0}(X) \right\} + \mathbb{E} \left\{ \mathbb{E} \left[\rho_1 \left(\epsilon \frac{\sigma_0}{\sigma} - a(X) \right) | X \right] \mathbb{I}_{\mathcal{A}_0^c}(X) \right\} \\ &> \mathbb{E} \left\{ \rho_1 \left(\epsilon \frac{\sigma_0}{\sigma} \right) \mathbb{I}_{\mathcal{A}_0}(X) \right\} + \mathbb{E} \left\{ \mathbb{E} \left[\rho_1 \left(\epsilon \frac{\sigma_0}{\sigma} \right) \right] \mathbb{I}_{\mathcal{A}_0^c}(X) \right\} = \mathbb{E} \left(\rho_1 \left(\epsilon \frac{\sigma_0}{\sigma} \right) \right), \end{aligned}$$

which together with (15) and the fact that $\mu_R(P_X) = \mu$, concludes the proof. \blacksquare

PROOF OF PROPOSITION 3.2. Note that as mentioned in Section 3.1, under **C2** and **C1**, for any $a \in \mathbb{R}$, $\beta \in L^2(0,1)$ and $\Upsilon \in \mathcal{F}$, we have that $L(\alpha, \beta, \Upsilon, \sigma_0) \geq L(\alpha_0, \beta_0, \Upsilon_0, \sigma_0)$. Thus for any $p \in \mathbb{N}$, $L(\alpha_0, \beta_0, \Upsilon_0, \mu, \sigma_0) \leq L(\alpha_p(P), \beta_p(P), \Upsilon_p(P), \mu, \sigma_0)$. Hence,

$$L(\alpha_0, \beta_0, \Upsilon_0, \mu, \sigma_0) \leq \liminf_{p \rightarrow \infty} L(\alpha_p(P), \beta_p(P), \Upsilon_p(P), \mu, \sigma_0).$$

On the other hand, taking into account that $\beta_{0,p} \in \mathcal{H}_p$ and $\Upsilon_{0,p} \in \mathcal{F}_p$, we get

$$L(\alpha_p(P), \beta_p(P), \Upsilon_p(P), \mu, \sigma_0) = \underset{a \in \mathbb{R}, \beta \in \mathcal{H}_p, \Upsilon \in \mathcal{F}_p}{\operatorname{argmin}} L(a, \beta, \Upsilon, \mu, \sigma_0) \leq L(\alpha_0, \beta_{0,p}, \Upsilon_{0,p}, \mu, \sigma_0). \quad (17)$$

Using that $\|\beta_{0,p} - \beta_0\|_{L^2(0,1)} \rightarrow 0$ and $\|\Upsilon_{0,p} - \Upsilon_0\|_{\mathcal{F}} \rightarrow 0$, the Cauchy-Schwartz inequality, the fact that ρ_1 is a bounded continuous function and the Bounded Convergence Theorem, we get that $L(\alpha_0, \beta_{0,p}, \Upsilon_{0,p}, \mu, \sigma_0) \rightarrow L(\alpha_0, \beta_0, \Upsilon_0, \mu, \sigma_0)$, which together with (17) leads to

$$\limsup_{p \rightarrow \infty} L(\alpha_p(P), \beta_p(P), \Upsilon_p(P), \mu, \sigma_0) \leq L(\alpha_0, \beta_0, \Upsilon_0, \mu, \sigma_0),$$

concluding the proof. \blacksquare

PROOF OF PROPOSITION 3.3. The proof uses similar arguments to those considered in the proof of Theorem 3.1 and Lemma S.1.4 in Boente et al. (2020) but adapted to the present situation of a quadratic model and L^2 -distances.

Let us denote as $\mathcal{C} = \mathbb{R} \times L^2(0,1) \times \mathcal{F}$, $\mathcal{C}^\star = \mathcal{C} \cap \mathbb{R} \times \mathcal{W}^{1,2} \times \mathcal{W}_2^{1,2}$, $\theta = (a, \beta, \Upsilon)$ and $\theta_0 = (\alpha_0, \beta_0, \Upsilon_0)$. We will begin showing that, for any $\epsilon > 0$,

$$\inf_{(a, \beta, v) \in \mathcal{A}_\epsilon} L(a, \beta, \Upsilon, \mu, \sigma_0) > L(\alpha_0, \beta_0, \Upsilon_0, \mu, \sigma_0), \quad (18)$$

where v the kernel related to the Hilbert-Schmidt operator Υ and $\mathcal{A}_\epsilon = \{(a, \beta, v) \in \mathcal{C}^\star : |a - \alpha_0| + \|\beta - \beta_0\|_{\mathcal{W}^{1,2}} + \|v - v_0\|_{\mathcal{W}_2^{1,2}} \leq M, d(\theta, \theta_0) \geq \epsilon\}$ with $d(\theta, \theta_0) = |a - \alpha_0| + \|\beta - \beta_0\|_{L^2(0,1)} + \|v - v_0\|_{L^2(\mathcal{T})}$ and $\mathcal{T} = (0,1) \times (0,1)$. From now on, we identify the quadratic operator with its kernel.

Let $(a_k, \beta_k, v_k) \in \mathcal{A}_\epsilon$ be such that $L_k = L(a_k, \beta_k, \Upsilon_k, \mu, \sigma_0) \rightarrow \inf_{(a, \beta, v) \in \mathcal{A}_\epsilon} L(a, \beta, \Upsilon, \mu, \sigma_0)$.

Recall that from the Rellich-Kondrachov Theorem, $\mathcal{W}^{1,2}$ and $\mathcal{W}_2^{1,2}$ are compactly embedded in $L^2(0,1)$ and $L^2(\mathcal{T})$, respectively, so using that $|a_k - \alpha_0| + \|\beta_k - \beta_0\|_{\mathcal{W}^{1,2}} + \|v_k - v_0\|_{\mathcal{W}_2^{1,2}} \leq M$, for all $k \geq 1$, we have that there exists a subsequence k_j such that $a_{k_j} - \alpha_0 \rightarrow a_0$, $\beta_{k_j} - \beta_0 \rightarrow b_0$ in $L^2(0,1)$ and $v_{k_j} - v_0 \rightarrow w_0$ in $L^2(\mathcal{T})$.

Denote as $\tilde{\alpha}_0 = \alpha_0 + a_0$, $\tilde{\beta}_0 = \beta_0 + b_0$ and $\tilde{v}_0 = v_0 + w_0$. Therefore, using that $(a_k, \beta_k, v_k) \in \mathcal{A}_\epsilon$, we get that $d(\theta_0, \theta_0) \geq \epsilon$ where $\tilde{\theta}_0 = (\tilde{\alpha}_0, \tilde{\beta}_0, \tilde{v}_0)$. Taking into account that ρ_1 is a bounded continuous function, from the Bounded Convergence Theorem and the Cauchy-Schwartz inequality, we get that $L_{k_j} \rightarrow L(\tilde{\alpha}_0, \tilde{\beta}_0, \tilde{v}_0, \mu, \sigma_0)$. Therefore, we obtain that $\inf_{(a, \beta, v) \in \mathcal{A}_\epsilon} L(a, \beta, \Upsilon, \mu, \sigma_0) = L(\tilde{\alpha}_0, \tilde{\beta}_0, \tilde{v}_0, \mu, \sigma_0)$. Using that $(\alpha_0, \beta_0, \Upsilon_0)$ is the unique minimizer of $L(\alpha, \beta, \Upsilon, \mu, \sigma)$ for any $\sigma > 0$, since **C7** holds, we obtain that $L(\tilde{\alpha}_0, \tilde{\beta}_0, \tilde{v}_0, \mu, \sigma_0) > L(\alpha_0, \beta_0, v_0, \mu, \sigma_0)$ which concludes the proof of (18).

The proof will be completed if we show that there exists $M > 0$ such that,

$$\limsup_{p \rightarrow \infty} |\alpha_p(P) - \alpha_0| + \|\beta_p(P) - \beta_0\|_{\mathcal{W}^{1,2}} + \|v_p(P) - v_0\|_{\mathcal{W}_2^{1,2}} \leq M. \quad (19)$$

Given $\delta > 0$, define K_δ such that for any $K \geq K_\delta$,

$$\mathbb{P}(\|X\| + \|X\|^2 \geq K) < \delta. \quad (20)$$

Fix $\theta = (a, \beta, v) \in \mathcal{C}^*$, $\theta \neq 0$, such that $|a| + \|\beta\|_{\mathcal{W}^{1,2}} + \|v\|_{\mathcal{W}_2^{1,2}} \leq 1$ and let $\varphi_\theta > 0$ be a continuity point of the distribution of $|a + \langle X, \beta \rangle + \langle X, \Upsilon X \rangle|$ such that

$$\mathbb{P}(|a + \langle X, \beta \rangle + \langle X, \Upsilon X \rangle| < \varphi_\theta) < c. \quad (21)$$

Then, if $a^* \in \mathbb{R}$, $\beta^* \in L^2(0, 1)$ and $v^* \in L^2(\mathcal{T})$ is such that

$$\Delta(\theta^*, \theta) = \max(|a^* - a|, \|\beta^* - \beta\|_{L^2(0,1)}, \|v^* - v\|_{L^2(\mathcal{T})}) < \vartheta_\theta,$$

where $\vartheta_\theta = \varphi_\theta/(2(K + 1))$, we have that

$$\mathbb{P}\left(|a^* + \langle X, \beta^* \rangle + \langle X, \Upsilon^* X \rangle| \geq \frac{\varphi_\theta}{2}\right) \geq A(\theta),$$

where $A(\theta) = \mathbb{P}(|a + \langle X, \beta \rangle + \langle X, \Upsilon X \rangle| \geq \varphi_\theta) - \mathbb{P}(\vartheta_\theta(1 + \|X\| + \|X\|^2) \geq \varphi_\theta/2)$. Hence, noting that from (20) and (21), $A(\theta) > 1 - c - \delta$, we conclude that

$$\inf_{\Delta(\theta^*, \theta) < \vartheta_\theta} \mathbb{P}\left(|a^* + \langle X, \beta^* \rangle + \langle X, \Upsilon^* X \rangle| \geq \frac{\varphi_\theta}{2}\right) \geq A(\theta) > 1 - c - \delta. \quad (22)$$

Taking into account that $\mathcal{V} = [-1, 1] \times \{\beta \in L^2(0, 1) : \|\beta\|_{\mathcal{W}^{1,2}} \leq 1\} \times \{v \in L^2(\mathcal{T}) : \|v\|_{\mathcal{W}_2^{1,2}} \leq 1\}$ is compact with the topology in $\mathbb{R} \times L^2(0, 1) \times L^2(\mathcal{T})$, we can take a finite sub-cover from the covering of \mathcal{V} given by $\{\mathcal{B}(\theta, \vartheta_\theta)\}_{\theta \in \mathcal{V}_1^{(1)} \times \mathcal{V}_1^{(1)}}$, where $\mathcal{B}(\theta, \rho)$ stands for the open ball with center θ and radius ρ , that is, $\mathcal{B}(\theta, \rho) = \{(u, f, w) \in \mathbb{R} \times L^2(0, 1) \times L^2(\mathcal{T}) : \max(|u - a|, \|f - \beta\|_{L^2(0,1)}, \|w - v\|_{L^2(\mathcal{T})}) < \rho\}$. The compactness of \mathcal{V} entails that there exist $\theta_j = (a_j, \beta_j, v_j) \in \mathcal{V}$, $1 \leq j \leq s$, such that $\mathcal{V} \subset \bigcup_{j=1}^s \mathcal{B}(\theta_j, \vartheta_j)$ with $\vartheta_j = \vartheta_{\theta_j}$. Therefore, from (22), we obtain that

$$\min_{1 \leq j \leq s} \inf_{\Delta(\theta, \theta_j) < \vartheta_j} \mathbb{P}\left(|a + \langle X, \beta \rangle + \langle X, \Upsilon X \rangle| > \frac{\varphi_j}{2}\right) > 1 - c - \delta,$$

with $\varphi_j = \varphi_{\theta_j}$, meaning that for any $(a, \beta, v) \in \mathcal{V}$, there exist $1 \leq j \leq s$ such that

$$\mathbb{P}\left(|a + \langle X, \beta \rangle + \langle X, \Upsilon X \rangle| > \frac{\varphi_j}{2}\right) > 1 - c - \delta. \quad (23)$$

Taking into account that from Proposition 3.2,

$$\lim_{p \rightarrow \infty} L(\alpha_p(P), \beta_p(P), \Upsilon_p(P), \mu, \sigma_0) = L(\alpha_0, \beta_0, \Upsilon_0, \mu, \sigma_0) = b_{\rho_1},$$

and that $c < 1 - b_{\rho_1}$, we have that there exists $p_0 \in \mathbb{N}$ such that for each $p \geq p_0$,

$$L(\alpha_p(P), \beta_p(P), \Upsilon_p(P), \mu, \sigma_0) \leq b_{\rho_1} + \frac{\xi}{2},$$

where $\xi < 1 - c - b_{\rho_1}$.

In order to derive (19), it will be enough to show that there exist $M > 0$ such that,

$$\inf_{(a, \beta, v) \in \mathcal{D}(\theta_0, M)} L(a, \beta, \Upsilon, \mu, \sigma_0) \geq b_{\rho_1} + \xi,$$

where $\mathcal{D}(\theta_0, M) = \{\theta = (a, \beta, v) \in \mathcal{C}^\star : |a - \alpha_0| + \|\beta - \beta_0\|_{\mathcal{W}^{1,2}} + \|v - v_0\|_{\mathcal{W}_2^{1,2}} > M\}$. Denote as $R(u) = \mathbb{E}\rho(\epsilon - u/\sigma_0)$. First note that, the independence between the errors and covariates entails that

$$\begin{aligned} L(a, \beta, \Upsilon, \mu, \sigma_0) &= \mathbb{E}\rho\left(\epsilon - \frac{(a - \alpha_0) + \langle X, \beta - \beta_0 \rangle + \langle X, (\Upsilon - \Upsilon_0)X \rangle}{\sigma_0}\right) \\ &= \mathbb{E}R((a - \alpha_0) + \langle X, \beta - \beta_0 \rangle + \langle X, (\Upsilon - \Upsilon_0)X \rangle). \end{aligned}$$

Using that $\lim_{|u| \rightarrow +\infty} R(u) = 1$, we get that for any $\delta > 0$, there exists u_0 such that, for any u such that $|u| \geq u_0$,

$$R(u) > 1 - \delta. \quad (24)$$

Choose $M > 2u_0/\min_{1 \leq j \leq s}(\varphi_j)$, where φ_j is given in (23) and let $(a_k, \beta_k, v_k) \in \mathbb{R} \times \mathcal{W}^{1,2} \times \mathcal{W}_2^{1,2}$ be such that $\nu_k = |a_k - a_0| + \|\beta_k - \beta_0\|_{\mathcal{W}^{1,2}} + \|v_k - v_0\|_{\mathcal{W}_2^{1,2}} > M$ and

$$\lim_{k \rightarrow \infty} L(a_k, \beta_k, v_k, \mu, \sigma_0) = \inf_{(a, \beta, v) \in \mathcal{D}(\theta_0, M)} L(a, \beta, v, \mu, \sigma_0).$$

Denote as $\tilde{a}_k = (a_k - \alpha_0)/\nu_k$, $\tilde{\beta}_k = (\beta_k - \beta_0)/\nu_k$ and $\tilde{v}_k = (v_k - v_0)/\nu_k$, then $(\tilde{a}_k, \tilde{\beta}_k, \tilde{v}_k) \in \mathcal{V}$, thus using (23), we obtain that there exists $1 \leq j = j(k) \leq s$ such that

$$\mathbb{P}\left(|\tilde{a}_k + \langle X, \tilde{\beta}_k \rangle + \langle X, \tilde{\Upsilon}_k X \rangle| > \frac{\varphi_j}{2}\right) > 1 - c - \delta.$$

Using that $\nu_k > M > 2u_0/\phi_j$ and denoting as $u_k(X) = \nu_k(\tilde{a}_k + \langle X, \tilde{\beta}_k \rangle + \langle X, \tilde{\Upsilon}_k X \rangle)$, we obtain that $|u_k(X)| > u_0$ whenever $|\tilde{a}_k + \langle X, \tilde{\beta}_k \rangle + \langle X, \tilde{\Upsilon}_k X \rangle| > \varphi_j/2$, which together with (24) leads to

$$\begin{aligned} L(a_k, \beta_k, \Upsilon_k, \mu, \sigma_0) &= \mathbb{E}R(a_k + \langle X, \beta_k \rangle + \langle X, \Upsilon_k X \rangle) = \mathbb{E}R(u_k(X)) \\ &\geq \mathbb{E}\left\{R(u_k(X)) \mathbb{I}_{|\tilde{a}_k + \langle X, \tilde{\beta}_k \rangle + \langle X, \tilde{\Upsilon}_k X \rangle| > \varphi_j/2}\right\} \\ &> (1 - \delta) \mathbb{P}\left(|\tilde{a}_k + \langle X, \tilde{\beta}_k \rangle + \langle X, \tilde{\Upsilon}_k X \rangle| > \frac{\varphi_j}{2}\right) \\ &> (1 - c - \delta)(1 - \delta), \end{aligned}$$

where the last inequality follows from (23). Therefore,

$$\inf_{(a, \beta, v) \in \mathcal{D}(\theta_0, M)} L(a, \beta, \Upsilon, \mu, \sigma_0) \geq (1 - c - \delta)(1 - \delta).$$

The proof follows now easily noting that $\lim_{\delta \rightarrow 0} (1 - c - \delta)(1 - \delta) = 1 - c > b_{\rho_1} + \xi$, so we can choose δ and consequently M such that

$$\inf_{(a, \beta, v) \in \mathcal{D}(\theta_0, M)} L(a, \beta, \Upsilon, \mu, \sigma_0) > b_{\rho_1} + \xi > L(\alpha_p(P), \beta_p(P), \Upsilon_p(P), \mu, \sigma_0),$$

which shows that $|\alpha_p(P) - \alpha_0| + \|\beta_p(P) - \beta_0\|_{\mathcal{W}^{1,2}} + \|v_p(P) - v_0\|_{\mathcal{W}_2^{1,2}} \leq M$, for any $p \geq p_0$, concluding the proof. \blacksquare

References

Aneiros-Pérez, G. and Vieu, P. (2006). Semi-functional partial linear regression. *Statistics and Probability Letters*, 76:1102–1110.

Arribas-Gil, A. and Romo, J. (2014). Shape outlier detection and visualization for functional data: the outliergram. *Biostatistics*, 15:603–619.

Bali, J. L. and Boente, G. (2009). Principal points and elliptical distributions from the multivariate setting to the functional case. *Statistics and Probability Letters*, 79:1858–1865.

Bali, J. L., Boente, G., Tyler, D. E., and Wang, J.-L. (2011). Robust functional principal components: A projection–pursuit approach. *Annals of Statistics*, 39:2852–2882.

Boente, G., Rodriguez, D., and Sued, M. (2019). The spatial sign covariance operator: Asymptotic results and applications. *Journal of Multivariate Analysis*, 170:115–128.

Boente, G. and Salibián-Barrera, M. (2015). S –estimators for functional principal component analysis. *Journal of the American Statistical Association*, 110:1100–1111.

Boente, G. and Salibián-Barrera, M. (2021). Robust functional principal components for sparse longitudinal data. *METRON*, 79:159–188.

Boente, G., Salibián-Barrera, M., and Tyler, D. (2014). A characterization of elliptical distributions and some optimality properties of principal components for functional data. *Journal of Multivariate Analysis*, 131:254–264.

Boente, G., Salibián-Barrera, M., and Vena, P. (2020). Robust estimation for semi–functional linear regression models. *Computational Statistics and Data Analysis*, 152.

Boente, G. and Vahnovan, A. (2017). Robust estimators in semi–functional partial linear regression models. *Journal of Multivariate Analysis*, 154:59–84.

Cai, T. and Hall, P. (2006). Prediction in functional linear regression. *Annals of Statistics*, 34:2159–2179.

Cardot, H., Cénac, P., and Zitt, P.-A. (2013). Efficient and fast estimation of the geometric median in Hilbert spaces with an averaged stochastic gradient algorithm. *Bernoulli*, 19:18–43.

Cardot, H., Ferraty, F., and Sarda, P. (2003). Spline estimators for the functional linear model. *Statistica Sinica*, 13:571–591.

Cardot, H. and Sarda, P. (2005). Estimation in generalized linear models for functional data via penalized likelihood. *Journal of Multivariate Analysis*, 92:24–41.

Cevallos-Valdiviezo, H. (2016). *On methods for prediction based on complex data with missing values and robust principal component analysis*. PhD thesis, Ghent University, (supervisors Van Aelst S. and Van den Poel, D.).

Chen, Y., Carroll, C., Dai, X., Fan, J., Hadjipantelis, P., Han, K., Ji, H., Müller, H., and Wang, J. (2020). *fdapace: Functional Data Analysis and Empirical Dynamics. R package version 0.5.2*.

Cuesta-Albertos, J. A., García-Portugués, E., Febrero-Bande, M., and González-Manteiga, W. (2019). Goodness–of–fit tests for the functional linear model based on randomly projected empirical processes. *Annals of Statistics*, 47:439–467.

Dai, W. and Genton, M. (2019). Directional outlyingness for multivariate functional data. *Computational Statistics and Data Analysis*, 131:50–65.

Febrero-Bande, M. and de la Fuente, M. O. (2012). Statistical computing in functional data analysis: The R package *fda.usc*. *Journal of Statistical Software*, 51:1–28.

Febrero-Bande, M., Galeano, P., and González-Manteiga, W. (2007). A functional analysis of NO_x levels: location and scale estimation and outlier detection. *Computational Statistics*, 22:411–427.

Febrero-Bande, M., Galeano, P., and González-Manteiga, W. (2008). Outlier detection in functional data by depth measures, with application to identify abnormal NO_x levels. *Environmetrics*, 19:331–345.

Febrero-Bande, M., Galeano, P., and González-Manteiga, W. (2017). Functional principal component regression and functional partial least-squares regression: An overview and a comparative study. *International Statistical Review*, 85:61–83.

Ferraty, F. and Vieu, P. (2006). *Nonparametric Functional Data Analysis: Theory and Practice*. Springer.

Fraiman, R. and Muñiz, G. (2001). Trimmed means for functional data. *Test*, 10:419–440.

García-Portugués, E., González-Manteiga, W., and Febrero-Bande, M. (2014). A goodness-of-fit test for the functional linear model with scalar response. *Journal of Computational and Graphical Statistics*, 23:761–778.

Genton, M. G., Johnson, C., Potter, K., Stenchikov, G., and Sun, Y. (2014). Surface boxplots. *Stat*, 3:1–11.

Gervini, D. (2008). Robust functional estimation using the median and spherical principal components. *Biometrika*, 95:587–600.

Hall, P. and Horowitz, J. L. (2007). Methodology and convergence rates for functional linear regression. *Annals of Statistics*, 35:70–91.

He, X. and Shi, P. (1998). Monotone B -spline smoothing. *Journal of the American Statistical Association*, 93:643–650.

Horváth, L. and Kokoszka, P. (2012). *Inference for functional data with applications*. Springer.

Horváth, L. and Reeder, R. (2013). A test of significance in functional quadratic regression. *Bernoulli*, 19:2120–2151.

Hsing, T. and Eubank, R. (2015). *Theoretical foundations of Functional Data Analysis with an introduction to Linear Operators*, volume 997. John Wiley and Sons.

Huang, L., Wang, H., Cui, H., and Wang, S. (2015). Sieve M -estimator for a semi-functional linear model. *Science China Mathematics*, 58:2421–2434.

Hubert, M., Rousseeuw, P., and Segaert, P. (2015). Multivariate functional outlier detection. *Statistical Methods and Applications*, 24:177–202.

Hyndman, R. and Shang, H. L. (2010). Rainbow plots, bagplots, and boxplots for functional data. *Journal of Computational and Graphical Statistics*, 19:29–45.

Hyndman, R. J. and Ullah, M. S. (2007). Robust forecasting of mortality and fertility rates: A functional data approach. *Computational Statistics and Data Analysis*, 51:4942–4956.

Kalogridis, I. and Van Aelst, S. (2019). Robust functional regression based on principal components. *Journal of Multivariate Analysis*, 173:393–415.

Kalogridis, I. and Van Aelst, S. (2021). Robust penalized estimators for functional linear regression. Available at <https://arXiv:1908.08760>.

Lee, S., Shin, H., and Billor, N. (2013). M -type smoothing spline estimators for principal functions. *Computational Statistics and Data Analysis*, 66:89–100.

Locantore, N., Marron, J., Simpson, D., Tripoli, N., Zhang, J., and Cohen, K. (1999). Robust principal component analysis for functional data. *Test*, 8:1–73.

Maronna, R., Martin, D., Yohai, V., and Salibián-Barrera, M. (2019). *Robust Statistics: Theory and Methods (with R)*. John Wiley and Sons.

Maronna, R. and Yohai, V. (2013). Robust Functional Linear Regression based on splines. *Computational Statistics and Data Analysis*, 65:46–55.

Patilea, V. and Sánchez-Sellero, C. (2020). Testing for lack-of-fit in functional regression models against general alternatives. *Journal of Statistical Planning and Inference*, 209:229–251.

Ramsay, J. and Silverman, B. (2002). *Applied Functional Data Analysis. Methods and Case Studies*. Springer.

Ramsay, J. and Silverman, B. (2005). *Functional Data Analysis, 2nd edition*. Springer.

Reiss, P. T., Goldsmith, J., Shang, H. L., and Ogden, R. T. (2017). Methods for scalar-on-function regression. *International Statistical Review*, 85:228–249.

Rousseeuw, P., Raymaekers, J., and Hubert, M. (2018). A measure of directional outlyingness with applications to image data and video. *Journal of Computational and Graphical Statistics*, 27:345–359.

Sawant, P., Billor, N., and Shin, H. (2012). Functional outlier detection with robust functional principal component analysis. *Computational Statistics*, 27:83–102.

Schumaker, L. (1981). *Spline Functions: Basic Theory*. Wiley.

Shang, H. L. (2014). Bayesian bandwidth estimation for a semi-functional partial linear regression model with unknown error density. *Computational Statistics*, 29:829–848.

Shen, Q. and Faraway, J. (2004). An F test for linear models with functional responses. *Statistica Sinica*, 14:1239–1257.

Sinova, B., González-Rodríguez, G., and Van Aelst, S. (2018). M –estimators of location for functional data. *Bernoulli*, 24:2328–2357.

Sun, Y. and Genton, M. G. (2011). Functional boxplots. *Journal of Computational and Graphical Statistics*, 20:316–334.

Yao, F. and Müller, H. G. (2010). Functional quadratic regression. *Biometrika*, 97:49–64.

Yao, F., Müller, H.-G., and Wang, J.-L. (2005). Functional data analysis for sparse longitudinal data. *Journal of the American Statistical Association*, 100:577–590.

Yohai, V. J. (1987). High breakdown-point and high efficiency robust estimates for regression. *Annals of Statistics*, 15:642–656.